

## 11. SITE 913<sup>1</sup>

### Shipboard Scientific Party<sup>2</sup>

#### HOLE 913A

**Date occupied:** 12 September 1993  
**Date departed:** 13 September 1993  
**Time on hole:** 20 hr, 45 min  
**Position:** 75°29.344'N, 6°56.830'E  
**Bottom felt (drill pipe measurement from rig floor, m):** 3330.0  
**Distance between rig floor and sea level (m):** 11.38  
**Water depth (drill pipe measurement from sea level, m):** 3318.6  
**Total depth (from rig floor, m):** 3433.6  
**Penetration (m):** 103.6  
**Number of cores (including cores with no recovery):** 13  
**Total length of cored section (m):** 103.6  
**Total core recovered (m):** 26.19  
**Core recovery (%):** 25.3  
**Oldest sediment cored:**  
Depth (mbsf): 103.6  
Nature: silty muds with dropstones  
Earliest age: Quaternary

#### HOLE 913B

**Date occupied:** 13 September 1993  
**Date departed:** 20 September 1993  
**Time on hole:** 7 days, 19 hr, 20 min  
**Position:** 75°29.356'N, 6°56.810'E  
**Bottom felt (drill pipe measurement from rig floor, m):** 3330.0  
**Distance between rig floor and sea level (m):** 11.57  
**Water depth (drill pipe measurement from sea level, m):** 3318.4  
**Total depth (from rig floor, m):** 4100.3  
**Penetration (m):** 770.3  
**Number of cores (including cores with no recovery):** 55  
**Total length of cored section (m):** 684.3  
**Total core recovered (m):** 219.99  
**Core recovery (%):** 32

#### Oldest sediment cored:

Depth (mbsf): 770.3  
Nature: siltstone  
Earliest age: middle Eocene

**Principal results:** Site 913 is located in the deep Greenland Basin on crust of magnetic Anomaly 24B age; it is the northernmost of the drill sites planned along the East Greenland Margin. The original scientific objectives aimed at describing the onset and evolution of the East Greenland Current, monitoring the deep-water formation in the Greenland Basin, and deciphering the history of the input of coarse ice-rafted debris. Two holes were drilled, the first one to conduct advanced hydraulic piston corer (APC) and extended core barrel (XCB) coring in the upper part of the sedimentary sequence, and the second one to conduct rotary core barrel (RCB) coring in the deeper part of the sequence to reach Paleogene sediments and basement. The poor recovery of the upper part of the drilled sequence prevented fulfillment of most of the previously defined scientific objectives. However, after penetrating a several-hundred-meter-thick sequence of Quaternary and Pliocene glacial-marine sediments having large ice-rafted components, we succeeded in reaching Oligocene to Eocene fossiliferous pelagic deposits having a rich variety of lithologies documenting a stratigraphic interval that had not been covered during previous DSDP and ODP legs. Throughout the entire sedimentary section of the site, headspace methane concentrations were very low.

Sediments in Hole 913A and the shallow part of Hole 913B (to 307.2 mbsf) are in large part glacially influenced. They consist of interbedded lithologies with a variety of textures, from clay to silty clay and clayey mud to silty sand, with 2%–6% carbonate and 0.1%–1% organic carbon. Although the colors are not monotonous, they are limited to dark grays, dark grayish browns, and olive grays. Beds are of decimeter- to meter-scale thickness and are generally massive. Coarse particles are common throughout, and sand and gravel layers occur as deep as 164 mbsf. Individual dropstones are particularly prevalent in the upper 131 mbsf. They are obviously many times larger than core barrel diameter. The lithology of the dropstones is diverse and includes a variety of sedimentary (quartz sand-, silt-, and limestones), igneous (gabbros, granites), and metamorphic (quartzites, amphibolites, gneisses, schists) lithologies. Crystalline rocks are predominant, in contrast with the lithologies at the Yermak Plateau and Fram Strait sites, where fine-grained clastic sedimentary rocks are most common. Siliciclastics dominate these shallow sediments, but planktonic and benthic foraminifers compose up to 40% in specific layers, and nannofossils are a trace component.

Siliciclastics are still present in sediments recovered below several washed intervals (375.2–509.9 mbsf), but are not dominant. Carbonate values are usually <1%, but in selected thin horizons they rise to 10%–23%. Organic carbon concentrations reach only 0.1%–0.5% (the exception being a value of 2.7% in Core 151-913B-27R). Alteration products such as zeolites are more important, as are siliceous microfossils. Diatoms and radiolarians both occur in concentrations as great as 20%. Total bio-silica reaches concentrations above 50%, the sediments thus constituting siliceous oozes. Particle size generally decreases, and silty clays and clays prevail. Layers within the deeper part of the section are typically of mm-

<sup>1</sup> Myhre, A.M., Thiede, J., Firth, J.V., et al., 1995. *Proc. ODP, Init. Repts.*, 151: College Station, TX (Ocean Drilling Program).

<sup>2</sup> Shipboard Scientific Party is as given in the list of participants preceding the Table of Contents.

to cm-thickness. Bedding styles range from fine, continuous, sharp laminations no thicker than 1 mm, to diffuse, discontinuous, gradational layers as thick as 10 cm. Burrows and other traces are absent from some packets of laminae, whereas mottled interfaces, cross-cutting burrows, and determinable traces such as *Chondrites* characterize the less well defined intervals. Perhaps the most distinctive aspect of these deeper sediments is the riotous color schemes associated with them. A full palette of greens characterizes the highly bioturbated zones. The laminated intervals are even more exotic, mixing the full range of greens with a stunning array of hues, including blues, browns, violets, tans, and yellows.

The entire sedimentary sequence of Site 913 can be subdivided into four lithologic units; Unit I has been further subdivided into two subunits, Unit III into three subunits:

Lithologic Unit I: 0–143.8 mbsf. Subunit IA (0–3.2 mbsf, age: Quaternary) consists of interbedded clays, silts, and sand; biocarbonate-bearing clay; and silty mud. Surprisingly few dropstones are found. Subunit IB (3.2–143.8 mbsf, age: Pliocene(?) to Quaternary) consists of interbedded clayey mud and silty mud with minor gravelly or gravel-bearing layers, defined by the presence of abundant large dropstones of various lithologies.

Lithologic Unit II: 143.8–378.7 mbsf; age: middle Miocene to Pliocene. The sequence comprises predominantly silty clay, clayey silt, and silty mud with very few dropstones.

Lithologic Unit III: 378.7–674.1 mbsf. Subunit IIIA (378.7–462.0 mbsf, age: middle Eocene to middle Miocene) consists of interbedded, massive, and laminated silty clay and clay, which at intervals is slightly bioturbated and can contain Mn-concretions. Subunit IIIB (462.0–500.3 mbsf, age: late Eocene to early Oligocene) contains biosilica-bearing clay, biosiliceous clay to silty clay, clayey and silty siliceous ooze with layers of dusky to bright greens, blues, and purples. Subunit IIIC (500.3–674.1 mbsf, age: middle Eocene to early Oligocene) consists of massive and laminated clays, minor silty clays, and muds. They contain rare microfossils.

Lithologic Unit IV: 674.1–770.3 mbsf; age: middle Eocene. The unit comprises laminated clays, silty clays, and massive silty clays, as well as clayey and silty muds in upward-fining sequences. In the lower part, some layers of well-cemented calcareous sandstone and siltstone have been penetrated; their presence is the probable cause of the reduced recoveries in the bottom of Hole 913B.

The uppermost sequence at Site 913 consists of poorly recovered Quaternary to Pliocene sediments containing planktonic and benthic foraminifers and nannofossils to a depth of 288.4 mbsf. Sediments in the interval 288.4–375.2 mbsf either are barren of microfossils or are of indeterminate age because of poor recovery. Diatoms, radiolarians, and benthic foraminifers recovered at 423.5 mbsf suggest an age of middle to early late Miocene for the overlying washed section. Sediments at 471.6 to 490.7 mbsf comprise lower Oligocene to upper Eocene radiolarians, diatoms, and benthic foraminifers; radiolarians and diatoms are particularly well preserved and abundant through the upper part of this interval, providing a first look at a Paleogene siliceous sequence along the East Greenland Margin. Diatoms are absent with the exception of pyritized forms at 558.1 mbsf. Radiolarians are reduced, but continuous from 490.7 to 558.1 mbsf, and co-occur with sporadic appearances of *Bolboforma*, planktonic and benthic foraminifers. Combined data from 500.3 to 558.1 mbsf indicate middle to upper Eocene sediments. Samples from 548.8 to 587.1 mbsf are barren of microfossils with the exception of agglutinated benthic Eocene foraminifers at 567.7 mbsf. The lower part of the hole has been marred by poor recoveries, but sediments are fossiliferous and, based on agglutinated foraminifers and *Bolboforma*, seem to belong to the middle Eocene, several million years younger than oceanic basement under Site 913. Shipboard magnetostratigraphic studies are inconclusive because of poor recovery and very low NRM intensities.

Measured bulk densities from the glacial marine sediments of this site range from 1.95 to 2.1 g/cm<sup>3</sup>, but decrease to values of 1.8 to 1.45 g/cm<sup>3</sup> as sediments become finely laminated further below and the amount of diatoms present in the sediments increases. Compressional velocities mea-

sured on the sediment from this laminated interval show typical thin-bedded anisotropic behavior (12% compressional-wave anisotropy). Along the bedding planes, the velocities are 1750 m/s. The lowered density in the biosiliceous material relative to the glacial marine sediments may partially explain the increased velocities.

## BACKGROUND AND OBJECTIVES

### Background

As part of the Leg 151 drilling program, a series of sites was proposed along a North-South transect along the East Greenland Margin, mainly to study the history of the East Greenland Current (see Figs. 14 and 15 of "Introduction" chapter and Fig. 1), one of the dominant elements of the Norwegian-Greenland Sea surface current regimes. Except planned Site EGM-4, the sites in this area also are located on relatively old oceanic crust (see Figs. 4 and 17 of "Introduction" chapter, this volume). Penetrating the deeper parts of the sedimentary columns, therefore, would also allow us to describe the depositional environment of the early Norwegian-Greenland Sea, which is only known from the fragments of evidence produced by DSDP Leg 38 (Talwani, Udintsev, et al., 1976) and ODP Leg 104 (Eldholm, Thiede, Taylor, et al., 1987b; 1989b).

The modern East Greenland Current can be traced from Fram Strait (see Fig. 14 of "Introduction" chapter, this volume) until it exits the Denmark Strait on its way to the southern tip of Greenland and the Labrador Sea. Its ice cover (Wadhams, 1986a) is fed by the Siberian and Polar branches of the Transpolar Drift, and its water masses are correspondingly cold and brackish (Johannessen, 1986). The ice cover consists henceforth mainly of pack ice, and the occurrence of icebergs is a rare exception. The East Greenland Current is mostly confined to the shelf regions along East Greenland (Dietrich, 1969) where it is often separated from the coast during the summer by open coastal waters. A particularly interesting feature of the modern satellite imagery is the high turbulence observed along the eastern ice edge and along the frontal boundaries, which are especially well expressed in the region immediately to the South of Fram Strait. The East Greenland Current in its present form is clearly an interglacial phenomenon, and little is known about its glacial-interglacial variability, or about its onset.

When comparing the stratigraphic distribution of the ice-rafted material in North Atlantic Ocean drill sites as an indicator of the onset of Northern Hemisphere glaciation, it is obvious that hitherto the oldest occurrences of such materials have been reported from Site 646 to the South of Greenland (Wolf and Thiede, 1991), whereas reports from sites immediately to the South of the Greenland-Scotland Ridge (Shackleton et al., 1984) and from the Vøring Plateau in the eastern Norwegian Sea (Jansen and Sjøholm, 1991) point to a considerably later onset of ice-rafting alternating with pelagic calcareous and fine-grained terrigenous deposits. Further details are described in the "Introduction" chapter (this volume).

The Paleogene sediments, which were planned to be sampled at Site 913 (proposed Site EGM 2, see Fig. 17 of "Introduction" chapter, this volume), were supposed to provide a key for deciphering the preglacial depositional environment of the Norwegian-Greenland Sea, at a time when this ocean basin did not possess a deep water connection allowing deep water exchange either with the Arctic or the Atlantic oceans. In this context it is interesting to note that, besides subaerial depositional environments that later subsided below sea level (such as on the Greenland-Scotland Ridge or on the Vøring Plateau), all available samples indicate a fully marine Norwegian-Greenland Sea during its early stages of existence. Evidence for the properties of the early Tertiary depositional environments from the surrounding shelf seas and land areas is in part conflicting. The outer continental margins, the Fennoscandian land mass, and maybe also Greenland, experienced important syn-rift uplift that rejuvenated ero-



sion during this time. The then small and narrow Norwegian-Greenland Sea was connected to the North Sea, with its thick sequence of highly variable Paleogene deposits.

The oldest deposits at Site 913 might have been generated under the influence of the intensive volcanism, which is related to the formation of a large province of volcanic rocks associated with the opening of the Norwegian-Greenland Sea, with the ensuing environmental impact thought to be of global significance (Eldholm and Thomas, 1993).

Site 913 is situated on the lower slope off the northeastern part of the East Greenland Margin South of the Greenland Fracture Zone at 75°29'N, 6°59'W. The site was planned in water depths of about 3300 m a few hundred meters above the basin floor, which lies between the 3600- and 3700-m isobaths (Perry, 1986). Limited bathymetric data exist from the shelf and upper slope at this part of the East Greenland Margin because of the ice cover. The East Greenland shelf has water depths between 250 and 350 m, typical for glaciated shelves with shallower banks situated on the outer shelf in water depths between 100 and 200 m. The shelf increases in width from 40 km at 69°30'N and attains its maximum width of 280 km at 77°25'N. A decrease in width again to only 30 km at 81°50'N is observed outside the northeastern tip of Greenland. Dominant geomorphologic features of the East Greenland shelf are the large transverse troughs, called straths, extending out from the shoreline. They are postulated as being erosional scars produced by advancing glaciers coming down from the Greenland ice cap. One of these straths is located just Northwest of the site at 75°40'N, 18°W (Perry, 1986).

The oldest identified magnetic seafloor spreading anomaly in the Norwegian-Greenland Sea is Anomaly 24B (Talwani and Eldholm, 1977), and Site 913 is located on Anomaly 24 crust. A Late Cretaceous-early Tertiary rifting phase affected large parts of the North Atlantic region from the Rockall Trough area, the Labrador-West Greenland, the Norwegian and Northeastern Greenland margins, and the western Barents Sea. The continental breakup was characterized by voluminous transient igneous activity resulting in rifted volcanic passive margins. The final separation of Greenland from Eurasia took place during Chron 24R, and the intensive volcanic activity had abated about 3 m.y. after breakup (Eldholm et al., 1989a; Eldholm, 1991). The margins are characterized by seaward-dipping reflectors, marginal highs, and volcanic flows with dikes and sills into the Mesozoic sedimentary basins bounded on the seaward side by the marginal highs. Figure 2 from Skogseid et al. (1992) shows a transect of the two conjugate margins affected by the Late Cretaceous-early Tertiary extension and magmatism.

According to Eldholm et al. (1989a), Skogseid et al. (1992), and Hinz et al. (1993), a tectono-volcanic zonation can be observed on both the Vøring and the Northeast Greenland conjugate passive margins in the Norwegian Sea (Fig. 3). The volcanic passive margin off Northeast Greenland can be divided into five zones where Zone I is part of the shelf province between the Jan Mayen and Greenland fracture zones. This zone is characterized by a horizon of flood basalt units forming the acoustic basement. A narrow window between 12° and 14°W shows weak indications of faulted and tilted Cretaceous sediments truncated by the rift phase unconformity similar to observations from the Norwegian continental margin. Hinz et al. (1993) suggested that the inner flows mark the beginning of an excessive volcanic episode resulting in the emplacement of the East Greenland plateau basalts immediately prior to breakup and during breakup. Zone II represents the virtually unexplored shelf North of 76°N where aeromagnetic data suggest a Northeast-trending horst and graben relief (Larsen, 1984; 1990). Seismic data (Hinz et al., 1991) confirm this and show a deep rift basin on the inner shelf with high velocity sediments of probable Carboniferous and Permian age. An equivalent of the Cretaceous Vøring Basin has also been suggested by Hinz et al. (1993) North of 76°N just landward of Zone III.

Seaward dipping reflectors have been observed under Zone III, which has been divided into IIIA and IIIB based on the extent of dip-

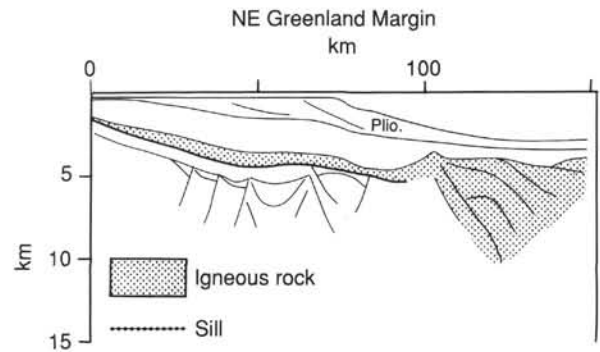


Figure 2. Conjugate margin transect across the region affected by Late Cretaceous-early Tertiary extension and magmatism. Constructed from seismic profiles on the Vøring and Northeast Greenland margins (Skogseid et al., 1992).

ping reflectors and the position of Anomaly 24. Zone IIIA is characterized by seaward dipping reflectors with partly subhorizontal layering landward of the double-peaked Anomaly 24. Where escarpments have been identified, they mark the landward edge of Zone IIIA. By analogy to the Vøring Plateau (Eldholm et al., 1989a), the lavas were probably emplaced in the last phase of rifting and first stage of seafloor spreading.

An outer zone of dipping reflectors, Zone IIIB is characterized by a well-defined smooth reflector, defined as top of the basaltic succession. Locally, short horizons dip seaward, and a pronounced escarpment forms its landward edge. This zone merges into normal oceanic crust, Zone IV, and is associated with magnetic Anomaly 24 North of 75°N (Hinz et al., 1993). Zones IIIA and IIIB represent the increased amount of new igneous material extruded in the last phase of rifting and first phase of seafloor spreading. Results from Site 642 on the Norwegian Margin suggest the continent ocean boundary to be just East of Anomaly 24B (Skogseid and Eldholm, 1989). Site 913 is located on crust dated as Anomaly 24B crust; the site, therefore, should be situated on oceanic crust, but still close to the transition zone.

The seismic line NGT-39/2 where Site 913 is located at shotpoint 1315 (Fig. 4) shows a sedimentary sequence overlying a high-amplitude, smooth, opaque, acoustic basement reflector, in places faulted or draping an underlying rough topography. Toward the landward side the smooth, opaque, seismic horizon shallows up almost to the seafloor and is appearing as a double-peaked basement ridge with a landward facing escarpment. Landward of the escarpment a system of westward-facing, downfaulted or laterally terminating, high-amplitude smooth reflectors occurs. These reflectors are interpreted as volcanic flows extruded into the Mesozoic-lower Tertiary basin analogous to the Vøring Basin.

The large-scale transient volcanic activity associated with breakup and the early drift phase of the North Atlantic margins have had profound environmental influence on the paleoenvironments by changing the oceanographic and atmospheric circulation patterns and compositions.

According to Eldholm and Thomas (1993), the volcanic activity during the Paleocene-Eocene transition was unusually violent with widespread deposition of volcanic ash and bentonite beds. Furthermore, the subaerially created volcanic structures between Greenland and Norway (see Fig. 9 of "Introduction" chapter, this volume) generated a change in basin geometries and restricted circulation and sedimentation probably through the Paleogene.

On the seaward side of the escarpment on seismic lines NGT-39/1 and 2 (Fig. 4), the sediments can be divided into three seismic sequences by two unconformities. The lowermost seismic sequence with low-amplitude, slightly disturbed reflectors appears to gradually onlap acoustic basement toward the escarpment. It is unconformably

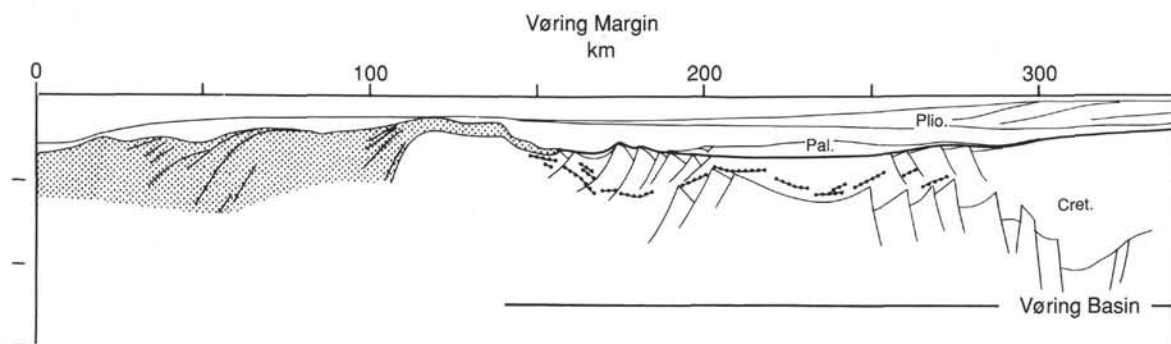


Figure 2 (continued).

overlain by a disturbed sequence of reflectors with a high amplitude and frequency content. The unconformity could either be the UII or UI described by Hinz et al. (1993). The disturbed seismic sequence, however, is most similar to their sequence between the UII and UIII unconformities. They have suggested the two unconformities to be lower and upper Pliocene, respectively, indicating a major hiatus between the lower and middle seismic sequences. The uppermost sequence is characterized by a low-amplitude continuous reflector pattern that downlaps onto the middle unit.

Hinz et al. (1993) interpreted Unconformity UII to represent a drastic change in the paleoceanography and in depositional processes. According to them, the UII truncates the older sediments and erodes deeply into the pre-upper Miocene paleoslope deposits between 74° and 76°N, representing increased water mass exchange through the Fram Strait that coincides with a lowering of eustatic sea level at 4–5 Ma. As a result, strong erosion and buildup of a sedimentary drift and/or contourite layer took place along the East Greenland Margin relating to increased Northern Hemisphere cooling. Furthermore, Hinz et al. (1993) suggest that UIII is representing the onset of the present circulation pattern of southward transport of polar water by the East Greenland Current.

### Scientific Objectives

EGM 2, the northernmost of the EGM sites, was selected to address the following major objectives, besides reaching basement:

1. The history and variability of the early pre-glacial depositional environments of the Norwegian-Greenland Sea when it was young. In the Paleogene, this region consisted of a number of isolated basins, which allowed only shallow water exchange with the world ocean.
2. The transition of the preglacial to the glacial as well as the variability of the early glacial depositional environments during the middle to late Miocene and Pliocene.
3. Dynamics of the glacial and interglacial depositional environments with particular emphasis on the history of the East Greenland Current and the Greenland ice sheet. The latter aspect was the particular target of planned Site EGM 4, which is located on the mouth-trough-fan off Scoresby Sound, one of the world's biggest fjord systems (Frontispiece).
4. Document the long-term history of the East Greenland Current and of deep-water flow out of the Arctic downstream from the Fram Strait.

## OPERATIONS

### Transit to Site 913

The 338-nmi transit to Site 913 required 30.6 hr for an average speed of 11.0 kt. Five course changes were required to avoid the edge

of the pack ice. Ice fields were noted near the location, and the survey course had to be altered twice to avoid ice. A 12-nmi seismic survey was conducted over the site in 1.75 hr at 6.8 kt. A Benthos 210 beacon was dropped at 1012 hr, 14 September. The survey continued for 15 nmi in 2.25 hr at 6.8 kt. The Benthos beacon had a weak signal; therefore, a Datasonics beacon was dropped at 1318 hr.

### Hole 913A

An advanced hydraulic piston corer/extended core barrel (APC/XCB) bottom-hole assembly (BHA) was run. The precision depth recorder (PDR) indicated a water depth of 3337.4 mbrf. Core 151-913A-1H established the water depth as 3330.0 mbrf. Core 151-913A-1H was taken from 0.0 to 4.4 mbsf, with advance by recovery. No cores were oriented because of the high latitude. The formation was unconsolidated silt with abundant large (up to 8 cm) dropstones. The APC core was a partial stroke that was stopped by the dropstones; therefore, the XCB system was used to penetrate further. Cores 151-913A-2X (4.4–9.3 mbsf) penetrated the upper layer of gravel, so the APC system was again used on Core 151-913-3H. Cores 3H through 5H (9.3–26.4 mbsf) recovered 17.18 m (100% recovery), but were all partial strokes (Table 1). The XCB was then run for the remainder of the hole. Cores 151-913A-6X through -13X (26.4–103.6 mbsf) recovered 4.45 m (<6% recovery) (Table 1). The hole was terminated because of the slow penetration rate of the XCB system.

### Hole 913B

An RCB BHA was run for Hole 913B. The water depth is 3330.0 mbrf. Hole 913B was spudded at 0828 hr, 16 September, and was washed down to 86.0 mbsf before coring began (Table 1). Cores 151-913B-1R through -9R were taken from 86.0 to 172.7 mbsf, and recovered 4.37 m (5.0% recovery). Heat-flow measurements were not taken in Hole 913A, but previous work in the area indicated a temperature gradient of about 55°C. Hydrocarbon gas was less than 10 ppm C<sub>1</sub>. Recovery was very poor again in the unconsolidated silt, and many dropstones jammed the core catcher and rotated under the bit, wiping out the fragile core pedestals before they could be caught. Permission was granted by ODP to spot core to 410 mbsf by alternately taking two cores and washing five cores. Approval also was given to core to 850 m total depth (TD) and to eliminate logging in an effort to reach basement.

Spot coring was done from wash Core 151-913B-10W (172.7–204.0 mbsf). The pipe was stuck at 201.0 mbsf when a boulder apparently fell into the hole. The pipe was worked free without drag; therefore, washing resumed to 204.0 mbsf, where the rotary stalled at 800 amps, and pump pressure increased from 200 to 2300 psi at 350 gpm (indicating that the hole caved in). The pipe was pulled up 3 m, where normal pressure and torque were resumed. Washing operations continued from 204.0 to 220.8 mbsf. Core 151-913B-10W recovered 1.16 m of core.

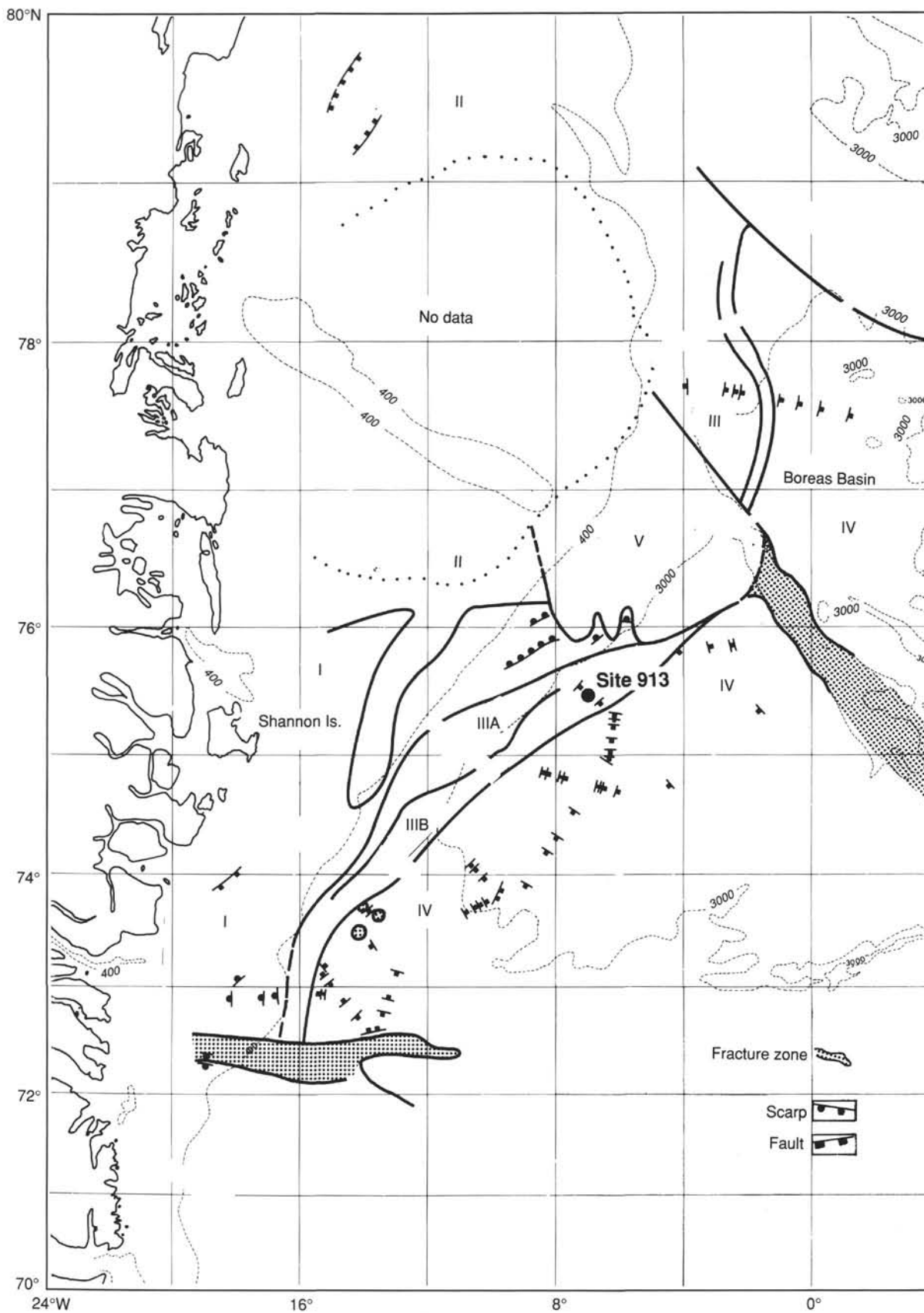


Figure 3. Tectono-volcanic zonation of the Northeast Greenland Margin. Bathymetry in meters (Hinz et al., 1993).

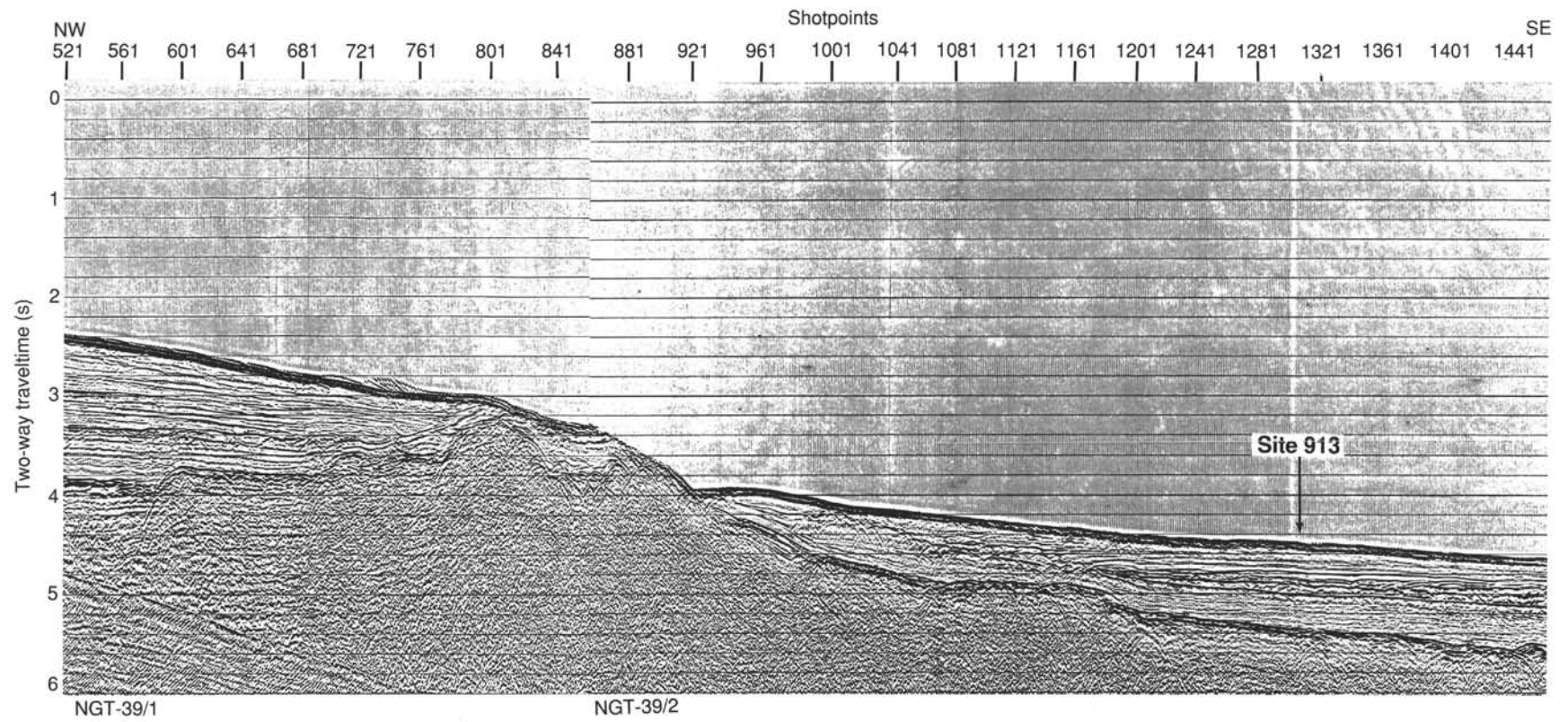


Figure 4. Seismic lines NGT-39/1 and -39/2. Location of Site 913 at shotpoint 1315.

Table 1. Coring summary, Holes 913A and 913B.

Core	Date (Sept. 1993)	Time (UTC)	Depth (mbsf)	Length cored (m)	Length recovered (m)	Recovery (%)
151-913A-						
1H	14	2000	0.0-4.4	4.4	4.36	99.1
2X	14	2110	4.4-9.3	4.9	0.20	4.1
3H	14	2250	9.3-17.6	8.3	8.32	100.2
4H	14	2345	17.6-23.6	6.0	6.01	100.2
5H	15	0105	23.6-26.4	2.8	2.85	102.0
6X	15	0335	26.4-36.1	9.7	0.03	0.3
7X	15	0520	36.1-45.8	9.7	0.87	9.0
8X	15	0740	45.8-55.5	9.7	0.13	1.3
9X	15	1020	55.5-65.1	9.6	1.44	15.0
10X	15	1200	65.1-74.7	9.6	1.58	16.5
11X	15	1305	74.7-84.4	9.7	0.15	1.5
12X	15	1500	84.4-94.0	9.6	0.25	2.6
13X	15	1620	94.0-103.6	9.6	0.00	0.0
Coring totals				103.6	26.19	25.3
151-913B-						
1R	16	1330	86.0-95.6	9.6	0.03	0.3
2R	16	1430	95.6-105.2	9.6	0.08	0.8
3R	16	1525	105.2-114.9	9.7	0.34	3.5
4R	16	1620	114.9-124.5	9.6	0.20	2.1
5R	16	1710	124.5-134.1	9.6	0.15	1.6
6R	16	1820	134.1-143.8	9.7	0.00	0.0
7R	16	1910	143.8-153.4	9.6	1.55	16.1
8R	16	2000	153.4-163.1	9.7	0.86	8.9
9R	16	2055	163.1-172.7	9.6	1.16	12.1
10W	17	0040	172.7-220.8	48.1	1.16	(wash core)
11R	17	0200	220.8-230.4	9.6	0.05	0.5
12R	17	0330	230.4-240.0	9.6	0.15	1.6
13W	17	0700	240.0-288.4	48.4	1.38	(wash core)
14R	17	0825	288.4-298.0	9.6	0.14	1.5
15R	17	1015	298.0-307.7	9.7	0.09	0.9
16W	17	1335	307.7-355.9	48.2	0.00	(wash core)
17R	17	1425	355.9-365.5	9.6	0.00	0.0
18R	17	1545	365.5-375.2	9.7	0.00	0.0
19W	17	2025	375.2-423.5	48.3	7.16	(wash core)
20R	17	2140	423.5-433.1	9.6	4.52	47.1
21R	17	2325	433.1-442.8	9.7	5.82	60.0
22R	18	0105	442.8-452.4	9.6	6.41	66.8
23R	18	0305	452.4-462.0	9.6	1.48	15.4
24R	18	0440	462.0-471.6	9.6	7.15	74.5
25R	18	0600	471.6-481.1	9.5	9.88	104.0
26R	18	0730	481.1-490.7	9.6	9.78	101.9
27R	18	0905	490.7-500.3	9.6	9.09	94.7
28R	18	1045	500.3-509.9	9.6	7.87	82.0
29R	18	1235	509.9-519.5	9.6	7.41	77.2
30R	18	1410	519.5-529.2	9.7	7.22	74.4
31R	18	1535	529.2-538.8	9.6	2.69	28.0
32R	18	1710	538.8-548.4	9.6	7.37	76.8
33R	18	1915	548.4-558.1	9.7	8.79	90.6
34R	18	2050	558.1-567.7	9.6	8.17	85.1
35R	18	2215	567.7-577.4	9.7	9.27	95.6
36R	18	2335	577.4-587.1	9.7	5.85	60.3
37R	19	0200	587.1-596.7	9.6	7.22	75.2
38R	19	0335	596.7-606.4	9.7	7.81	80.5
39R	19	0515	606.4-616.0	9.6	8.75	91.1
40R	19	0705	616.0-625.7	9.7	9.67	99.7
41R	19	0855	625.7-635.4	9.7	5.07	52.3
42R	19	1050	635.4-645.1	9.7	7.05	72.7
43R	19	1230	645.1-654.7	9.6	8.24	85.8
44R	19	1400	654.7-664.4	9.7	6.83	70.4
45R	19	1540	664.4-674.1	9.7	2.24	23.1
46R	19	1710	674.1-683.7	9.6	4.21	43.9
47R	19	1905	683.7-693.0	9.3	4.38	47.1
48R	19	2030	693.0-702.7	9.7	2.32	23.9
49R	19	2200	702.7-712.3	9.6	7.17	74.7
50R	19	2325	712.3-721.9	9.6	5.50	57.3
51R	20	0135	721.9-731.6	9.7	0.23	2.4
52R	20	0310	731.6-741.3	9.7	0.00	0.0
53R	20	0445	741.3-751.0	9.7	0.00	0.0
54R	20	0620	751.0-760.7	9.7	0.00	0.0
55R	20	0945	760.7-770.3	9.6	0.03	0.3
Coring totals				491.3	210.29	42.8
Washing totals				193.0	9.70	
Combined totals				684.3	219.99	32.1

Cores 151-913B-11R through -12R (220.8-240.0 mbsf) recovered 0.20 m. Wash Core 151-913B-13W was taken from 240.0 to 288.4 mbsf, and recovered 1.38 m. Cores 151-913B-14R and -15R were taken from 288.4 to 307.7 mbsf and recovered 0.23 m. Wash Core 151-913B-16W (307.7-355.9 mbsf) and Cores 151-913B-17R and -18R (355.9-375.2 mbsf) did not recover any core. The silty formation was not entering the core barrel; however, a deplunger was

dropped as a precaution. Wash Core 151-913B-19W was taken from 375.2 to 423.5 mbsf, and recovered 7.16 m of core. Gas was negligible, with 20 ppm of C<sub>1</sub> and no C<sub>2</sub>.

ODP gave approval to spot core to 490 mbsf; however, the formation changed from silty mud with dropstones to firm diatom-bearing silty claystone, and from Quaternary to middle Miocene in age. The drilling time and recovery rate both improved. Continuous RCB

Table 2. Summary of lithologic units, Site 913.

Unit	Lithology	Interval, mbsf (thickness, m)	Age	Occurrence (hole-core-section)
IA	Interbedded clay, silt, and sand, and foraminifer clay, biocarbonate-bearing clay, and silty mud. Paucity of dropstones.	0–3.2 (3.2)	Quaternary	913A-1H-1 to 1H-3
IB	Interbedded clayey mud and silty mud with minor gravelly and gravel-bearing layers. Defined by presence of abundant large dropstones of various lithologies.	3.2–143.8 (140.6)	Pliocene to Quaternary	913A-1H-3 to 12X-CC 913B-1R-1 to 6R
II	Predominantly silty clay, clayey silt, and silty mud. Paucity of large dropstones.	143.8–378.7 (234.9)	middle Miocene to Pliocene	913B-7R-1 to 19W-3
IIIA	Interbedded silty clay and clay, massive and laminated. Slightly bioturbated. Mn concretions.	378.7–462.0 (83.3)	late Eocene to middle Miocene	913B-19W-3 to 23R-CC
IIIB	Biosilica-bearing clay, biosiliceous clay to silty clay, clayey and silty siliceous ooze. Layers of dusky to bright greens, blues, and purples.	462.0–500.3 (38.3)	late Eocene to early Oligocene	913B-24R-1 to 27R-CC
IIIC	Laminated and massive clay. Minor silty clay and silty mud. Rare biogenic components.	500.3–674.1 (178.3)	middle Eocene to early Oligocene	913B-28R-1 to 45R-CC
IV	Laminated silty clay and clay, and massive silty clay, clayey mud, silty mud in fining upward sequences. Slump structures.	674.1–770.3 (96.2)	middle Eocene	913B-46R-1 to 55R

Cores 151-913B-20R through -55R were taken from 423.5 to 770.7 mbsf and recovered 205.49 m (59.2% recovery). Recovery was poor below 721.9 mbsf in unconsolidated silt interbedded with some hard carbonate-rich sandstone. Coring was terminated when time ran out. The bit cleared the rotary table at 2030 hr, 20 September, ending Hole 913B (Table 1).

Daily position reports were sent via radio telex to the authorities of the Danish Forsvars Ministeriet in Greenland.

### Transit to Reykjavik

The 871-nmi transit to Reykjavik, Iceland, required 80.5 hr for an average speed of 10.8 kt.

## LITHOSTRATIGRAPHY

### Introduction

The 770.3-m-long sedimentary sequence recovered at Site 913 is divided into four lithologic units (Table 2). They are composed of predominantly siliciclastic sediments that range from clay to gravel. Units are distinguished by differences in texture, biogenic composition, sedimentary structures, and color (Fig. 5, Table 2). The dominant lithologies in the upper 380 m are the coarsest in the sequence and include clayey mud, silty mud, clayey silt, and silty clay with granule- and cobble-sized dropstones. Below this interval, clay and biosilica-bearing clay and biosilica ooze predominate, and in turn are underlain by silty clay, clayey mud, and silty mud. Authigenic components occur throughout the sequence and include carbonate and manganese concretions and, below 490 m, altered sodic micas(?).

#### Lithologic Unit I:

Subunit IA: Sections 151-913A-1H-1 through 151-913A-1H-3, 20 cm (0–3.2 mbsf);  
Thickness: 3.2 m  
Age: Quaternary

Subunit IA at Site 913 is characterized by alternating layers of interbedded clay, silt, and sand, as well as layers of dark grayish brown and olive gray foraminifer clay, biocarbonate-bearing clay, and silty mud. These layers are of decimeter- to meter-scale thickness and

have gradational top and bottom contacts. A single red sandstone dropstone, 1.2 cm in diameter and rounded, occurs in a thin sandy layer at 0.96 mbsf.

The upper interval is massive and contains a few diffuse patches of iron sulfide. Planktonic and benthic foraminifers compose up to 40% of the sediment; nannofossils occur at 0.03 mbsf. Detrital constituents include clay, quartz, and minor amounts of feldspar, accessory minerals, and inorganic carbonate.

The lower boundary of Unit IA is a sharp contact between foraminifers bearing silty mud and the underlying soupy layer of gravel to silt at the top of Unit IB.

Subunit IB: Sections 151-913A-1H-3, 20 cm, through -12X-CC; Sections 151-913B-1R-1 through -6R (3.2–143.8 mbsf)

Thickness: 140.6 m  
Age: Pliocene to Quaternary

This subunit is characterized by very dark gray to dark grayish brown clayey mud and silty mud, containing granule- and pebble-sized dropstones composed of a variety of lithologies (Fig. 6). Clayey mud and mud are homogeneous and contain quartz (20%–40%) and feldspar (5%–15%). Accessory minerals, inorganic carbonate, opaques, and mica are minor constituents. Biogenic components are very rare; molluscan shell fragments occur at 23.41–23.46 mbsf.

Poor recovery in Hole 913A precludes detailed investigation of dropstone distribution. However, the dropstones appear to be dispersed throughout the subunit, and locally there are gravel-bearing to gravelly layers, decimeters to meters in thickness. Cores 151-913A-8X and -11X have less than 5% recovery and contain only pebble-sized dropstones. The size and composition of these dropstones are similar to those observed elsewhere in the subunit, suggesting that they may be either drilling contamination from uphole or were originally part of gravelly sediment from which the finer sediment was washed out during coring. The uppermost part of the subunit in Core 151-913A-1H, 3.2–4.36 mbsf, consists of gravel that grades upward into silt. However, the sediment is soupy and the core liner is only half full, suggesting that the grading was probably generated during core recovery.

Dropstone lithology is diverse and includes a variety of sedimentary (e.g., quartz sandstones and siltstones, limestones), igneous (e.g., gabbros, granites), and metamorphic (e.g., metaquartzites, metagabbros, amphibolites, gneisses, schists) rocks (Table 3). Obvious down-

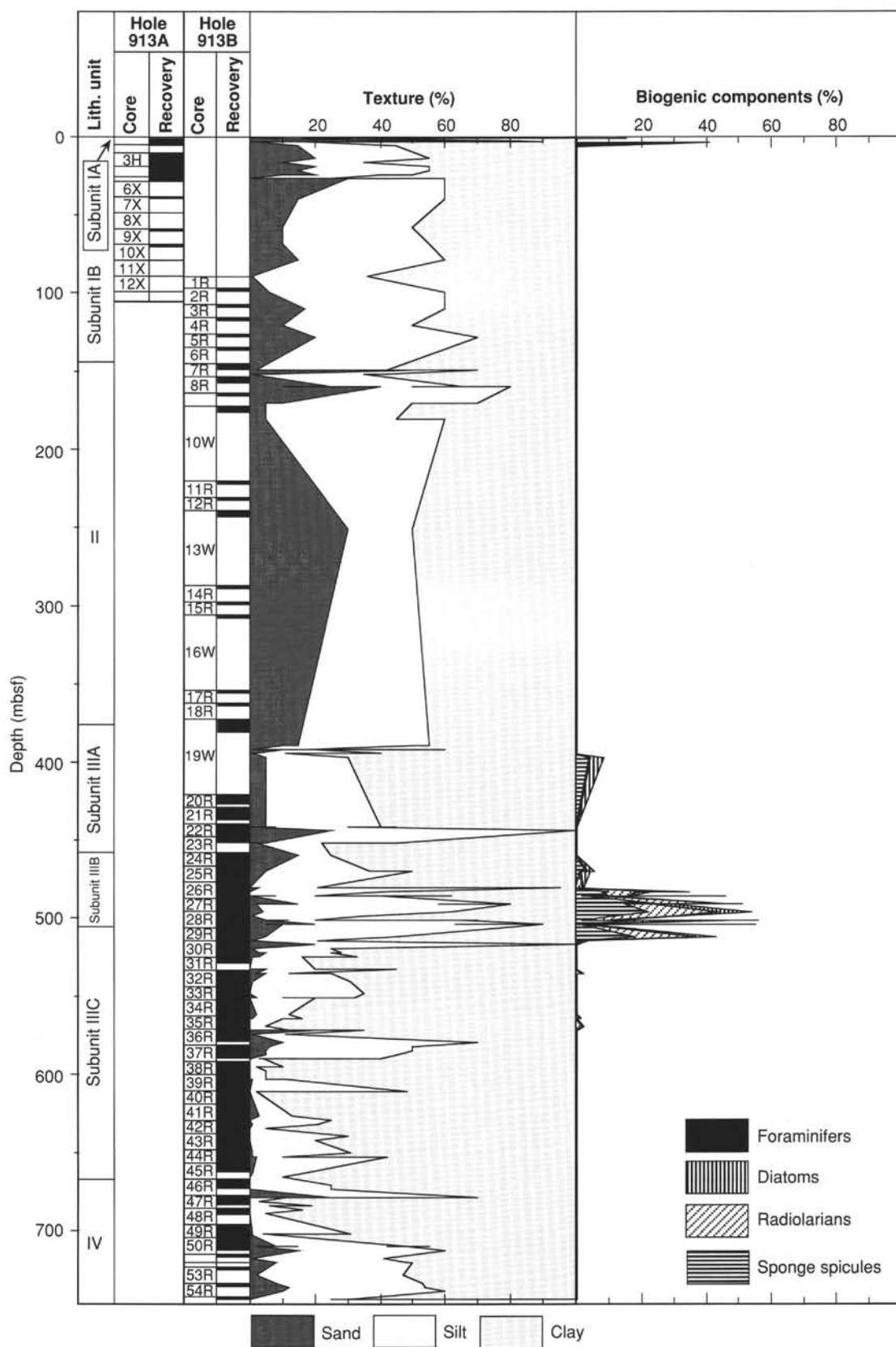


Figure 5. Schematic of lithostratigraphic units showing recovery, texture, and biogenic components.

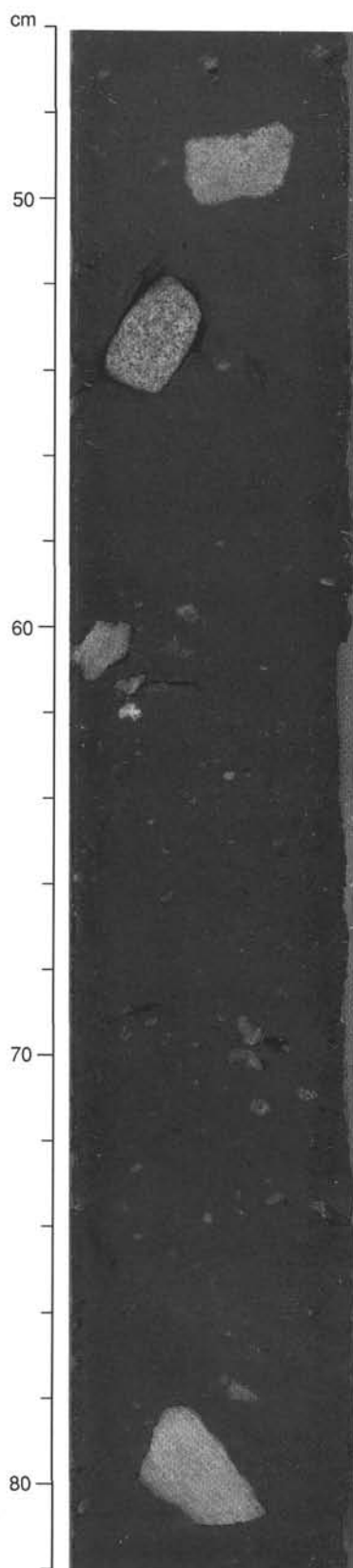


Figure 6. Abundant dropstones of sedimentary and igneous lithologies in black clayey mud. Subunit IB, interval 151-913A-9X-1, 46–82 cm.

Table 3. Occurrence of dropstones ( $\geq 1$  cm size) at Site 913.

Core, section, interval (cm)	Depth (mbsf)	Size (cm)	Lithology
151-913A-			
1H-1, 96	1.0	1.2	Red rounded sandstone
2X-CC, 13	9.2	1.5	Granite
3H-1, 27	9.6	1.9	Angular red quartzite
3H-1, 31	9.6	1.3	Subangular quartz sandstone
3H-1, 75	10.1	2.0	Rounded gray limestone
3H-1, 110	10.4	4.0	Rounded metaquartzite
3H-1, 123	10.5	2.0	Angular orange sandstone
3H-1, 130	10.6	2.3	Subrounded gneiss
3H-2, 26	11.1	1.8	Subangular gray sandstone
3H-2, 26	11.1	1.2	Subangular gray sandstone
3H-2, 33	11.1	1.2	Angular granite
3H-2, 46	11.3	4.4	Rounded light red quartzite
3H-2, 79	11.6	2.2	Rounded gabbro
3H-2, 81	11.6	2.7	Rounded amphibolite
3H-2, 87	11.7	2.2	Subangular gabbro
3H-3, 48	12.8	3.7	Rounded chert
3H-3, 60	12.9	1.8	Subangular red quartzite
3H-3, 66	13.0	1.5	Subangular gray quartz sandstone
3H-3, 117	13.5	1.8	Subangular crystalline rock
3H-4, 20	14.0	5.3	Subrounded gray limestone
3H-4, 32	14.1	1.2	Subangular gneiss
3H-4, 38	14.2	1.2	Angular sandstone
3H-4, 60	14.4	7.0	Angular metagabbro
3H-4, 122	15.0	1.8	Subangular light orange sandstone
3H-4, 138	15.2	1.2	Angular light red sandstone
3H-5, 15	15.5	2.5	Angular biotite schist
3H-5, 22	15.5	1.9	Subangular black limestone
3H-5, 36	15.7	1.6	Rounded black siltstone
3H-5, 77	16.1	2.6	Subrounded granite
3H-5, 100	16.3	2.2	Subrounded quartz sandstone
3H-5, 105	16.4	3.5	Subrounded quartzite
3H-5, 122	16.5	1.8	Angular gabbro
3H-6, 71	17.5	5.0	Subrounded mica schist
3H-6, 79	17.6	2.9	Rounded mica schist
3H-6, 79	17.6	2.0	Subangular quartzite
3H-6, 81	17.6	3.5	Rounded marble
4H-1, 103	18.6	3.0	Limestone
4H-1, 134	18.9	2.0	Limestone
4H-1, 140	19.0	1.7	Granite
4H-1, 147	19.1	1.4	Gneiss
4H-2, 23	19.3	3.5	Limestone
4H-2, 35	19.5	2.6	Amphibolite
4H-2, 39	19.5	2.2	Amphibolite
4H-2, 41	19.5	1.5	Sandstone
4H-2, 55	19.7	1.4	Sandstone
4H-2, 70	19.8	1.2	Shale?
4H-2, 85	20.0	3.3	Quartzite
4H-2, 91	20.0	5.3	Plutonic?
4H-2, 100	20.1	1.2	Amphibolite?
4H-2, 107	20.2	3.7	Gneiss
4H-2, 111	20.2	3.2	Sandstone
4H-2, 119	20.3	1.2	Granite
4H-2, 128	20.4	2.0	Sandstone
4H-2, 133	20.4	1.3	Quartzite
4H-2, 140	20.5	1.2	Schist?
4H-3, 18	20.8	1.2	Siltstone
4H-3, 25	20.9	1.4	Siltstone
4H-3, 28	20.9	3.0	Sandstone
4H-3, 36	21.0	2.5	Sandstone
4H-3, 51	21.1	3.5	Limestone
4H-3, 66	21.3	2.8	Felsic?
4H-3, 72	21.3	1.5	Siltstone
4H-3, 90	21.5	3.5	Calcareous sandstone
4H-3, 119	21.8	2.0	Sandstone
4H-3, 123	21.8	3.7	Amphibole-biotite schist
4H-3, 139	22.0	2.7	Sandstone
4H-3, 144	22.0	4.3	Calcareous sandstone
4H-4, 23	22.3	1.5	Siltstone
4H-4, 24	22.3	1.2	Schist
4H-4, 44	22.5	1.6	Granite
4H-4, 48	22.6	3.5	Amphibolite
4H-4, 60	22.7	1.2	Red sandstone
4H-4, 67	22.8	1.5	Granite
4H-4, 70	22.8	1.2	Schist
4H-4, 86	23.0	2.0	Bryozoan limestone
4H-4, 93	23.0	2.0	Amphibolite
4H-4, 99	23.1	1.5	Sandstone
4H-CC, 7	23.3	3.5	Gray sandstone
4H-CC, 26	23.5	1.3	Granite
5H-1, 13	23.7	1.6	Amphibolite
5H-1, 15	23.8	2.6	Amphibolite
5H-1, 39	24.0	2.0	Sheared quartzite
5H-1, 45	24.1	2.0	Quartzite
5H-1, 47	24.1	2.3	Schist
5H-1, 49	24.1	1.9	Quartzite
5H-1, 53	24.1	1.8	Red sandstone
5H-1, 55	24.2	4.2	Amphibolite
5H-1, 64	24.2	4.0	Amphibolite

Table 3 (continued).

Core, section, interval (cm)	Depth (mbsf)	Size (cm)	Lithology	Core, section, interval (cm)	Depth (mbsf)	Size (cm)	Lithology
5H-1, 70	24.3	5.0	Granodiorite	10X-1, 92	66.0	1.5	Siltstone
5H-1, 83	24.4	2.7	Gneiss	10X-1, 108	66.2	2.0	Quartzitic
5H-1, 100	24.6	1.3	Sandstone	10X-CC, 4	66.2	1.0	Red sandstone
5H-1, 103	24.6	2.7	Amphibolite	10X-CC, 8	66.3	4.5	Black siltstone
5H-1, 107	24.7	4.0	Quartzite	10X-CC, 9	66.3	1.5	Black siltstone
5H-1, 114	24.7	3.4	Gneiss	10X-CC, 15	66.3	1.5	Sandstone
5H-1, 124	24.8	3.9	Amphibolite	10X-CC, 22	66.4	1.5	Metamorphic
5H-1, 126	24.9	2.2	Amphibolite	10X-CC, 30	66.5	1.0	Schist
5H-1, 131	24.9	1.9	Quartzite	10X-CC, 33	66.5	1.0	Sandstone
5H-1, 134	24.9	3.0	Siltstone	10X-CC, 41	66.2	1.5	Metamorphic
5H-1, 141	25.0	2.0	Mafic plutonic	10X-CC, 45	66.6	2.5	Black metamorphic
5H-2, 2	25.1	1.9	Granite pegmatite	11X-CC, 7	74.8	7.5	Metamorphic (migmatic)
5H-2, 48	25.6	2.0	Metamorphic	12X-CC, 4	84.4	5.0	Subangular quartzite
5H-2, 50	25.6	1.6	Quartzite	12X-CC, 7	84.5	3.5	Subangular quartzite
5H-2, 51	25.6	1.2	Sandstone	12X-CC, 7	84.5	4.5	Shale
5H-2, 52	25.6	4.3	Quartzite	12X-CC, 9	84.5	4.0	Siltstone
5H-2, 53	25.6	2.2	Gabbro	12X-CC, 11	84.5	4.5	Subrounded gneiss
5H-3, 1	25.7	1.9	Granite pegmatite	12X-CC, 15	84.6	6.0	Sandstone
5H-3, 11	25.8	2.6	Quartzite	12X-CC, 20	84.6	6.0	Gneiss
5H-3, 21	25.9	3.7	Quartzite	151-913B-			
5H-3, 28	26.0	4.8	Sandstone?	1R-CC, 0	86.0	4.5	Rounded quartzite
5H-3, 35	26.0	4.0	Metamorphic	3R-1, 0	105.2	5.0	Gneissic schist subangular
5H-3, 36	26.1	2.0	Quartzite	3R-1, 1	105.2	2.5	Quartzite subangular
5H-CC, 2	26.1	1.4	Sandstone	3R-1, 7	105.3	4.0	Green sandstone subangular
5H-CC, 4	26.2	4.0	Quartzite	3R-1, 13	105.3	1.0	Siltstone slate-like
5H-CC, 18	26.3	2.5	Andesite	3R-1, 13	105.3	6.0	Mica schist subrounded
7X-1, 4	36.1	2.5	Subrounded amphibolite	3R-1, 28	105.5	3.0	Amphibolite
7X-1, 5	36.2	2.0	Subangular amphibolite	4R-CC, 0	114.9	1.0	Quartzite rounded
7X-1, 5	36.2	2.0	Angular amphibolite	4R-CC, 2	114.9	2.0	Granitic rock subangular
7X-1, 6	36.2	2.5	Subangular schist	4R-CC, 6	115.0	6.5	Quartzite subangular
7X-1, 13	36.2	7.0	Rounded sandstone	4R-CC, 12	115.0	9.0	Diorite?
7X-1, 19	36.1	3.0	Amphibolite	5R-CC, 2	124.5	1.0	Igneous pegmatite
7X-CC, 2	36.7	1.5	Amphibolite	5R-CC, 3	124.5	1.5	White quartzite
7X-CC, 12	36.8	2.5	Subangular sandstone	5R-CC, 5	124.6	1.5	Pink quartzite
7X-CC, 21	36.9	4.5	Subrounded quartzite	5R-CC, 6	124.6	1.2	White quartzite
7X-CC, 23	36.9	5.0	Subrounded quartzite	8R-1, 1	153.4	1.0	Amphibolite
9X-1, 9	55.6	4.0	Dark pink subrounded sedimentary	12R-CC, 0	230.4	8.2	Black sheared metamorphic
9X-1, 40	55.9	1.0	Subangular igneous	13W-1, 20	240.2	1.3	Subangular quartz
9X-1, 48	56.0	2.8	Pink subrounded sedimentary	13W-1, 83	240.8	1.5	Angular layered sandstone
9X-1, 52	56.0	2.6	Subrounded igneous	13W-1, 115	241.2	1.0	Angular gneiss
9X-1, 60	56.1	1.6	Subrounded igneous	13W-1, 121	241.2	4.1	Rounded gabbro
9X-1, 78	56.3	3.3	Subangular igneous	13W-CC, 0	241.3	8.1	Rounded gray gneiss
9X-1, 97	56.5	1.9	Yellow-brown subangular sedimentary	13W-CC, 0	241.3	5.2	Rounded green metagabbro
9X-1, 121	56.7	1.7	Light and dark green angular igneous	13W-CC, 0	241.3	4.1	Rounded green metagabbro
10X-1, 7	65.2	4.5	Red sandstone	13W-CC, 0	241.3	3.8	Angular black amphibolite
10X-1, 15	65.3	6.0	Red sandstone	13W-CC, 0	241.3	1.8	Angular pink gneiss
10X-1, 26	65.4	1.0	White siltstone	13W-CC, 0	241.3	1.0	Angular pink gneiss
10X-1, 32	65.4	1.0	Black siltstone	14R-CC, 0	288.4	8.0	Gneiss
10X-1, 35	65.5	1.0	Black siltstone	14R-CC, 10	288.5	6.0	Gneiss
10X-1, 38	65.5	1.5	Red sandstone	15R-CC, 0	298.0	6.5	Granite
10X-1, 38	65.5	1.0	Red sandstone	19W-2, 20	376.9	1.5	Sandstone
10X-1, 59	65.7	1.5	Metamorphic	23R-1, 79	453.2	1.2	Quartzite?
10X-1, 83	65.9	1.0	Black slate				

hole trends in lithology and grain diameter are lacking in this subunit (Fig. 5). Dropstones are subspherical to tabular, and range from angular to well rounded, but are predominantly rounded. There is no obvious correlation between lithology, roundness, and shape.

The abundance of large dropstones (Figs. 7 and 8) ranges from 4 to 28 per meter and averages 15 per meter, based on data normalized for recovery. Cores that recovered only a few pebble-sized dropstones and no other sediment were not included in the analyzed data. Peak values occur in Cores 151-913A-12X (84.4–94.0 mbsf) and 151-913B-5R (124.5–134.1 mbsf).

#### Lithologic Unit II:

Sections 151-913B-7R-1, 0 cm, through -19W-3, 50 cm (143.8–378.7 mbsf)

Thickness: 234.9 m

Age: middle Miocene(?) to Pliocene

This unit is characterized by the paucity of dropstones  $\geq 1$  cm in diameter and the predominance of silty clay to clayey silt and silty mud. Determination of unit boundaries is problematic because of the poor recovery in the upper and lower parts of Hole 913B. The top boundary of this unit is placed at the top of Core 151-913B-7R, below

which only a few large dropstones occur. The lower boundary of Unit II is placed at the lowest occurrence of beds of clayey, silty, and sandy muds (Core 151-913B-19W, 50 cm; 378.7 mbsf). This boundary is poorly defined, as Cores 913B-16W to-18R had no recovery and Core 151-913B-19W is a wash core.

The major lithologies of silty clay to clayey silt and silty mud are typically very dark gray and homogeneous. Locally they have thin and medium color bands of brown, dark greenish gray, and black. The main nonclay components are quartz (20%–50%) and feldspar (10%–25%); minor constituents include accessory minerals and opaques.

Minor lithologies of dark olive gray and very dark gray sandy mud, and dark grayish brown sandy silt occur as thin beds. They are typically homogeneous, but an interval of sandy mud in Core 151-913B-7R is graded with a gradational top contact and a sharp base.

Although large dropstones are rare from 143.8 to 220.8 mbsf, a gravel-bearing silty mud layer occurs from 163.4 to 163.5 mbsf (Core 151-913B-9R, 30–38 cm). The top contact is sharp, and the bottom contact is gradational. The layer contains poorly sorted, subangular to rounded granules and pebbles, up to 9 mm in diameter, composed of a variety of lithologies.

The interval 220.8–423.5 mbsf (Cores 151-913B-11R through -19W) is difficult to characterize because recovery was 0%–2% (ex-

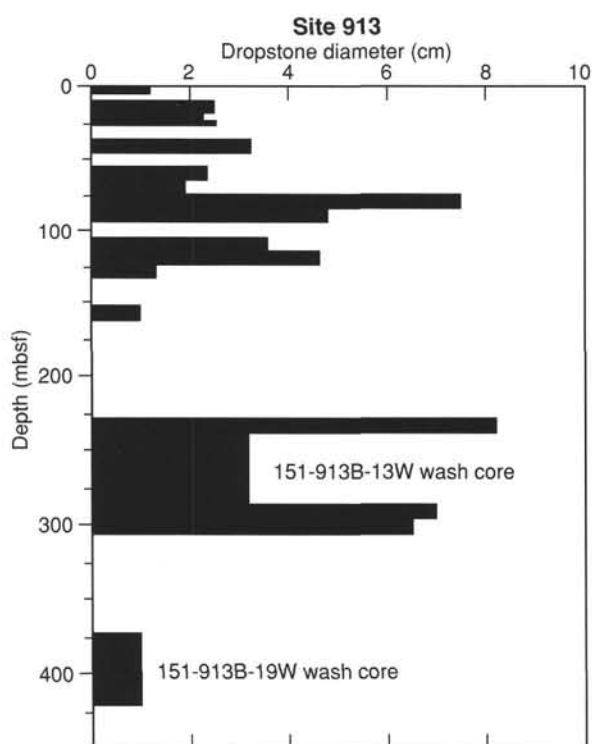


Figure 7. Average size of dropstones ( $\geq 1$  cm size) per core.

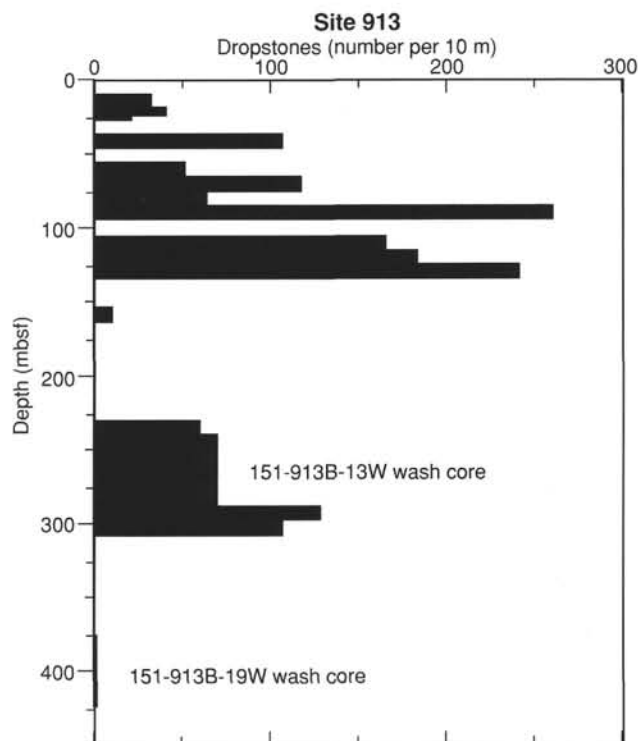


Figure 8. Number of dropstones per 10 m of section (normalized for recovery).

cluding the wash core). It contains large dropstones that are interpreted to be drilling contamination. The variety of lithologies, size, roundness, and shape are similar to those observed for dropstones in Subunit IB. Although Cores 13W and 19W are wash cores, they provide some indication of the sediment composing this interval. Clayey and sandy muds are the dominant lithologies and contain color bands of very dark gray to dark greenish gray, cm in thickness. Laminated, very dark gray clay layers occur locally. Some clay layers have sharp lower contacts and grade upward into sandy mud. The major silt and sand-sized grains in clayey and sandy muds are quartz and accessory minerals. Minor components include feldspars, micas, and opaques.

#### Lithologic Unit III:

Subunit IIIA: Sections 151-913B-19W-3, 50 cm, through -23R-CC (378.7–462.0 mbsf)

Thickness: 83.3 m

Age: early Oligocene/late Eocene to middle Miocene/Pliocene(?)

This subunit is distinguished by the predominance of interbedded silty clay and clay. These slightly bioturbated layers are of centimeter to decimeter scale and have both gradational and sharp boundaries. Dark gray to dark greenish gray silty clay is the dominant lithology. It is commonly massive and mottled but is locally laminated. Quartz and feldspar are the main silt- and sand-sized components. Olive gray and very dark gray clay occurs irregularly throughout the subunit and is typically laminated. Wavy laminae in both lithologies are olive gray, dark greenish gray, dark grayish brown and very dark gray, and may be continuous or discontinuous. Laminae of very dark gray and dark greenish gray sandy mud, 1–5 mm in thickness, are interbedded with silty clay and clay in Core 20R. Light gray silty burrows, up to centimeter-sized, and agglutinated foraminifers are scattered throughout the subunit. A single quartz pebble was found at 453.16 mbsf but may be drilling contamination.

Different authigenic constituents in silty clay and clay were observed on the split core surfaces and in smear slides. Two manganese concretions, 10 cm in thickness, occur at 378.4 and 444.51 mbsf (Fig. 9). The upper concretion is dark brown at the top and grades downward to yellowish brown, whereas the lower one is dark grayish brown. Both concretions have Liesegang rings and sharp upper and gradational lower contacts. Clay- and silt-sized, altered sodic micas(?) appear to be locally abundant in silty clay and clay.

The lower boundary of Subunit IIIA is placed at the lowest occurrence of poorly fossiliferous silty clay and clay.

Subunit IIIB: Sections 151-913B-24R-1, 0 cm, through -27R-CC, 13 cm (462.0–500.3 mbsf)

Thickness: 38.3 m

Age: late Eocene to early Oligocene

Subunit IIIB is characterized by biosilica-bearing clay, biosiliceous clay to silty clay, clayey siliceous ooze and silty siliceous ooze. These lithologies occur in layers of various dusky to bright green, blue, and purple hues that lend a distinctive appearance to this subunit. They may be either laminated and mottled, and have slight to moderate bioturbation. Biogenic components are diatoms, radiolarians, sponge spicules, and silicoflagellates. Detrital components include quartz, volcanic glass, opaques, and accessory minerals. Clay- and silt-sized, altered sodic micas(?) grains are abundant.

Clayey siliceous ooze is generally composed of wavy laminae of various green hues, ranging from pale green to dark greenish gray, and laminae of dark gray to greenish black (Fig. 10). This lithology also occurs in laminated layers, 25–55 cm thick, of variegated grayish blue, pale purple, grayish purple, as well as in a few thin bands of dusky purple and bright azure blue (Fig. 11). These layers are locally faulted. The other biosilica-bearing and biosiliceous sediments tend to be muted colors, ranging from greenish gray to dark gray. Burrows are dark colored and parallel to bedding. Silt laminae, <3 mm thick,

are interbedded with the above lithologies. Rare constituents include dropstones, <1 cm in diameter, at 481.1–490.7 mbsf (Core 151-913B-26R) and a thin ash layer at 463.9 mbsf (Core 151-913B-24R-2, 43 cm).

The basal boundary of Subunit IIIB occurs at the lowest occurrence of abundant biosilica and the first thick layers of clay.

Subunit IIIC: Sections 151-913B-28R-1 through -45R-CC (500.3–674.1 mbsf)

Thickness: 173.8 m

Age: middle Eocene to early Oligocene

This subunit is characterized by grayish olive green to dark greenish gray and dark gray to very dark gray clays. These clays consist of alternating fissile, laminated layers and massive layers, centimeters to decimeters in thickness. The top and bottom contacts of these layers are gradational.

Laminated clays are dusky yellowish green, grayish olive green, and greenish black. Laminae are wavy and discontinuous but are locally planar and continuous. Burrowing is slight to moderate and includes *Zoophycos*, *Chondrites*, and *Planolites*. A few of the thicker laminae, light gray to grayish green, are graded with bioturbated tops and sharp bases.

In both laminated and massive clays, quartz, opaques, and accessory minerals are the main silt- and sand-sized components. Altered sodic micas(?) are the main clay-sized component. Rare biogenic components are agglutinated benthic foraminifers, diatoms, radiolarians, sponge spicules, and molluscan shell fragments.

Laminae of grayish brown to very dark gray silty clay and silty mud occur below 665 mbsf. Laminated silty clay increases in abundance and thickness downward to the base of the subunit, becoming interbedded with homogeneous, very dark gray clay.

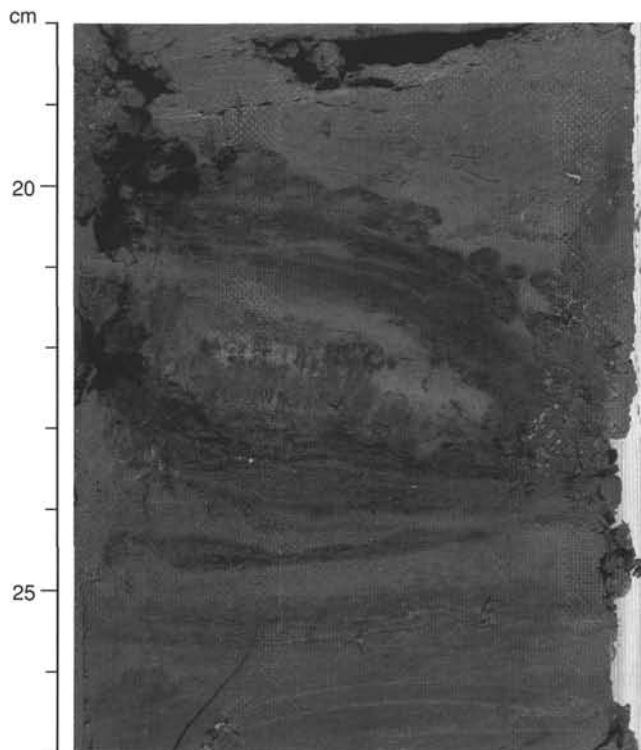


Figure 9. Laminated, dark gray silty clay containing a manganese concretion of dark grayish brown and dark greenish gray. Top contact of concretion is sharp. Subunit IIIA, interval 151-913B-22R-2, 18–27 cm.

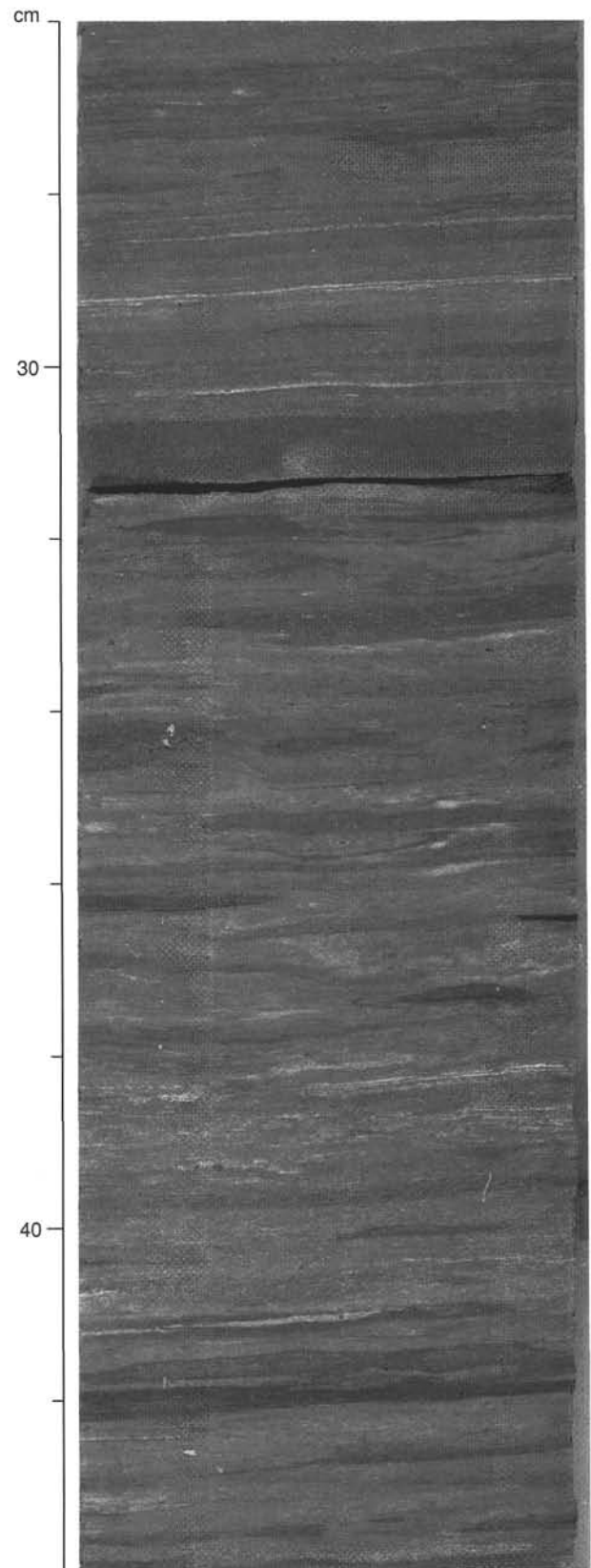


Figure 10. Biosiliceous clay composed of bioturbated laminae of pale green to dark greenish gray and dark gray to greenish black. Subunit IIIB, interval 151-913B-27R-3, 26–44 cm.

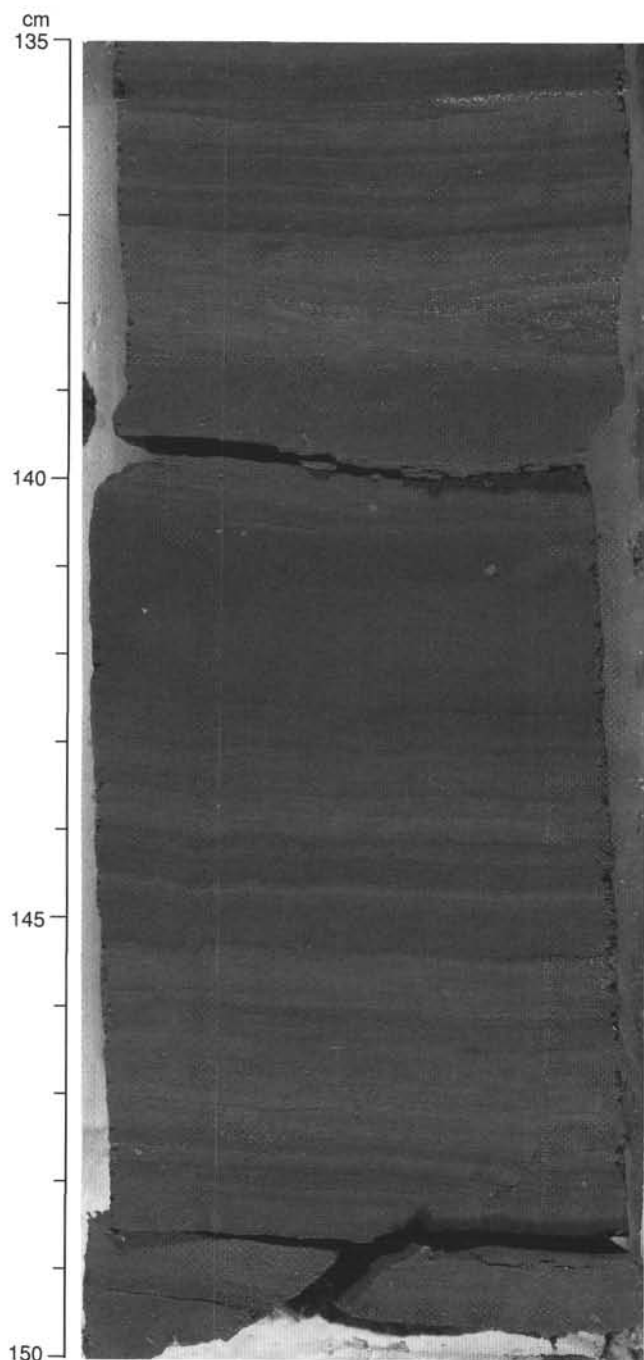


Figure 11. Laminated, biosilica-bearing silty clay, grayish brown (135–140 cm) and grayish blue (140–150 cm). Small faults and folds occur at 146 cm and 148 cm. Subunit IIIB, interval 151-913B-24R-4, 135–150 cm.

Light gray to dark yellowish brown carbonate clay and carbonate concretions of centimeter-scale thickness are present sporadically throughout the subunit (Fig. 12). They are massive to moderately bioturbated and have abruptly gradational or sharp top and bottom contacts. *Bolboforma* occurs scattered through some of these layers and makes up light gray to dark yellow orange *Bolboforma* ooze in centimeter-thick beds. Coarse barite crystals were recovered from these layers in Core 151-913B-38R and -39R (596.7–616.0 mbsf), and rhodochrosite was identified by preliminary X-ray diffraction data.

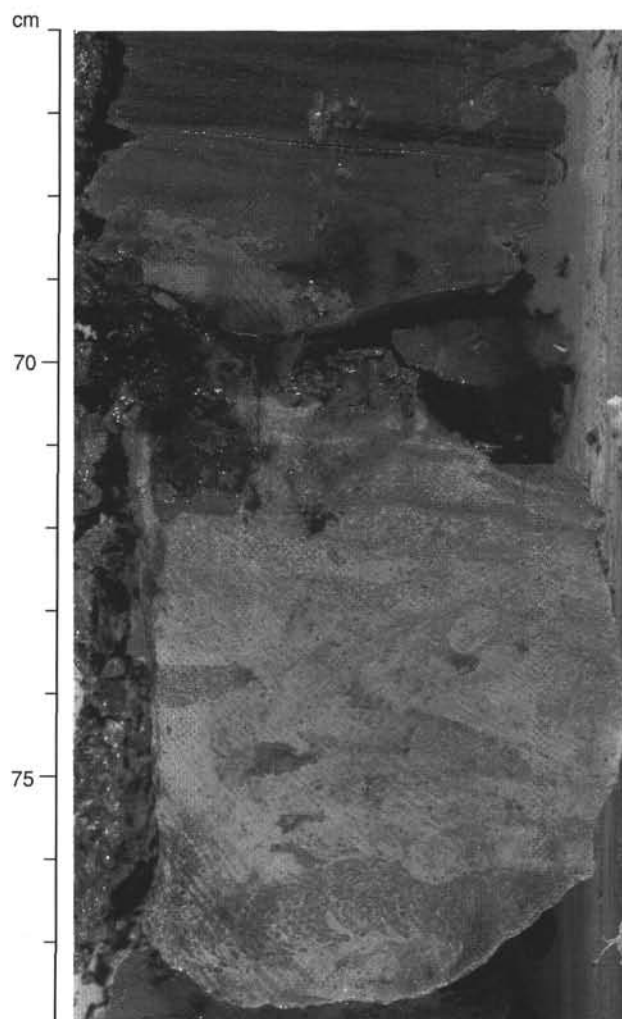


Figure 12. Laminated, grayish olive green clay (66–70 cm) and pale olive gray carbonate concretions (70–78 cm) with unpacted burrows. Pelleted *Zoophycos* occurs in the concretion at 76–77 cm. Subunit IIIC, interval 151-913B-32R-2, 66–78 cm.

The lower boundary of Subunit IIIC is placed at 674.1 mbsf at the lowest occurrence of clay as the major lithology.

#### **Lithologic Unit IV:**

Section 151-913B-46R-1 through -55R (674.1–770.3 mbsf)  
Thickness: 96.2 m  
Age: middle Eocene

The lowermost unit is characterized by alternating layers of laminated silty clay and clay and massive silty clay, silty mud, and sandy mud beds, decimeters in thickness. Laminated silty clay and clay consist of wavy laminae of olive gray to dark greenish gray and grayish brown to black. Bioturbation is slight to moderate. In contrast, massive layers are very dark gray and lack bioturbation. Isolated layers are commonly silty and sandy mud, which may be laminated, grading upward into silty clay and clay. Elongated green clay clasts, centimeter-sized, in silty mud locally decrease upward in size within single layers. Coal fragments, millimeter- to centimeter-sized, are scattered throughout the massive layers below 702 mbsf. In both laminated and massive layers, silt- and sand-sized grains include quartz, accessory

minerals, opaques, feldspar, and inorganic carbonate. *Bolboforma* occurs locally in olive gray, silty clay layers.

In Cores 151-913B-49R and -50R (702.7–721.9 mbsf), massive and laminated layers compose fining-upward packages that have sharp bases. A complete package appears to consist of the following centimeter- to decimeter-thick layers, from bottom to top: (1) massive or faintly laminated, very dark gray clayey mud; (2) laminated, very dark gray and green clay; (3) black clay; and (4) a cap of olive gray, carbonate clay.

Slump structures occur in very dark gray silty clay and silty mud in Cores 151-913-48R to -50R (693.0–721.9 mbsf). They have distorted laminae and laminated clay clasts of dark grayish green and black. Irregular patches of light yellowish-brown carbonate clay, centimeter-sized, are rare. Pyritized burrows and irregularly shaped pyrite concretions occur locally, particularly in coal-rich layers.

The lithology of the lowermost interval, 721.9–760.73 mbsf, is poorly known because of poor core recovery. Core 151-913B-51R (721.9–731.6 mbsf) is a 23-cm-thick plug of very dark gray, calcareous sandstone underlain by calcareous siltstone. These lithologies are well indurated and similar in texture to the silty and sandy mud in the overlying cores.

### Interpretation

In the lowest part of Unit IV, the coarse-grained, poorly sorted, graded beds with large clay clasts and coal, as well as laminations throughout, suggest rapidly deposited sediment gravity flows and proximity to land. The large clay clasts argue against long-distance transport or very high energy flows; deposition from a mud flow, debris flow or turbidity current is more likely. In contrast, the silt laminations are more typical of Bouma B or channel-levee deposition, both of which are possible in this depositional environment. The compositional relationship between the coarse clasts and the silt laminae is not clear enough to determine genetic relationships.

The finer sediments and color laminations may reflect less energetic deposition. Their increased abundance upsection, and the thinning of the coarser units, could be caused by one or more of the following: (1) a change in the sediment source, (2) relocation of the depocenter, and (3) rise in sea level.

The silty clay and clay composing Unit III are interpreted to be hemipelagic sediments delivered to the site primarily by relatively low-energy currents and by eolian transport.

The clays that characterize Subunit IIIC most likely represent a transition to deposition of fine particles from suspension. Variable, generally light bioturbation indicates sub-oxic bottom waters and/or limited organic-carbon supply. The absence of planktonic microfossils may indicate dissolution of calcium carbonate and amorphous silica. In addition, a tectonically restricted basin, stratified water column, and little exchange with nutrient-rich deep waters outside the basin all may have played a role in restricting productivity. Although clay-particle dominance might be caused by any of the possibilities mentioned for the finer parts of Unit IV, the complete lack of coarse sediments suggests that a tectonic barrier may have existed, a barrier that was gradually emplaced during the deposition of Unit IV.

A notable increase in surface productivity is documented in the transition to Subunit IIIB. An enhanced supply of nutrients would account for the observed biosilica-rich sediments. Oxidation at depth of the organic matter associated with surface productivity may have tipped the balance toward less oxic conditions, resulting in the absence of benthic activity and the preservation of fine laminations. The marked color contrasts that occur throughout the subunit are likely linked to variations in chemical and/or mineralogical composition. Their formation and preservation attest to subtle changes in sediment, pore water, or diagenetic processes, within a generally stable hydrography.

Subunit IIIA is interpreted to reflect diminished productivity as evidenced particularly by biosilica-poor sediments. The lack of cal-

careous microfossils also may be related to dissolution of calcite. Corrosive bottom and pore waters also are consistent with the common occurrence of agglutinated benthic foraminifers only.

The increase in grain size to silty clays, and the preponderance of mottled, burrowed, and otherwise bioturbated sediment may reflect a variable and episodically energetic circulation. Dark, massive-bedded sediments may be related to increased terrigenous input to this site, and possibly to the basin in general. Enhanced circulation may have delivered relatively coarser sediment to this somewhat distal site, and it may be that erosion of the surrounding source areas began to increase.

The boundary between Units II and III represents a change from primarily nonglacial to glacial deposition. Interpretation of Unit II is problematic because of the poor core recovery. Recovered sediments are very similar in composition and texture to terrigenous sediments of Unit I. Unit II differs from Subunit IB, by the paucity of dropstones, and from Subunit IA, by the lack of biogenic components. The lack of dropstones suggests little ice-rafting activity in this area during the middle Miocene to Pliocene.

In contrast, the abundant dropstones of diverse lithologies in Subunit IB are interpreted to have been deposited primarily from melting icebergs indicative of intensified glacial conditions. Several explanations are possible for the high abundance of dropstones (up to 28 per meter). Possibly, the East Greenland Current or precursory currents were major iceberg trajectories during the late Pliocene to Quaternary. Alternatively, a weaker East Greenland Current may have permitted icebergs to stay in the Greenland Sea for longer times during the glacial periods, and the enhanced mechanical weathering would allow the abundant dropstones to be produced and then collected in this area.

No interglacial/glacial sedimentological differences are evident in Subunit IB, although this, too, could be an artifact of recovery. Subunit IA also does not contain clear glacial/interglacial sections and lacks dropstones. The presence of planktonic foraminifers, however, indicates the only favorable conditions for their production and preservation in the entire recovered section.

## BIOSTRATIGRAPHY

### Introduction

Poor recovery severely hampered the late Neogene and Quaternary paleoceanographic objectives of Site 913. However, an excellent middle Eocene to lower Oligocene/upper Eocene record was obtained below 462.0 mbsf in Core 151-913B-24R, as well as a middle Miocene siliceous sequence in wash Core 151-913B-19W.

Stratigraphic control on the upper 450 m of sediment is minimal (Fig. 13). The upper Quaternary is represented by calcareous nannofossils and planktonic foraminifers in Hole 913A. Diatoms and ebridians were used to date the middle Miocene interval recovered in Core 151-913B-19W. Middle Eocene to lower lower Oligocene/upper Eocene sediments were dated by occurrences of diatoms, silicoflagellates, ebridians, radiolarians, benthic foraminifers, dinoflagellates, and *Bolboforma*. There was little recovery and no biostratigraphic control in the lower 50 m of the section, which ended in a lithified siltstone with Core 151-913B-55R.

### Diatoms

Core-catcher and shipboard samples from Hole 913A, and all samples from Hole 913B down to Core 151-913B-18R are barren of diatoms. Core 151-913B-19W is a wash core; however, it includes short, relatively undisturbed sedimentary sequences with diatoms. The exact depth below seafloor of Core 151-913B-19W is not well constrained. The possible depth of this 7.16-m section ranges from 375.2 mbsf to 423.5 mbsf. Sample 151-913B-19W-CC contains abundant but severely fragmented diatoms. The diatom assemblage

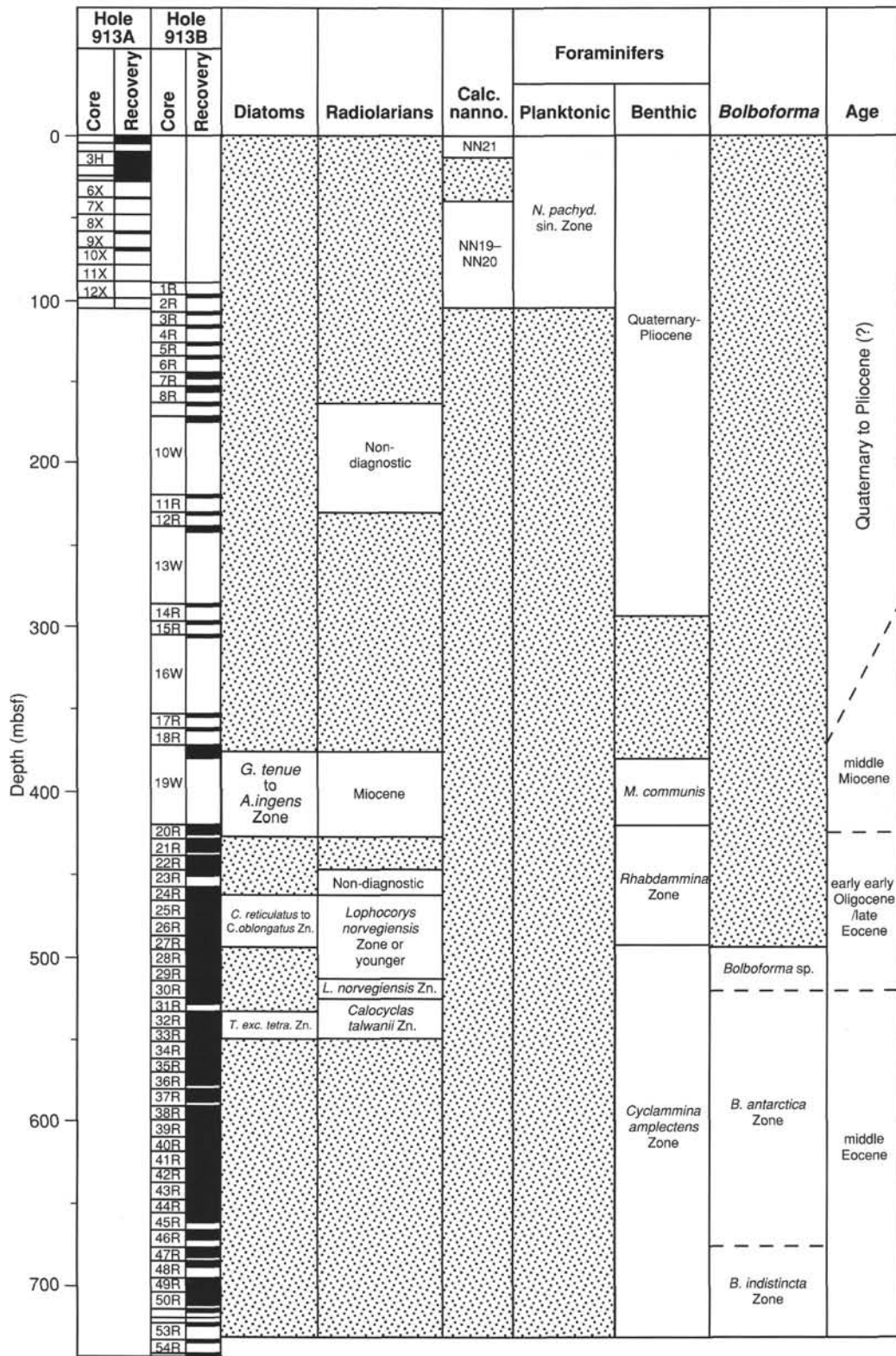


Figure 13. Summary of biostratigraphy of Site 913.

contains few specimens of *Actinocyclus ingens*, *Coscinodiscus plicatus*, and *Stephanogonia hanzawae*, suggesting the upper middle Miocene *G. tenue* to *A. ingens* zones of Schrader and Fenner (1976).

Core-catcher and shipboard samples from Cores 151-913B-20R to -23R are barren of diatoms. Samples 151-913B-24R-CC through -27R-5, 75 cm, contain abundant diatoms, particularly in the finely laminated sections of these cores. Samples from Core 151-913B-24R contain an unusually high abundance of radiolarians relative to diatoms. Cores 151-913B-26R and -27R are diatomites with reduced numbers of radiolarians and silicoflagellates, and diatom-rich layers occur down to Core 29R (519.5 mbsf). The diatom assemblages in these cores include many species characteristic of the upper Eocene diatom assemblage of DSDP Leg 38, as described by Schrader and Fenner (1976) and Dzinoridze et al. (1978), although there are some differences.

Samples from this interval include *Asterolampra insignis*, *Hemaulus polycystinorum*, *H. polymorphus*, *Monobrachia unicornuta*, *Actinopticus* sp. (triangular), *Riedelia claviger*, *Stictodiscus kittonianus*, *Trococira trochlea*, *Coscinodiscus monicae*, *Cymatosira* sp. 1 of Schrader and Fenner (1976), and *Macrora barbadensis*, among numerous others, which suggest the upper Eocene *Craspedodiscus oblongus* Zone of Schrader and Fenner (1976) and Dzinoridze et al. (1978). However, several taxa that characterize this zone are conspicuously absent. These include *C. oblongus*, and most surprisingly, *Triceratium barbadense*, which ranges through the upper Eocene and dominates the Eocene diatom assemblages of Leg 38 in certain intervals. The absence of these taxa suggests that the diatom assemblage represented in Cores 151-913B-24R through -29R may be younger than the Eocene assemblages recovered during Leg 38.

A younger age also is supported by the occurrence of *A. schmidtii*, *Xanthopyxis panduraeformis*, *Cestodiscus* sp. 9 of Baldauf and Monjanel (1989), and *Thalassiosira* sp. aff. *T. irregularata* sensu Baldauf and Monjanel (1989). These taxa define the lower Oligocene *Cestodiscus reticulatus* Zone of Baldauf and Monjanel (1989) from the Labrador Sea (ODP Leg 105), which is correlated to the upper part of calcareous nannofossil Zone NN21. The diatom assemblage of Cores 151-913B-24R through -29R is older than the Leg 105 material, based on the occurrence of "upper Eocene" diatoms of Leg 38 and the absence of *C. reticulatus*, which defines the lower Oligocene zone of Baldauf and Monjanel (1989). The diatom assemblage of this interval, therefore, may correlate to a previously unrecovered interval between the lower Oligocene *C. reticulatus* Zone of Baldauf and Monjanel (1989) and the upper Eocene *C. oblongus* Zone of Schrader and Fenner (1976). This section may include the Oligocene/Eocene boundary, but stratigraphic control on diatoms of this region is not good enough to recognize this boundary.

Cores 151-913B-30R and -31R are barren of diatoms. Sample 151-913B-32R-CC contains a remarkable assemblage of diatoms replaced by pyrite, with fine detail preserved. Identifiable diatoms include specimens of *Trinacria subcoronata*, *R. claviger*, *C. oligocenicus*, *C. senarius*, and *T. excavata* sp. cf. *tetragona*. This assemblage is correlated to the middle Eocene *T. excavata* sp. cf. *tetragona* Zone of Dzinoridze et al. (1978). Although preservation of these diatoms includes fine detail, abundance of identifiable diatoms is low and most specimens are fragmented. Consequently, shipboard identification of the above taxa is based on a few whole specimens, and additional post-cruise studies are needed to verify and refine the diatom-based age of this interval. All samples below 151-913B-32R-CC are barren of diatoms, with the exception of Samples 151-913B-35R-5, 135 cm, -45R-CC, and -42R-3, 119 cm, which contain trace quantities of unidentifiable pyritized diatom fragments.

### Silicoflagellates and Ebridians

No silicoflagellates or ebridians were observed in Hole 913A or in Hole 913B, from the top down to Core 151-913B-18R. Core 151-

913B-19R contains few silicoflagellates and common ebridians, including *Spongebria miocenica*. Locker and Martini (1989) described this large species from Leg 104 material on the Vøring Plateau and assigned it a lower middle Miocene age. Relatively rare reworked lower Oligocene to Eocene silicoflagellates, including *Dictyocha frenguelli*, also occur in Core 151-913B-19W.

Cores 151-913B-24R through -29R contain lower Oligocene to upper Eocene ebridians and silicoflagellates. Silicoflagellates include: *Corbisema triacantha*, *C. hastata*, *C. hastata globulata*, *C. sp. cf. katharinae*, *Mesocena apiculata/inflata* transitional forms, *M. apiculata glabra*, *Naviculopsis ponticula*, *N. biapiculata* and *N. eo-biapiculata* transitional forms, and the ebridian *Ebriopsis crenulata*. This diverse assemblage indicates lower lower Oligocene to upper Eocene for this interval.

Core 151-913B-32R contains a diverse assemblage of pyritized silicoflagellates and ebridians, including *C. triacantha/glezerae* transitional forms, *C. inermis minor*, *Dictyocha deflandrei*, *D. frenguelli*, *Distephanus antiquus*, and *Naviculopsis* sp. cf. *N. minor/foliacea*. This assemblage suggests a middle Eocene age. Below Sample 151-913B-32R-CC, only very rare and unidentifiable fragments of silicoflagellates and ebridians have been found.

### Radiolarians

Sediments recovered from Site 913 on the East Greenland margin are mostly silica-poor in the Neogene and Quaternary portion of the sequence, but contain abundant and well-preserved lower lower Oligocene to middle and upper Eocene radiolarians from 471.6 to 548.4 mbsf (Core 151-913B-24R through -32R). Overall diversity is low, as is typical of high-latitude radiolarian assemblages, although a large portion of the fauna is not described at the species level. Two radiolarian biostratigraphic zonations for the Paleogene of the Norwegian-Greenland Sea have been proposed by previous studies of DSDP Leg 38 material (Bjørklund, 1976; Dzinoridze et al., 1978). In each of these studies, however, the lower Oligocene remained unzoned or very poorly zoned, and the Oligocene/Eocene boundary is not clearly defined. Well-established upper Eocene radiolarian marker taxa are present at Site 913 and provide good stratigraphic control for the age of the sediments in this interval.

Core-catcher samples analyzed from Hole 913A and the upper part of the sedimentary sequence in Hole 913B are barren of radiolarians with the exception of rare, recrystallized, and non-age-diagnostic radiolarians in Cores 151-913B-8R, -10W, and -11R (163.1 to 230.4 mbsf). Core-catcher samples from 230.4 mbsf to 375.2 mbsf also are barren of radiolarians, although recovery in this interval is very poor and includes three wash cores.

Wash Core 151-913B-19W, which recovered material from 375.2 to 423.5 mbsf, has relatively undisturbed, short sequences of sediment within the core. Siliceous intervals are present, and Sample 151-913B-19W-CC contains an assemblage of moderately well-preserved Miocene diatoms and radiolarians. Radiolarian species include *Porodiscus parvus* group, *Stylodictya* sp. cf. *S. stellata*, and unnamed species of the genera *Stylodictya*, *Prunopyle*, *Spongodiscus*, and *Actinomma*. Age constraints for this assemblage herein are based on the presence of diagnostic diatoms until shore-based studies are completed.

Radiolarians are absent in Samples 151-913B-20R-CC and -21R-CC, but occur as broken fragments and rare, poorly preserved specimens in Samples 151-913B-22R-CC and -23R-CC. Underlying these fragmented assemblages is a rich, well-preserved succession of radiolarian faunas extending from 471.6 mbsf (or slightly shallower; Sample 151-913B-24R-CC) to 548.4 mbsf (Sample 151-913B-32R-CC). Siliceous skeletons are best preserved and most abundant from about 470 mbsf to 497 mbsf. Faunas from the lower part of this interval contain fewer species and lower absolute numbers of radiolarians, but age-diagnostic taxa are present. The lowermost occurrence of ra-

diolarians in Hole 913B consists of a sparse, pyritized fauna in Sample 151-913B-32R-CC.

Sample 151-913B-24R-CC is dominated by an abundance of volcanic glass and large spumellarian radiolarians, particularly unnamed species of the genera *Actinomma*, *Axoprimum*, and *Stylotractus*. Age-diagnostic species within this sample are typically the smaller nassellarians (e.g., artoströbiids) and include *Lithomitrella stathmeporoides*, *L. minuta*, *Cornutella* sp. aff. *C. californica*, and *Botryostrobus joides*. Age ranges for these species, determined largely by Petrushevskaya (1979), place this sample in the early Oligocene to late Eocene. Mostly undescribed species of the genera *Prunopyle*, *Stylodictya*, *Spongurus*, *Porodiscus*, *Peripyramis*, and *Siphocampe* also are represented, in addition to rare trissocyclids.

The assemblage in Sample 151-913B-24R-CC cannot easily be related to the biostratigraphic zonations established by either Dzinoridze et al. (1978) or Bjørklund (1976). Little is known about high-latitude lower Oligocene radiolarians, with the exception of a lower Oligocene radiolarian assemblage described in the Labrador Sea (Lazarus and Pallant, 1989). The assemblage in Sample 151-913B-24R-CC appears to have little in common taxonomically with the Labrador Sea fauna. Dzinoridze et al. (1978) did not distinguish zones for the lowermost Oligocene based on Leg 38 material; Bjørklund defined a single zone from this material based on the taxon "*Lithomitra* sp. A," but did not figure *Lithomitra* sp. A in the report. Diatoms co-occurring with radiolarians in Hole 913B also indicate an age just above or below the Oligocene/Eocene boundary.

Sample 151-913B-25R-CC contains a more diverse radiolarian assemblage with a higher abundance of nassellarians, although large spumellarians such as *Actinomma* spp. still dominate. Species identified include *Lithomitra*(?) sp. "P" of Dzinoridze et al. (1978), *L.*(?) *elegans* group, *L. minuta*, *Lithomitrella* sp. aff. *L. elizabethae*, *Theocyrtis litos* (= *Calocyclus* sp. of Bjørklund, 1976), and *T. andriashevi*. *T. litos* ranges from the base of Dzinoridze et al.'s *Lophocorys norvegiensis* Zone to the top of their *T. litos* "Cr" Zone, all of which are correlated to the upper Eocene. This interval should be approximately equivalent to Bjørklund's (1976) *L. norvegiensis* Zone (also correlated with the upper Eocene), but the marker taxon for this zone (*L. norvegiensis*) has its last stratigraphic occurrence thus far at Site 913 below this level. The final occurrence of *L. norvegiensis* marks the top of the Eocene in Bjørklund's (1976) zonation and lies just below the Oligocene/Eocene boundary, according to Dzinoridze et al. (1978). Thus, the radiolarian assemblage in Sample 151-913B-25R-CC may be a slightly younger assemblage than the *L. norvegiensis* Zone of Bjørklund.

Radiolarians are less abundant in Sample 151-913B-26R-CC than in stratigraphically higher samples, an event which co-occurs with increased abundance of diatoms and silicoflagellates in Hole 913B. Radiolarians in this sample include *Lithomitra embrionalis*, *Lithomitra* sp. aff. *L. nodosaria*, and undescribed species of *Actinomma*, *Spongurus*, *Spongodiscus*, *Lithomitrella*, and rare trissocyclids. Sample 151-913B-27R-CC has specimens of *L. stathmeporoides*, *A.*(?) *spinulosa*, and *Ceratocyrtis* sp. of Petrushevskaya (1979). Radiolarians recovered from core-catcher Samples 151-913B-28R and -29R are less well preserved and few age-diagnostic taxa have been identified thus far. Based on the species present in Cores 151-913B-26R and -27R and the underlying occurrences of upper Eocene marker taxa, Cores 151-913B-26R to -29R are correlated tentatively to the Upper Eocene *L. norvegiensis* Zone, although these samples also may be slightly younger than Bjørklund's zone.

The assemblage preserved in Sample 151-913B-30R-CC is similar to the radiolarian fauna described in Cores 26 and 27 at Site 338, DSDP Leg 38 (Bjørklund, 1976). Species present include *L. norvegiensis*, *A.*(?) *spinulosa*, *A. spinulosa*, *Hexaconthium* sp. aff. *H. pachydermum*, and *Stylospongia communis*. Sample 151-913B-31R-CC contains the first downhole occurrence of *Calocyclus talwanii*, which consistently makes its first downhole appearance stratigraphically

below *L. norvegiensis* in Norwegian-Greenland Sea sediments of Leg 38. Sample 151-913B-31R-CC is assigned to the upper part of the *Calocyclus talwanii* Zone of Bjørklund (1976), which is correlated to the lower upper Eocene. Dzinoridze et al. (1978) correlate this same interval to the upper middle to lower upper Eocene.

Sample 151-913B-32R-CC contains a sparse, but well-preserved, pyritized radiolarian assemblage that includes *L. norvegiensis* and is assigned to the upper middle to lower upper Eocene. Although very rare sporadic fragments of pyritized radiolarians are present in smear slides below this interval, no whole, identifiable radiolarians have been recovered from core-catcher samples from Cores 151-913B-33R through -51R.

### Calcareous Nannofossils

All core-catcher and some additional samples from Holes 913A and 913B were studied for calcareous nannofossil biostratigraphy. Well-preserved nannofossils are rare in the upper part of the sequence. Reworked calcareous nannofossils from the Cretaceous such as *Cribrosphaerella ehrenbergii*, *Prediscosphaerella cretacea*, *Manivittela pemmatoidea*, *Eiffelithus eximius*, *Gartnergo obliquum*, and *Vagalapilla matalosa*, are also found in the upper part of the sequence.

*Emiliania huxleyi*, which indicates NN21 Zone, is found in Samples 151-913A-1H-CC (4.4 mbsf) and -2X-CC (9.3 mbsf). Samples 151-913A-6X-CC (36.1 mbsf) through -12X-CC (94.0 mbsf) also contain Quaternary marker species *Gephyrocapsa caribbeana* and *G. oceanica*, but without *E. huxleyi*, and are correlated to Quaternary Zones NN19 to NN20. *G. oceanica*, which indicates the Quaternary, also occurs in Samples 151-913B-1R-CC (95.6 mbsf) and -2R-CC (105.2 mbsf). Calcareous nannofossils are absent below this depth.

### Planktonic Foraminifers

Planktonic foraminifer biostratigraphy of Site 913 is based on the examination of all core-catcher samples from Holes 913A and 913B. Four additional samples were analyzed from Core 151-913A-1H. Planktonic foraminifers are abundant in the upper sequence of the Quaternary sediments and occur sporadically in the downhole sequence. The planktonic foraminifers are well preserved. *Neoglobobulimina pachyderma* in the sinistral and dextral coiling direction co-occur with *N. sp. cf. N. dutertrei*, *Turborotalia quinqueloba*, and *Globigerinita glutinata*, indicating an age of Quaternary for Cores 151-913A-1H through -12X-CC and Sample 151-913B-2R-CC (105.2 mbsf). Samples 151-913A-3H-CC, -6X-CC, and -9X-CC and all core-catcher samples from Hole 913B, except Sample 151-913B-2R-CC, are barren of planktonic foraminifers.

### Benthic Foraminifers

Benthic foraminifers were analyzed in all core-catcher samples from Holes 913A and 913B. Quaternary and Pliocene benthic foraminifers are abundant to rare in the upper 10 core catchers of Hole 913A, and the upper 13 core-catcher samples of Hole 913B. The Pliocene foraminifer *Cibicides grossa* occurs sporadically in this interval and is assumed to be reworked because of the poor preservation. Given the preservation of this species, it is uncertain whether Pliocene sediments were actually recovered at Site 913. Poor recovery from 151-913B-14R-CC through -18R-CC hinders efforts to define boundaries from the Quaternary through the Miocene.

Fragments of the Miocene benthic foraminifers *Martinottiella communis* and *Spirosigmoidella compressa* are rare in Samples 151-913B-19W-CC and -20R-CC. No Oligocene benthic foraminifers were observed in the core-catcher samples from Hole 913B.

Eocene agglutinated benthic foraminifers are found from Sample 151-913B-22R-CC to the bottom of the hole. The last occurrence of

fragments of *Rhabdammina* spp. is found in Sample 151-913B-22R-CC, and the encrusting agglutinate *Ammolagena clavata* is common to abundant below Sample 151-913B-27R-CC. The last occurrence of *Cyclammina amplexens* is in Sample 151-913B-37R-CC. This Eocene assemblage is similar to Eocene agglutinated benthic foraminifer assemblages from the Labrador Sea (Miller et al., 1982; Kaminski et al., 1989) and from the Vøring Plateau (Kaminski et al., 1990).

### Bolboforma

All core-catcher samples in Holes 913A and 913B were examined for *Bolboforma*. *Bolboforma* occur sporadically from Sample 151-913B-27R-CC through -51R-CC; additional samples taken from certain intervals of yellow-gray siltstone within the cores contain very high abundances of this microfossil. Preservation is generally poor because of replacement of the low magnesium calcite skeletons by rhodochrosite ( $MnCO_3$ ), and most ornamentation of the tests has been destroyed. Nevertheless, some of the specimens are preserved well enough to allow the identification of *Bolboforma antarctica*, *B. indistincta*, and *B. praespinosa*. All of these taxa are indicative of the middle Eocene (Spiegler and von Daniels, 1991). The *B. antarctica* Zone extends from Sample 151-913B-30R-CC through -45R-CC. The shorter-ranging *B. indistincta* Zone occurs from Sample 151-913B-46R-CC through -51R-CC.

It is important to note that *Bolboforma* have the potential to become a useful biostratigraphic tool in the Cenozoic middle- and higher-latitude sediments. They have been found in Paleogene sediments of ODP Site 647, Labrador Sea (Pallant and Kaminski, 1989), as well as in the Paleogene of Leg 113, Maud Rise, Antarctica (Kennett and Kennett, 1990); from the subantarctic Atlantic, ODP Leg 114 (Spiegler, 1991); and the southern Indian Ocean from Leg 120 (Mackensen and Spiegler, 1992).

Barite crystals were observed in three core samples collected for *Bolboforma* analyses. Isolated barite crystals (2–3 mm) were seen in Samples 151-913B-39R-5, 2–5 cm, and -40R-2, 23–25 cm. The

former sample contains *Bolboforma* with sulfide linings and includes one *Bolboforma* enclosed within a barite crystal. The latter sample contains rare *Bolboforma* and agglutinated benthic foraminifers. Barite is widespread in marine sediment but usually constitutes less than 1% of most sediments. This mineral has been reported to occur in certain primitive protozoans. The possible relationship between barite and *Bolboforma* and agglutinated foraminifers will be investigated in post-cruise studies.

### Palynology

Only selected samples were processed for palynomorphs from Hole 913B. Cores 151-913B-11R and -12R contain abundant amorphous organic matter (AOM) and common terrestrial pollen and spores, similar to the upper Neogene sequences of all other Leg 151 sites.

From Core 151-913B-20R through -51R, AOM and pollen are much less abundant, except in a few samples where they are common. Dinoflagellates are rare to few, owing to the dilution of the samples with biogenic silica and clays, which were not completely dissolved by abbreviated shipboard treatments with hydrofluoric acid. Nonetheless, there is a diverse assemblage, which shore-based processing should improve. Specimens of the following genera occur: *Achomosphaera*, *Aptodinium*, *Areoligera*, *Batiacasphaera*, *Cleistosphaeridium*, *Corrudinium*, *Cribroperidinium*, *Deflandrea*, *Dinopterygium*, *Hystrichosphaeropsis*, *Impagidinium*, *Kallosphaeridium*, *Lejeuncysta*, *Lingulodinium*, *Operculodinium*, *Palaeocystodinium*, *Phelodinium*, *Phthanoperidinium*, *Pxydiella*, *Selenopemphix*, *Spiniferites*, *Thalassiphora*, and *Wetzeliella*. *Wetzeliella* ranges from Eocene to Oligocene, giving a broad age constraint for the lower part of Hole 913B. *Phthanoperidinium* sp. cf. *P. stockmansii* occurs in Sample 151-913B-32R-CC. This species occurs in the middle Eocene of Site 643 (Manum et al., 1989), and indicates a middle Eocene age for this sample. *Deflandrea* sp. cf. *D. leptoderma* occurs in Sample 151-913B-48R-CC, and likewise has a range restricted to middle Eocene or younger at Site 643 (Manum et al., 1989).

### Biostratigraphic Synthesis

The 94-m-thick sequence of glacial sediments in Hole 913A is dated as Quaternary, based on calcareous nannofossils and planktonic and benthic foraminifers. No siliceous microfossils are present in this part of the hole.

The upper 423.5 m of Hole 913B was alternately washed and spot-cored. Hence, biostratigraphic control is minimal on this upper interval. Benthic foraminifers suggest Quaternary to Pliocene to a depth of 288.4 mbsf (Core 151-913B-13R). Wash core 151-913B-19W contains a short undisturbed sedimentary sequence containing middle Miocene diatoms and ebridians.

Cores 151-913B-24R to -29R contain rich biosiliceous faunas and floras, which indicate an early early Oligocene to late Eocene age. This biosiliceous interval may not have been recovered previously from the North Atlantic Ocean or Norwegian-Greenland Sea, and thus represents part of the stratigraphic gap between Oligocene sediments of Leg 105 and upper Eocene sediments of Leg 38 (Fig. 14). The interpreted age of Cores 151-913B-24R through -29R is early early Oligocene to late late Eocene. Post-cruise paleomagnetic and biostratigraphic correlation may establish the position of Eocene/Oligocene Boundary in Site 913. Pyritized middle Eocene diatoms, silicoflagellates, and radiolarians are recognized in Sample 151-913B-32R-CC. The middle Eocene is recognized by the occurrence of *Bolboforma* in Samples 151-913B-27R-CC through -51R-CC.

Little can be said about stratigraphic continuity in the upper Neogene and Quaternary stratigraphic successions, because of very poor recovery in the sequence. Pliocene and upper Miocene sediments are not recognized biostratigraphically. The lower Neogene and Paleo-

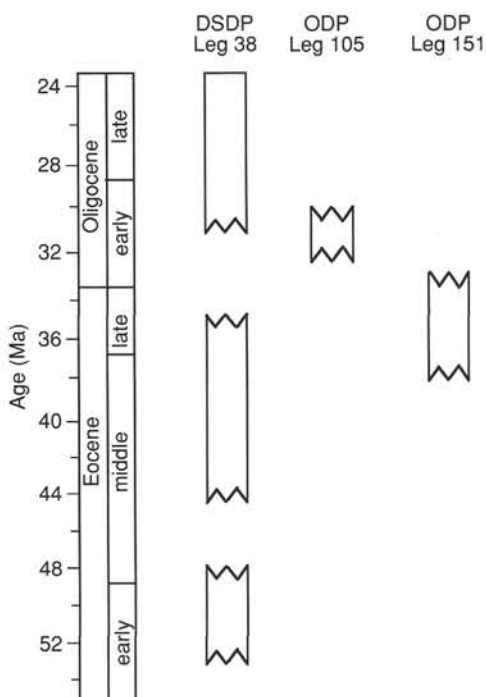


Figure 14. Comparison of Paleogene biosiliceous sedimentary intervals of Norwegian-Greenland and Labrador seas (DSDP Leg 38, ODP Legs 105 and 151).

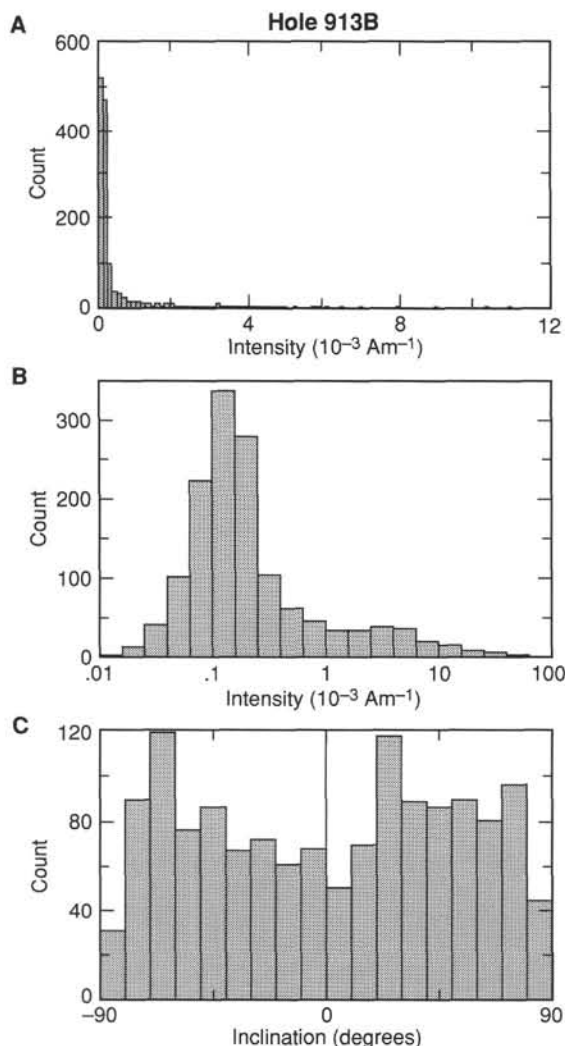


Figure 15. The distribution of (A) remanent intensity values and (B) the log of the remanent intensity, after 30-mT AF demagnetization in Hole 913B. The practical sensitivity in the 2G pass-through magnetometer system is approximately  $5 \times 10^{-4} \text{ Am}^{-1}$ . C. The distribution of the inclination of remanent magnetization in Hole 913B after 30-mT AF demagnetization.

gene sedimentary successions of Site 913 may contain hiatuses. No lower Miocene or upper Oligocene successions were recovered, and a hiatus is suggested, in addition to the fact that as much as 87 m of sediment was not recovered between middle Miocene wash Core 151-913B-19W and lower lower Oligocene/upper Eocene Core 151-913B-24R. This suggestion is supported by the occurrence of reworked Eocene diatoms and silicoflagellates, which occur in Core 151-913B-19W.

## PALEOMAGNETICS

Shipboard paleomagnetic studies performed at Site 913 followed the general methods described in the "Explanatory Notes" chapter (this volume). Poor recovery and very weakly magnetized sediments prevented a definitive determination of a continuous and reliable magnetostratigraphy at this site. However, the poorly defined normal and reversed paleomagnetic record indicates seven successive reversals in interpreted polarity between 540 and 670 mbsf.

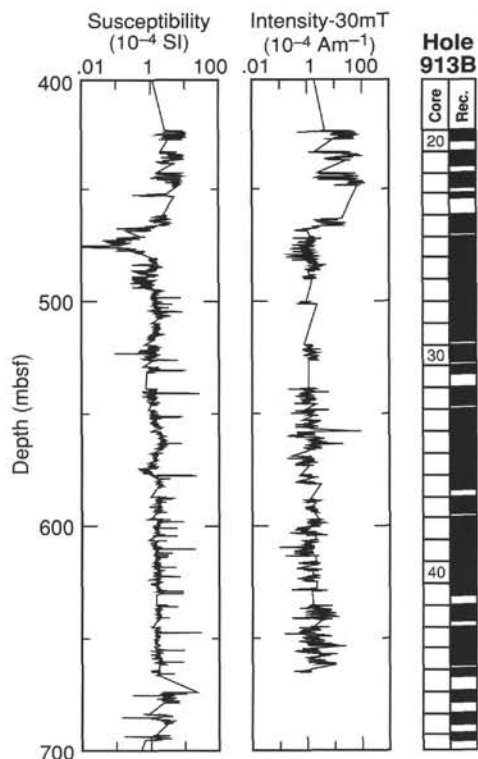


Figure 16. The variation with depth of magnetic susceptibility and NRM intensity after 30-mT AF demagnetization in Hole 913B.

## General Magnetic Character of the Site 913 Sediments

The upper 400 m of Hole 913A and 913B yielded extremely poor recovery because of an abundance of coarse ice-rafted debris. The small amount of sediment that was recovered in this interval was strongly deformed and useless for paleomagnetic studies. Drilling recovery improves below this zone, at a depth of about 420 mbsf. Magnetic susceptibility and remanent intensity values are fairly high, on the order of  $5 \times 10^{-4} \text{ SI}$  units and  $2 \times 10^{-3} \text{ Am}^{-1}$ , respectively. However, susceptibility and intensity dropped by more than 10 times these initial mean values from 465 mbsf to the bottom of the hole, with a pronounced sharper drop in susceptibility between 465 and 476 mbsf.

Similar to the Yermak Plateau and Fram Strait sedimentary columns, the lower magnetic susceptibility zone (465–480 mbsf) corresponds to maximum values in the total sulfur concentrations, which rise up to 6% in Cores 151-913B-24R, -25R, and -26R (see the "Organic Geochemistry" section, this chapter). Although the distribution of intensity values as presented on Figure 15A shows that 85% of these values are lower than  $3 \times 10^{-4} \text{ Am}^{-1}$  and lie close to the noise-level of the pass-through cryomagnetometer, some tendency toward a bimodal distribution is observed in the intensity log values. A tail in the distribution toward values higher than  $10^{-3} \text{ Am}^{-1}$  reflects zones that are less affected by reducing processes (see Fig. 16, and the "Organic Geochemistry" and "Inorganic Geochemistry" sections, this chapter).

## Inclination Record

As observed in Figure 15C, inclinations are equally distributed between  $\pm 80^\circ$  without the tendency toward a well-developed bimodal distribution, which, in previous sites, has been the hallmark of a reliably isolated characteristic magnetization. This distribution suggests that our alternating field (AF) demagnetization treatment has been ineffective in dealing with spurious magnetizations. However, the in-

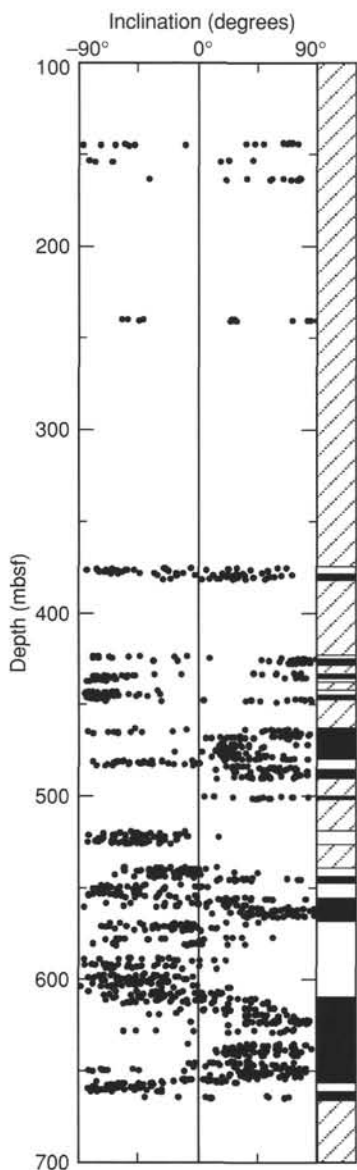


Figure 17. The variation with depth of inclination for the NRM after 30-mT AF treatment (left column). The right column indicates our polarity interpretation for the section (black = normal polarity, white = reversed polarity, hatched = missed recovery).

clination record does suggest consistent patterns of positive and negative inclination, which we have tentatively interpreted in terms of normal and reversed magnetozones in Figure 17. These normal and reversed magnetozones are largely interrupted by missing recovery intervals; however, in the interval between 540 and 660 mbsf, we can discern a pattern of seven polarity transitions.

### Comparison Between Magnetostratigraphy and Biostratigraphy

The sequence of reversed and normal polarity magnetozones interpreted in Figure 17 is entirely consistent with the latest Eocene to earliest Oligocene age proposed for this interval (519 to 462 mbsf) on the basis of biostratigraphy (see "Biostratigraphy" section, this chapter); however, the present level of uncertainty in the definition of magnetozones does not permit us to refine or add to the biostratigraphic ages. The Eocene and Oligocene are indeed of mixed polarity (Cande and Kent, 1992), but there is not a distinctive pattern of reversed and normal polarity zones that suggests a unique correlation to the geomagnetic polarity time scale (GPTS). Further refinements to the age control in this interval might come from other independent sources (e.g., spectral analysis of lithostratigraphic character).

## INORGANIC GEOCHEMISTRY

### Interstitial Water

Table 4 and Figure 18 show the composition of interstitial waters collected from Holes 913A and 913B. The interval from 25 mbsf to 425 mbsf was not sampled, and there are no interstitial water data for this interval. Sodium shows a moderate decrease with depth from nearly seawater values at the sediment water interface to about 350 mmol/L at the bottom of Hole 913B. Potassium shows a sharp drop in Hole 913A and a more gradual decrease at depth. Both show a spike in abundance in Core 151-913B-24R (462.0–471.6 mbsf).

Magnesium decreases with depth below seafloor; calcium appears to remain relatively constant down to about 550 mbsf, then increases to high levels, above 60 mmol/L below 650 mbsf.

Ammonia rises sharply in the cores from Hole 913A, but the ultimate levels reached at depth are quite low compared with other sites in the region. Ammonia at depth does not exceed 600 μmol/L. Silica similarly rises sharply in Hole 913A but peaks in Hole 913B at 778 mmol/L in Core 151-913B-24R, the same core in which sodium, potassium, and ammonia peak. Below 550–580 mbsf silica is very low, in the quartz equilibrium range.

Chloride falls gently from seawater levels in Hole 913A to about 500 mmol/L in Hole 913B. Chlorine and sodium appear to covary, and no special effects appear to affect the sea salt elements except for the usual mild dilution due to clay diagenesis.

Table 4. Composition of interstitial waters in Holes 913A and 913B.

Core, section	Depth (mbsf)	Na (mmol/L)	K (mmol/L)	Mg (mmol/L)	Ca (mmol/L)	Cl (mmol/L)	SO <sub>4</sub> (mmol/L)	NH <sub>4</sub> (μmol/L)	SiO <sub>2</sub> (μmol/L)	pH	Alkalinity (meq/L)
151-913A-											
1H-2	2.95	440	11.1	49.9	10.9	544	31.3	0	89	7.6	2.652
3H-5	16.75	456	8.7	46.5	16.3	551	30.7	262	154	8.06	1.856
4H-3	22.05	452	7.5	45.3	18.6	552	30.1	178	179	8.04	1.627
5H-1	25.03	453	7.1	44.1	18.7	551	29.0	212	173	8.09	1.635
151-913B-											
20R-2	426.40	361	5.0	32.0	25.1	503	15.2	356	147		
24R-3	466.40	420	7.4	34.7	29.7	533	17.8	579	778	7.59	2.236
27R-4	496.60	350	4.0	34.0	27.6	462	14.7	325	540		
30R-2	522.40	313	3.3	31.0	27.7	432	13.6	309	405		
33R-4	554.30	364	3.8	32.0	39.2	500	13.5	371	334		
36R-3	581.74	286	2.7	23.8	30.5	403	9.0	317	51		
39R-5	613.77	345	3.5	26.4	45.3	480	11.0	437	51		
42R-3	639.50	347	2.5	26.3	52.4	509	8.4	333	83		
45R-1	665.19	351	2.6	28.5	63.4	517	6.5	348	96		
48R-1	693.77	356	2.3	23.7	66.6	529	6.0	401	89		

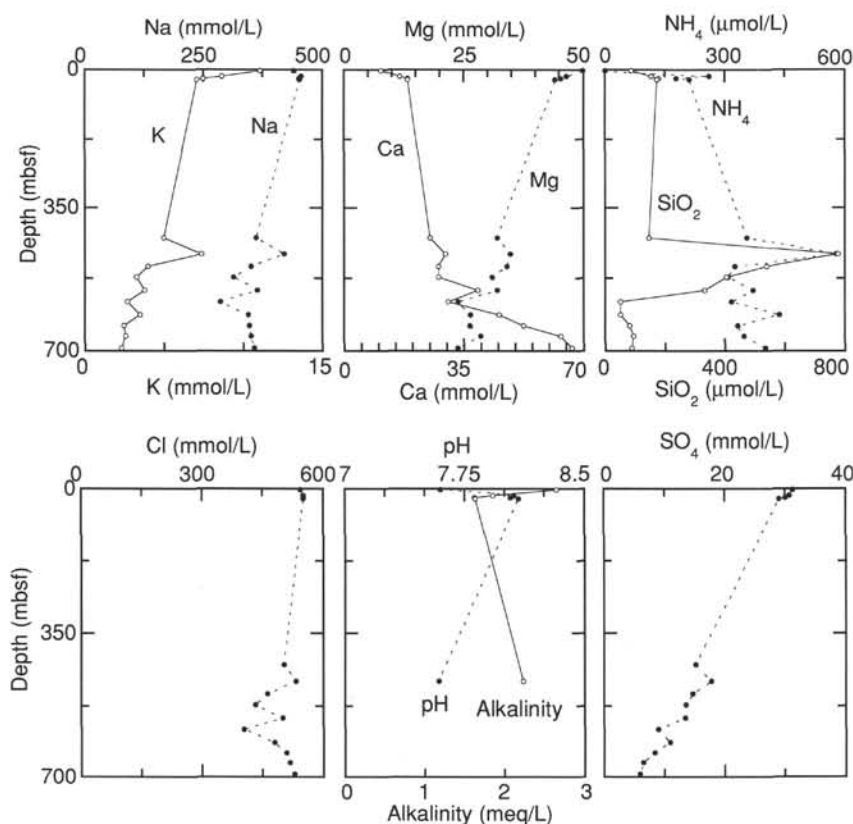


Figure 18. Interstitial water compositions at Site 913.

Alkalinity behaves anomalously in these holes, dropping rapidly from seawater values to below 1.5 meq/L. Only one interstitial water sample from Hole 913B was sufficiently large for an alkalinity determination, but it, too, is low relative to the overlying seawater.

Sulfate shows truly anomalous behavior. Samples from Hole 913A are close to seawater values. Samples from Hole 913B at much greater depth appear to define a trend passing through the Hole 913A samples. Sulfate does not decrease to zero at the top of the section but appears to decrease gradually downhole, indicating a very low level of sulfate reducing activity. Methane in samples from Holes 913A and 913B is similarly very low (see "Organic Geochemistry" section, this chapter).

### Sediment Geochemistry

Table 5 shows major element abundances measured on samples from Holes 913A and 913B by X-ray fluorescence on pressed pellets. Silica (Fig. 19) shows a constant background level of around 60 wt% throughout the section; occasional much higher values reflect the presence of abundant siliceous microfossils. Titanium (Fig. 19) shows a similarly constant abundance, diluted occasionally by the high silica abundance in fossiliferous layers. Alumina (Fig. 19) is somewhat higher in the lower part of the section, and total iron (Fig. 19) is substantially higher in the lower parts except where diluted by high silica.

Magnesium (Fig. 19) is quite high (near 4 wt%) at the top of the section, then decreases to about 3 wt% in Hole 913A. In Hole 913B magnesium is below 3 wt% in the section between 350 and 600–650 mbsf, then rises up to about 3.3 wt% below this level. Calcium (Fig. 19) is abundant in the upper parts of Hole 913A (where carbonates are relatively abundant; see "Organic Geochemistry" section, this

chapter), then drops to about 1.5 wt% (typical of other sediments in the region) in Hole 913B.

Sodium (Fig. 19) is nearly constant in sediments from both holes at this site except for dilution in high silica layers and a few high-sodium/low-potassium regions from about 450 to 550 mbsf. Manganese is relatively constant in these sediments except for isolated high abundances in Cores 151-913B-45R and -47R. Phosphorus is relatively abundant in samples from Hole 913A, probably associated with high carbonate levels. It is substantially lower in Hole 913B except for cores below about 650 mbsf, where fish teeth are reported by the biostratigraphers (see "Biostratigraphy" section, this chapter).

### Discussion

The chemistry of interstitial waters at Site 913 is peculiar. The behavior of silica may be explained by changes in basin circulation and water sources as at Site 909. It is notable that the two deepest holes show this silica-depleted interstitial water, which suggests a lack of siliceous microfossils and, perhaps, nutrient scarcity in the basin, or more likely, a diagenetic system that has achieved the complete conversion of opal to quartz.

The sulfate profile is difficult to explain. The general lack of sulfate-reducing activity suggests a lack of organic carbon, but at least a modest level of carbon is present in these sediments; at the same time, these sediments are notably poor in methane (see "Organic Geochemistry" section, this chapter). The increased abundance of sedimentary organic carbon and methane at the bottom of Hole 913B may set the lower boundary condition for the diffusive (?) sulfate profile (Fig. 18) at this site.

Once again sediments with very high silica contents have been recovered, suggesting a continental (acid igneous rock) source. The ex-

Table 5. Major element composition of sediments in Holes 913A and 913B.

Core, section	Depth (mbsf)	SiO <sub>2</sub> (wt%)	TiO <sub>2</sub> (wt%)	Al <sub>2</sub> O <sub>3</sub> (wt%)	Fe <sub>2</sub> O <sub>3</sub> (wt%)	MnO (wt%)	MgO (wt%)	CaO (wt%)	Na <sub>2</sub> O (wt%)	K <sub>2</sub> O (wt%)	P <sub>2</sub> O <sub>5</sub> (wt%)	Total (wt%)
151-913A-												
1H-2	2.00	60.26	0.81	12.68	6.41	0.08	3.81	3.79	1.78	3.39	0.21	93.22
3H-3	12.93	61.98	0.82	12.42	5.36	0.05	3.38	3.33	1.80	2.99	0.20	92.32
4H-3	21.22	66.00	0.67	10.69	4.59	0.05	2.94	3.09	1.73	2.73	0.20	92.69
7X-1	36.37	64.79	0.73	12.16	5.29	0.05	3.07	2.91	1.79	2.84	0.21	93.84
9X-1	56.11	61.73	0.81	13.74	5.82	0.05	3.19	3.03	1.76	2.90	0.19	93.21
10X-1	65.74	62.41	0.77	12.69	5.51	0.06	3.18	3.08	1.81	2.83	0.20	92.53
151-913B-												
3R-1	105.40	63.77	0.78	12.19	5.46	0.05	3.34	2.98	1.83	2.96	0.22	93.59
5R-CC	124.57	63.99	0.79	13.35	6.16	0.12	2.91	1.91	2.09	2.72	0.21	94.25
7R-1	144.10	65.31	0.80	13.58	5.62	0.05	2.92	1.89	2.20	3.28	0.20	95.84
8R-1	153.68	60.33	0.90	15.02	7.95	0.07	3.19	1.90	2.11	3.44	0.25	95.15
19W-3	378.83	58.10	0.87	15.77	9.86	0.06	2.70	1.67	1.67	2.27	0.08	93.04
20R-3	427.13	62.14	1.14	14.38	8.27	0.05	2.44	1.81	1.70	2.97	0.12	95.02
21R-R	436.97	61.49	1.02	14.91	8.34	0.06	2.63	1.79	1.72	2.51	0.11	94.59
22R-3	446.43	64.58	0.88	13.19	7.66	0.07	2.53	1.66	1.70	2.23	0.09	94.59
23R-3	465.63	64.64	0.78	14.03	8.23	0.06	2.73	1.65	1.87	1.61	0.06	95.66
24R-5	468.09	92.68	0.15	1.74	2.57	0.02	0.63	1.05	0.85	0.42	0.02	100.13
25R-3	475.23	83.78	0.39	4.96	3.88	0.04	1.10	1.24	1.38	1.01	0.04	97.81
26R-3	484.73	64.02	0.82	16.60	6.97	0.05	2.80	1.69	2.56	1.37	0.04	96.93
27R-3	494.32	81.04	0.60	7.70	4.92	0.04	1.55	1.43	1.33	1.29	0.05	99.94
28R-3	503.93	61.00	0.77	18.26	7.70	0.07	2.58	1.77	2.30	0.75	0.04	95.25
29R-3	513.53	71.24	0.70	11.34	7.20	0.06	2.15	1.56	1.70	1.58	0.05	97.58
30R-3	523.13	71.87	0.70	11.43	6.61	0.05	2.22	1.55	1.69	1.45	0.04	97.62
32R-3	542.46	62.18	0.84	15.67	8.16	0.05	2.47	1.76	1.96	1.16	0.08	94.34
33R-3	552.04	76.48	0.58	9.34	6.06	0.06	2.04	1.46	1.44	1.70	0.04	99.18
34R-3	561.83	59.89	0.88	15.76	8.73	0.07	2.62	1.74	1.61	2.62	0.05	93.97
35R-3	571.35	72.12	0.70	11.10	6.43	0.04	2.25	1.59	1.57	1.56	0.04	97.38
36R-3	581.02	63.65	0.80	13.97	7.59	0.05	2.59	1.67	1.55	2.81	0.05	94.72
37R-3	590.66	59.50	1.32	16.22	8.67	0.06	2.54	2.08	1.58	2.21	0.05	94.22
38R-3	599.38	61.45	0.82	15.43	7.46	0.05	2.55	1.89	1.83	2.07	0.15	93.70
39R-3	610.06	70.31	0.67	11.48	6.63	0.05	2.17	1.63	1.50	1.63	0.03	96.09
40R-3	619.63	61.17	0.98	14.83	8.32	0.06	2.59	1.98	1.61	2.08	0.09	93.72
41R-3	628.50	61.84	0.86	14.82	8.11	0.06	2.80	1.85	1.64	2.24	0.06	94.27
42R-3	639.03	61.73	0.90	15.39	7.65	0.05	2.73	1.77	1.47	3.22	0.10	95.02
43R-3	648.48	63.30	0.83	14.90	7.81	0.06	3.19	1.88	1.61	2.36	0.05	95.98
44R-3	658.14	64.96	0.79	14.58	7.26	0.05	2.93	1.71	1.48	3.07	0.10	96.94
45R-2	665.95	59.13	0.98	16.10	7.98	0.52	3.41	2.50	1.67	1.89	0.50	94.68
46R-3	677.73	60.89	0.97	16.78	7.57	0.10	3.20	1.87	1.43	3.60	0.12	96.52
47R-3	687.33	58.86	0.99	16.23	8.22	0.38	3.16	1.90	1.43	3.41	0.15	94.75
48R-2	694.60	61.86	0.88	14.05	6.25	0.08	3.01	1.71	1.69	2.47	0.16	92.17
49R-3	706.30	64.47	0.97	13.20	6.63	0.18	2.92	1.79	1.45	2.69	0.19	94.50
50R-3	715.54	53.26	1.09	19.15	9.28	0.08	3.37	1.92	1.35	2.58	0.07	92.13

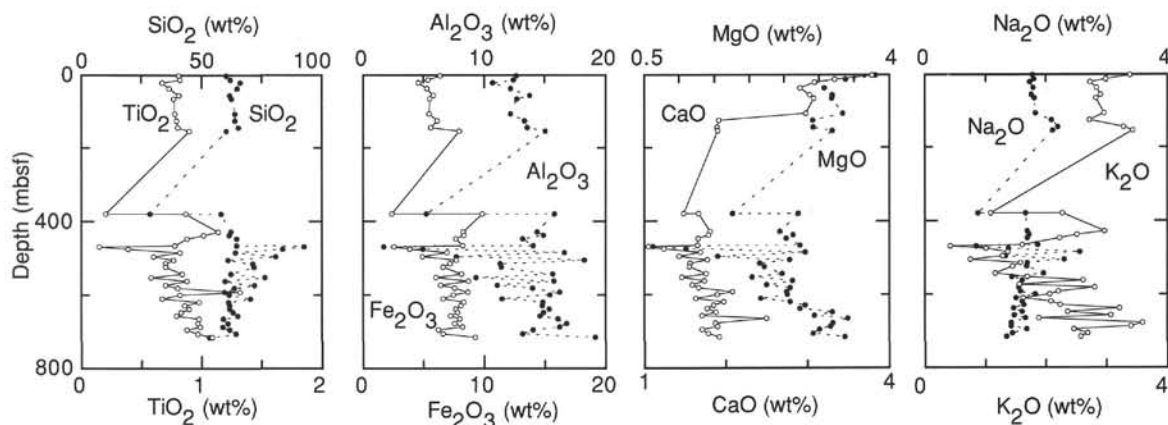


Figure 19. Sediment compositions at Site 913.

cursor to anomalously high sodium to potassium ratios in the samples from 450 to 550 mbsf is interesting, and shore-based mineralogical and minor-element studies may shed more light on the sources of these sediments.

## ORGANIC GEOCHEMISTRY

The shipboard organic geochemistry program at Site 913 consisted of analyses of volatile hydrocarbons and determinations of inor-

ganic carbon, total nitrogen, total carbon, and total sulfur (for methods see "Explanatory Notes" chapter, this volume).

## Volatile Hydrocarbons

As part of the shipboard safety and pollution monitoring program, concentrations of methane (C<sub>1</sub>) and ethane (C<sub>2</sub>) gases were monitored every core using standard ODP headspace-sampling techniques.

Throughout the 770.3-m-thick sedimentary section of Site 913, headspace methane concentrations are low. Almost all of the values

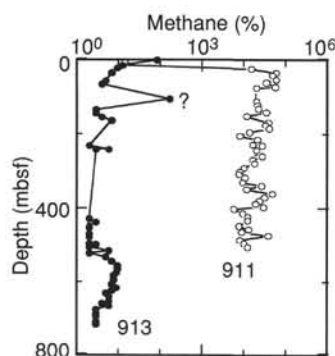


Figure 20. Record of headspace methane ( $C_1$ ) concentrations in sediments from Site 913. For comparison, methane concentrations at Site 911 (see "Organic Geochemistry" section, "Site 911" chapter, this volume) are shown, too.

are <10 ppm (i.e., about four orders of magnitude lower than those recorded at Site 911; Fig. 20, Table 6). Only in the uppermost sample at about 3 mbsf and near 105 mbsf, some slightly increased methane values of 84 ppm and 172 ppm, respectively, occurred. In the interval between 550 and 660 mbsf where methane reached concentrations of up to 10 ppm, traces of ethane were determined, too (Table 6, Fig. 20).

### Carbon, Nitrogen, and Sulfur Concentrations

The results of determinations of inorganic carbon, carbonate, total carbon, total nitrogen, and total sulfur are summarized in Table 7 and presented in Figures 21 and 22.

Most of the carbonate values of the sedimentary sequence of Site 913 are low and vary between 0.2% and 5% (Fig. 21). According to the carbonate record, the sequence can be divided into three intervals. In the upper approximately 60m (Quaternary to late Pliocene in age) corresponding to lithologic Unit I, the higher carbonate values of 4% to 6% are typical. The maximum values in the uppermost 3 m (Sub-unit IA) coincide with the occurrence of foraminifers (see "Biostratigraphy" section, this chapter), suggesting a biogenic source of the carbonate. Except for single peaks of carbonate contents as high as 6% to 1% at depths of 145, 448, and 578 mbsf (Fig. 21, Table 7), carbonate contents are <1% between 60 and 670 mbsf. This interval corresponds to the lower part of lithologic Unit I as well as Units II and III. In the lowermost part of the sedimentary sequence of Site 913 (674.1–716 mbsf, lithologic Unit IV, middle Eocene in age), carbonate values are higher, varying between 1% and 11%.

In general, total organic carbon (TOC) values vary between 0.1% and 1%, with some single peaks of TOC as high as 2% to 5.2% in the lower part of the sequence (Fig. 21). Whereas the lower values of 0.1% to 0.5% are dominant in the upper 460 mbsf, the higher values are more typical below 460 mbsf. Distinct maxima in total organic carbon values of 0.5%–1%, 1.7%–2.7%, and 0.6%–5.2% occur at 460 to 500 mbsf (earliest Oligocene to late Eocene in age), 525 to 548 mbsf, and 638 to 716 mbsf (the two lower intervals are early Oligocene to middle Eocene), respectively. C/N ratios <10 (Figs. 21 and 22) may indicate that major proportions of marine organic matter are present in the sediments at Site 913. The maximum TOC peaks in the lower part of the record are probably caused by increased supply of terrigenous material as indicated by high C/N ratios of up to 37 (Figs. 21 and 22).

According to the sulfur data, the sedimentary sequences of Site 913 can be divided into four intervals (Fig. 21). Sulfur values of dominantly <0.3% are typical in the upper 460 mbsf and between 550 and 635 mbsf. Between 460 to 550 mbsf and below 635 mbsf, sulfur val-

Table 6. Results of headspace gas analysis from Site 913.

Core, section, interval top	Depth (mbsf)	$C_1$ (ppm)	$C_2$ (ppm)
151-913A-			
1H-3, 0	3	84	
3H-6, 0	17	13	
4H-4, 0	22	11	
5H-2, 0	25	10	
7X-1, 0	36	7	
9X-1, 134	57	5	
10X-1, 104	66	4	
151-913B-			
3R-1, 30	106	172	1
5R-7, 10	134	3	
7R-1, 0	144	3	
8R-1, 0	153	4	
9R-1, 0	163	7	
11R-7, 0	230	2	
12R-7, 0	239	6	
13W-1, 0	240	3	
20R-3, 0	427	2	
21R-4, 0	438	3	
22R-3, 145	447	2	
23R-1, 0	452	2	
24R-4, 0	467	2	
24R-4, 145	468	2	
25R-6, 0	479	2	
26R-6, 0	494	2	
27R-5, 0	497	3	
28R-4, 0	505	2	
29R-4, 0	514	6	
30R-2, 0	521	2	
31R-2, 0	531	5	
32R-4, 0	543	7	
33R-5, 0	554	10	1
34R-6, 0	566	10	1
35R-6, 0	575	9	1
36R-4, 0	582	8	1
37R-5, 0	593	8	1
38R-6, 0	604	7	
39R-6, 0	614	9	1
40R-5, 0	622	7	
41R-3, 0	629	5	
42R-4, 0	640	6	1
43R-5, 0	651	6	
44R-3, 0	658	4	1
45R-2, 0	666	6	
46R-2, 0	676	3	
47R-3, 0	687	3	
48R-2, 0	695	3	
49R-5, 0	709	3	
50R-4, 0	717	3	

ues are distinctly increased, reaching values of 1.2% to 2.7%, with a single sulfur spike as high as 6.3% at 546 mbsf. The sulfur maxima partly coincided with organic carbon maxima and with a major drop in magnetic susceptibility and magnetic intensity (see "Paleomagnetism" section, this chapter).

In the upper 423.5 mbsf (Quaternary to middle Miocene in age), total organic carbon values at Site 913 are similar to those typical for modern open-ocean environments. In the lowermost Oligocene/upper Eocene to middle Eocene interval, however, the sediments are distinctly enriched in organic carbon. In the lowermost Oligocene/upper Eocene interval, the maximum contents of organic carbon coincide with maximum occurrences of biogenic opal (i.e., diatoms and radiolarians; see "Biostratigraphy" section, this chapter). This may reflect a distinct high-productivity event that also was recorded in the Labrador Sea during that time (ODP Site 647; Bohrmann and Stein, 1989). The maximum organic carbon values in the lowermost part of the sequence characterized by slump deposits (see "Lithostratigraphy" section, this chapter) are probably caused by increased supply of terrigenous material (indicated by maximum C/N ratios of 37). However, more detailed organic geochemical data and fluxes of (marine) organic matter as well as paleontological data are required before more precise paleoenvironmental reconstructions can be performed.

Table 7. Summary of geochemical analyses of sediments from Site 913.

Core, section, interval top (cm)	Depth (mbsf)	TC (%)	IC (%)	TOC (%)	CaCO <sub>3</sub> (%)	TN (%)	TS (%)	C/N	C/S
151-913A-									
1H-1, 64	0.64	1.02	0.81	0.21	6.7	0.06	0.05	3.5	4.2
1H-1, 101	1.01	0.97	0.65	0.32	5.4		0.00		
1H-2, 26	1.76	0.98	0.75	0.23	6.2		0.00		
1H-2, 73	2.23	1.08	0.81	0.27	6.7		0.00		
1H-2, 128	2.78	3.17	2.80	0.37	23.3	0.06	0.00	6.2	
3H-1, 80	10.10	0.88	0.48	0.40	4.0		0.09		4.4
3H-2, 81	11.61	0.83	0.42	0.41	3.5	0.04	0.22	10.2	1.9
3H-3, 81	13.11	1.06	0.52	0.54	4.3		0.16		3.4
3H-4, 82	14.62	0.87	0.50	0.37	4.2		0.18		2.1
3H-5, 82	16.12	0.76	0.54	0.22	4.5		0.22		1.0
4H-1, 130	18.90	0.89	0.53	0.36	4.4		0.17		2.1
4H-3, 72	21.32	0.84	0.51	0.33	4.2		0.15		2.2
5H-1, 17	23.77	0.85	0.50	0.35	4.2	0.08	0.22	4.4	1.6
5H-3, 10	25.79	0.72	0.50	0.22	4.2	0.08	0.15	2.8	1.5
7X-1, 16	36.26	0.85	0.50	0.35	4.2	0.08	0.09	4.4	3.9
9X-1, 106	56.56	1.09	0.50	0.59	4.2	0.08	0.20	7.4	3.0
151-913B-									
3R-1, 22	105.42	0.77	0.39	0.38	3.2	0.06	0.00	6.3	
5R-CC, 9	124.59	0.41	0.11	0.30	0.9	0.08	0.00	3.8	
7R-1, 15	143.95	0.44	0.02	0.42	0.2	0.09		4.7	
7R-1, 52	144.32	0.22	0.04	0.18	0.3	0.09		2.0	
7R-1, 59	144.39	0.20	0.04	0.16	0.3	0.08		2.0	
7R-1, 69	144.49	0.24	0.04	0.20	0.3	0.07		2.9	
7R-1, 86	144.66	0.57	0.17	0.40	1.4	0.07		5.7	
7R-1, 98	144.78	0.80	0.11	0.69	0.9	0.10		6.9	
7R-1, 110	144.90	1.86	1.27	0.59	10.6	0.07		8.4	
7R-1, 132	145.12	1.11	0.73	0.38	6.1	0.07		5.4	
8R-1, 10	153.50	0.17	0.04	0.13	0.3				
8R-1, 69	154.09	0.33	0.15	0.18	1.2		0.12		1.5
9R-1, 22	163.32	0.42	0.12	0.30	1.0		0.16		1.9
11R-CC, 0	220.80	1.05	0.59	0.46	4.9	0.08	0.07	5.8	6.6
19W-1, 120	376.40	0.14	0.04	0.10	0.3	0.05	0.10	2.0	1.0
19W-3, 27	378.47	0.05	0.04	0.01	0.3		0.13		0.1
19W-3, 61	378.81		0.03		0.2				
19W-5, 26	381.46		0.05		0.4				
20R-1, 27	423.77	0.16	0.05	0.11	0.4	0.05	0.06	2.2	1.8
20R-2, 72	425.72		0.01		0.1				
20R-3, 33	426.83		0.05		0.4				
21R-1, 71	433.81	0.25	0.04	0.21	0.3	0.06	0.09	3.5	2.3
21R-3, 72	436.82	0.45	0.06	0.39	0.5	0.06	0.09	6.5	4.3
22R-1, 77	443.57	0.10	0.06	0.04	0.5		0.07		0.6
22R-2, 22	444.52	0.36	0.28	0.08	2.3		0.08		1.0
22R-3, 77	446.57		0.06		0.5				
22R-3, 78	446.58		0.05		0.4				
22R-3, 145	447.25		0.13		1.1				
22R-4, 72	448.02	1.00	0.75	0.25	6.2		0.11		2.3
22R-4, 102	448.32	0.04	0.07		0.6		0.20		
23R-1, 0	452.40		0.06		0.5				
23R-1, 23	452.63	0.21	0.05	0.16	0.4		0.06		2.7
23R-1, 72	453.12	0.02	0.01	0.01	0.1		0.00		
24R-1, 29	462.29	0.40	0.06	0.34	0.5		0.17		2.0
24R-2, 21	463.71	0.11	0.08	0.03	0.7		0.08		0.4
24R-2, 33	463.83	0.02	0.06		0.5		0.06		
24R-3, 29	465.29	0.13	0.03	0.10	0.2		0.04		2.5
24R-4, 0	466.50		0.03		0.2				
24R-4, 134	467.84		0.02		0.2				
24R-4, 139	467.89	0.46	0.03	0.43	0.2		0.57		0.8
24R-4, 143	467.93	0.62	0.06	0.56	0.5		2.10		0.3
24R-4, 145	467.95		0.01		0.1				
24R-5, 94	468.94	0.46	0.05	0.41	0.4		0.67		0.6
25R-1, 47	472.07	0.71	0.02	0.69	0.2		1.60		0.4
25R-3, 16	474.76	0.76	0.06	0.70	0.5		1.35		0.5
25R-5, 19	477.79	1.00	0.06	0.94	0.5		0.81		1.2
25R-6, 0	479.10		0.03		0.2				
25R-7, 67	481.27	0.26	0.05	0.21	0.4		0.17		1.2
27R-1, 39	491.09	0.16	0.06	0.10	0.5		0.18		0.6
27R-3, 96	494.66	0.17	0.06	0.11	0.5	0.05	0.10	2.2	1.1
27R-5, 0	496.70		0.05		0.4				
27R-5, 139	498.09	0.43	0.06	0.37	0.5	0.05	1.70	7.4	0.2
28R-1, 79	501.09	0.21	0.07	0.14	0.6		0.23		0.6
28R-2, 85	502.65	0.21	0.07	0.14	0.6		0.09		1.6
28R-3, 85	504.15		0.04		0.3				
28R-4, 67	505.47	0.21	0.05	0.16	0.4		0.14		1.1
28R-CC, 4	508.04		0.08		0.7				
29R-1, 67	510.57	0.18	0.04	0.14	0.3		0.10		1.4
29R-2, 101	512.41		0.03		0.2				
29R-3, 97	513.87	0.13	0.09	0.04	0.7		0.07		0.6
29R-4, 69	515.09		0.08		0.7				
29R-5, 87	516.77	0.35	0.08	0.27	0.7		0.11		2.5
30R-1, 32	519.82	0.13	0.01	0.12	0.1		0.14		0.9
30R-2, 47	521.47		0.02		0.2				
30R-3, 47	522.97		0.07		0.6				
30R-4, 48	524.48		0.07		0.6				
30R-5, 40	525.90	1.71	0.06	1.65	0.5	0.11	1.56	15.0	1.1
30R-5, 49	525.99	0.38	0.07	0.31	0.6		1.38		0.2
31R-1, 36	529.56	0.16	0.08	0.08	0.7		0.17		0.5

Table 7 (continued).

Core, section, interval top (cm)	Depth (mbsf)	TC (%)	IC (%)	TOC (%)	CaCO <sub>3</sub> (%)	TN (%)	TS (%)	C/N	C/S
32R-1, 72	539.52	0.44	0.04	0.40	0.3	0.06	0.17	6.7	2.4
32R-2, 86	541.16	2.04	0.07	1.97	0.6	0.14	2.68	14.1	0.7
32R-3, 83	542.66	0.36	0.07	0.29	0.6		0.82		0.4
32R-5, 38	545.32	0.41	0.02	0.39	0.2	0.07	0.42	5.6	0.9
32R-CC, 0	546.31	2.71	0.02	2.69	0.2	0.16	6.34	16.8	0.4
33R-1, 32	548.72	0.52	0.03	0.49	0.2	0.06	0.32	8.2	1.5
33R-5, 23	554.68	0.46	0.01	0.45	0.1		0.32		1.4
34R-1, 23	558.33	0.43	0.05	0.38	0.4	0.06	0.11	6.3	3.5
34R-3, 62	561.83	0.34	0.06	0.28	0.5	0.04	0.08	7.0	3.5
34R-5, 15	564.43	0.17	0.07	0.10	0.6		0.07		1.4
35R-1, 46	568.16	0.44	0.04	0.40	0.3		0.80		0.5
35R-3, 34	571.06	0.61	0.05	0.56	0.4	0.06	0.32	9.3	1.8
35R-5, 37	574.11	0.44	0.07	0.37	0.6	0.08	0.31	4.6	1.2
35R-7, 20	577.00	0.11	0.08	0.03	0.7		0.13		0.2
36R-1, 31	577.71	1.39	1.28	0.11	10.7		0.12		0.9
36R-3, 44	580.83	0.17	0.03	0.14	0.2	0.07	0.13	2.0	1.1
37R-1, 78	587.88	0.17	0.07	0.10	0.6		0.05		2.0
37R-3, 107	591.11	0.21	0.02	0.19	0.2	0.07	0.10	2.7	1.9
37R-5, 35	593.40	0.29	0.02	0.27	0.2				
38R-1, 21	596.91	0.15	0.08	0.07	0.7				
38R-3, 68	599.44	0.24	0.06	0.18	0.5		0.10		1.8
38R-5, 70	602.46	0.27	0.07	0.20	0.6	0.13		1.5	
39R-1, 100	607.40	0.30	0.08	0.22	0.7				
39R-2, 7	607.97	0.24	0.07	0.17	0.6	0.08	0.33	2.1	0.5
39R-3, 53	609.95	0.13	0.07	0.06	0.6	0.06	0.11	1.0	0.5
39R-4, 73	611.65	0.23	0.03	0.20	0.2	0.10	0.15	2.0	1.3
39R-5, 45	612.87	0.13	0.07	0.06	0.6	0.06	0.09	1.0	0.7
39R-6, 69	614.61	0.15	0.09	0.06	0.7	0.06	0.15	1.0	0.4
40R-1, 57	616.57	0.19	0.04	0.15	0.3				
40R-3, 71	619.71	0.18	0.04	0.14	0.3		0.11		1.3
40R-5, 18	622.19	0.69	0.06	0.63	0.5	0.08	0.09	7.9	7.0
40R-7, 18	625.22	0.15	0.06	0.09	0.5		0.12		0.8
41R-1, 21	625.91	0.31	0.05	0.26	0.4	0.07	0.13	3.7	2.0
41R-3, 77	628.64	0.27	0.04	0.19	0.3		0.15		1.3
42R-1, 30	635.70	0.25	0.08	0.17	0.7	0.09	0.38	1.9	0.4
42R-3, 28	638.68	1.14	0.08	1.06	0.7	0.09	1.25	11.8	0.8
42R-3, 130	639.70		0.02		0.2				
42R-5, 75	642.15	0.40	0.09	0.31	0.7	0.08	0.88	3.9	0.4
43R-1, 76	645.86	0.36	0.02	0.34	0.2	0.05	0.23	6.8	1.5
43R-3, 74	648.60	0.29	0.08	0.21	0.7		0.55		0.4
43R-5, 80	651.66	0.89	0.05	0.84	0.4	0.10	0.93	8.4	0.9
44R-1, 19	654.89	0.28	0.07	0.21	0.6		0.80		0.3
44R-3, 69	658.20	0.51	0.10	0.41	0.8		0.71		0.6
44R-5, 29	660.80	0.66	0.07	0.59	0.6		0.56		1.1
45R-1, 29	664.69	0.70	0.11	0.59	0.9	0.08	0.34	7.4	1.7
46R-1, 55	674.65	0.90	0.27	0.63	2.2	0.12	0.36	5.2	1.8
46R-3, 67	677.77	0.74	0.19	0.55	1.6	0.06	0.73	9.2	0.8
47R-1, 79	684.49	0.78	0.05	0.73	0.4	0.06	1.16	12.2	0.6
47R-3, 20	686.90	1.16	0.85	0.31	7.1		0.39		0.8
49R-1, 126	703.96	5.27	0.16	5.11	1.3	0.14	0.80	36.5	6.4
49R-3, 85	706.52	0.73	0.09	0.64	0.7		0.28		2.3
49R-5, 37	709.00	1.31	0.12	1.19	1.0	0.08	1.20	14.9	1.0
50R-1, 56	712.86	2.36	1.29	1.07	10.7		0.73		1.5
50R-3, 95	715.86	0.97	0.11	0.86	0.9		0.50		1.7

Notes: IC = inorganic carbon; CaCO<sub>3</sub> = carbonate; TC = total carbon; TOC = total organic carbon; TN = total nitrogen; TS = total sulfur; C/N = total organic carbon/total nitrogen ratios; C/S = total organic carbon/total sulfur ratios.

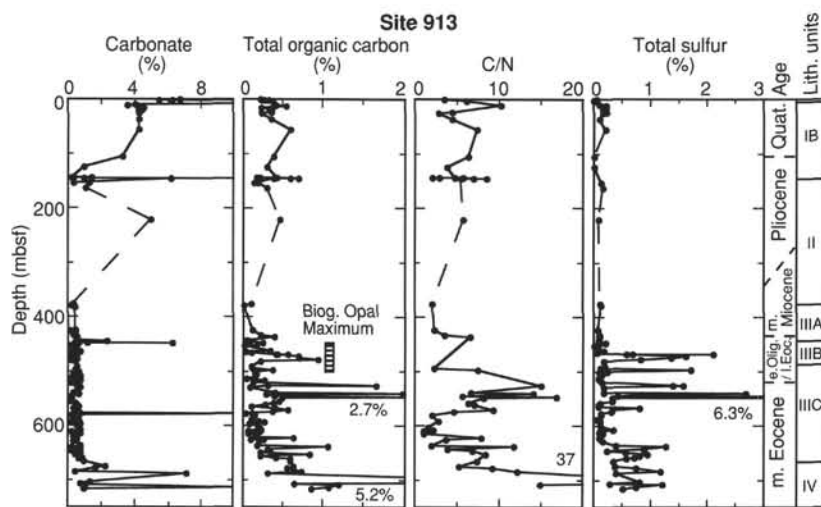


Figure 21. Carbonate contents, total organic carbon contents, organic carbon/total nitrogen (C/N) ratios, and total sulfur contents in sediments at Site 913. Dashed line in the C/N record marks range of dominantly marine organic matter; C/N ratios >10 may suggest significant amounts of terrigenous organic matter.

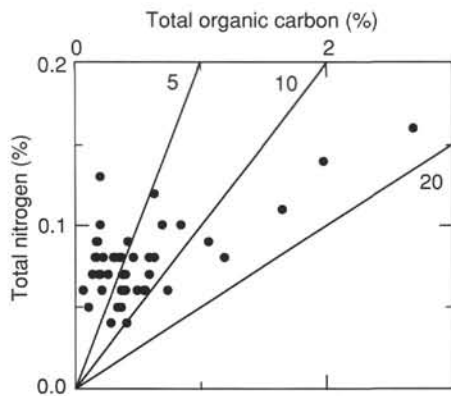


Figure 22. Total organic carbon vs. total nitrogen diagram for Site 913. Lines of C/N ratios of 5, 10, and 20 are indicated.

## PHYSICAL PROPERTIES

### Introduction

The shipboard physical properties program at Site 913 included nondestructive measurements of bulk density, bulk magnetic susceptibility, and total natural gamma activity on whole sections of core using the multi-sensor track (MST), as well as discrete measurements of thermal conductivity, compressional-wave velocities, shear strength, and index properties. Methodology is discussed in the "Explanatory Notes" chapter (this volume).

Two holes were drilled at Site 913 in sediments of Quaternary to Eocene age. Hole 913A consisted of five APC cores and eight XCB cores, penetrating to a depth of 103.6 mbsf with a recovery of 25.3%. Hole 913B was washed to a depth of 86.0 mbsf; then, rotary drilling was alternated with washed coring to 423.5 mbsf, where a significant increase in recovery began with Core 151-913B-20R (47.1%). Rotary drilling continued to the bottom of Hole 913B at 770.3 mbsf. The poor recovery in the upper 423.5 m of Hole 913B created large segments of missing data in the physical property record.

### Whole-core Measurements

The poor recovery in Hole 913A severely limits the value of the multi-sensor track data from this hole. Figure 23 shows records of GRAPE density, magnetic susceptibility, and natural gamma activity for the interval 420–715 mbsf for Hole 913B. The interval ~420–460 mbsf exhibits the highest magnetic susceptibility values in this part of the section, with values generally above 40 uncorrected cgs units. GRAPE densities are in the range 1.5–1.9 g/cm<sup>3</sup>. The interval ~460–480 mbsf is characterized by relatively low values of all three parameters: GRAPE densities drop to a minimum of ~1.1 g/cm<sup>3</sup>, magnetic susceptibilities are close to zero, and natural gamma activities are around 300 counts. Below ~480 mbsf there is an overall trend of increasing GRAPE density, which reaches values greater than 2.00 g/cm<sup>3</sup> at the base of the hole. Natural gamma activity shows a similar trend, rising to values greater than 1000 counts at the base of the hole. Magnetic susceptibility is relatively uniform from ~480 to 665 mbsf, with values of about 20 uncorrected cgs units, and then shows a pattern of greater variability from ~665 mbsf to the base of the hole, with values ranging from near zero to ~100.

The multi-sensor track records correlate well with the lithologic units recognized at this site (see "Lithostratigraphy" section, this chapter). The interval of low GRAPE density, magnetic susceptibility, and natural gamma activity from ~460 to 480 mbsf corresponds to lithologic Subunit IIIB, characterized by biosiliceous clays and siliceous oozes, which were intermittently laminated. The interval of ris-

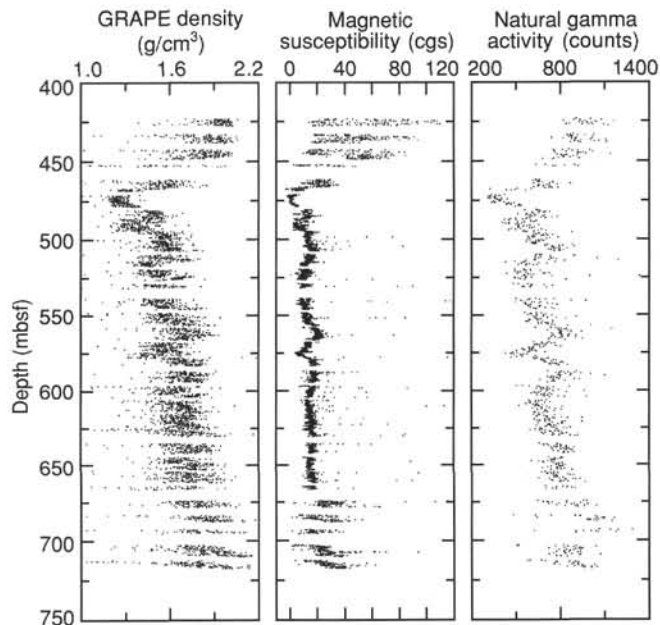


Figure 23. Multi-sensor-track results for Hole 913B.

ing GRAPE density and natural gamma activity from 480 to 680 mbsf corresponds to lithologic Subunit IIIC, characterized by olive green and gray clays, which again were intermittently laminated. The interval of relatively high but fluctuating magnetic susceptibility from 685 mbsf to the base of the hole corresponds to lithologic Unit IV, consisting of alternating layers of laminated and massive silty clays.

### Thermal Conductivity

Thermal conductivity measurements were performed in cores from both Holes 913A and 913B. Measurements were generally performed in four whole-round sections from each core at 75 cm using both a red and black rubber standard (conductivity = 0.96 + 0.05 W/m-K and 0.54 + 0.02 W/m-K, respectively) each time to evaluate the degree of error in the measurements. Thermal conductivities ranged between 0.916 and 2.27 W/m-K ± 0.35 for Hole 913A and 0.533 and 2.795 W/m-K ± 0.36 for Hole 913B (see Table 8). Figures 24 and 25 present plots of thermal conductivity values alongside wet-bulk density, wet water content, and porosity combined from Holes 913A and 913B for 0–175 mbsf and for 350–750 mbsf of Hole 913B. Some of the scatter in thermal conductivity may be caused by variations in the water content and porosity, as lower thermal conductivity correlates with higher water contents and porosity. The average thermal conductivity for Holes 913A and 913B is 1.780 W/m-K and 1.259 W/m-K, respectively (although the value for Hole 913A reflects only the first 94 m of sediment at Site 913).

### Split-core Measurements

#### Compressional Velocity

Velocities were generally higher than at other Leg 151 sites, ranging between 1480 and 1825 m/s (see Table 9). Except for the sediments in the deepest part of Hole 913B, velocities above 2000 m/s were measured only on carbonate concretions.

The sonic transducers of the digital sound velocimeter (DSV) were inserted along the core axis in Cores 151-913A-1H through -7X (0 to 19.60 mbsf). After washing to 86.0 mbsf in Hole 913B, highly consolidated sediment was encountered that precluded use of the

DSV. Therefore, only the Hamilton Frame was used to obtain compressional velocities in Hole 913B. All measurements on Hole 913B sediments were performed using pieces of core removed from the liner. Because the sediments showed such fine lamination, acoustic anisotropy was anticipated. Therefore, several measurements were performed in which the propagation path was both perpendicular and parallel to the bedding planes. These direction-dependent propagation values allow a measure of anisotropy to be determined. In the interval ~460–700 mbsf, the degree of compressional-wave anisotropy is approximately 10%. Velocity measurements are presented in Table 9 and shown in Figure 26 alongside wet-bulk density, porosity, and strength, and in Figure 27 alongside dry-bulk density, void ratio, and dry water content.

### *Shear Strength*

Both the mechanical vane shear and the hand-held penetrometer were used to measure strength where possible to provide a means of

comparison between the two instruments. Strength measurements were performed as deep as Section 151-913A-10X-1 (to 65.64 mbsf) of Hole 913A and to 151-913B-10W-CC (to 173.8 mbsf) in Hole 913B. The data are presented in Table 10. The vane shear measurements from both holes are combined in Figure 26 and plotted alongside wet-bulk density, velocity, and porosity.

### **Index Properties**

Index properties were determined by gravimetric methods using discrete samples taken at a rate of two samples/core section in each hole at Site 913. Values of index properties from both methods are presented in Table 11. Figure 28 presents the wet-bulk density, grain density, wet water content, and porosity. Figure 27 shows dry-bulk density, velocity, void ratio, and dry water content.

### **MS 151IR-111**

**NOTE:** For all sites drilled, core-description forms (“barrel sheets”) and core photographs can be found in Section 6, beginning on page 465. Forms containing smear-slide data can be found in Section 7, beginning on page 849. Thin-section descriptions are given in Section 8, beginning on page 885, and sediment thin sections in Section 9, beginning on page 895. Dropstone descriptions are included in Section 10, beginning on page 903.

Table 8. Thermal conductivity measurements from Holes 913A and 913B.

Core, section, interval top (cm)	Depth (mbsf)	M	P #	TC <sub>corr</sub> (W/m-K)	Std dev (W/m-K)	Drift (°C/min)
151-913A-						
1H-1, 50	0.50	F	332	1.215	0.00217	0.027
1H-1, 100	1.00	F	338	0.916	0.00391	-0.017
1H-2, 75	2.25	F	339	1.409	0.00218	0.023
1H-2, 75	2.25	F	339	1.437	0.00166	0.027
3H-2, 75	11.55	F	332	1.747	0.00098	0.029
3H-3, 75	13.05	F	338	1.639	0.00209	0.024
3H-3, 75	13.05	F	338	1.686	0.00180	0.029
4H-1, 75	18.35	F	332	2.027	0.00199	0.020
4H-2, 75	19.85	F	338	2.002	0.00215	0.036
4H-3, 75	21.35	F	339	2.274	0.00226	0.025
4H-4, 75	22.85	F	350	2.070	0.00298	0.006
5H-1, 50	24.10	F	332	2.252	0.00235	0.028
5H-1, 0	24.60	F	338	1.867	0.00417	0.027
5H-3, 25	25.94	F	350	2.167	0.00217	-0.002
9X-1, 25	55.75	F	332	1.900	0.00285	0.033
9X-1, 25	55.75	F	332	1.843	0.00198	0.029
9X-1, 37	55.87	F	338	1.643	0.00321	0.010
10X-1, 25	65.35	F	332	1.863	0.00222	0.037
10X-1, 48	65.58	F	338	1.858	0.00302	0.019
151-913B-						
7R-1, 80	144.60	F	332	1.622	0.00359	0.010
7R-1, 116	144.96	F	338	1.138	0.00316	-0.017
8R-1, 25	153.65	F	339	1.418	0.00360	0.028
8R-1, 53	153.93	F	350	1.479	0.00335	0.005
9R-1, 25	163.35	F	332	2.100	0.00343	0.013
9R-1, 50	163.60	F	338	1.431	0.00388	-0.011
9R-1, 75	163.85	F	339	1.748	0.00527	0.019
9R-1, 100	164.10	F	350	2.668	0.00245	0.038
19W-1, 25	375.45	F	332	1.561	0.00333	0.039
19W-2, 15	376.85	F	338	1.415	0.00252	0.010
19W-3, 25	378.45	F	332	1.008	0.00197	0.021
19W-5, 20	381.40	F	350	1.049	0.00641	0.006
20R-1, 50	424.00	F	332	1.251	0.00174	0.034
21R-3, 50	436.60	F	350	1.196	0.00285	0.037
22R-1, 130	444.10	F	332	1.165	0.00211	0.013
22R-2, 105	445.35	F	338	1.483	0.00282	0.027
22R-3, 85	446.65	F	339	1.105	0.00483	0.025
24R-4, 19	466.69	F	339	1.189	0.00733	0.035
25R-1, 45	472.05	F	332	0.884	0.00304	0.016
25R-2, 70	473.80	F	338	0.610	0.00642	-0.037
25R-4, 80	476.90	F	350	0.992	0.00264	0.039
26R-1, 74	481.84	F	332	1.035	0.00306	0.033
26R-2, 68	483.28	F	338	0.995	0.00811	0.013
26R-4, 85	486.45	F	350	0.927	0.01241	-0.030
27R-2, 75	492.95	F	332	1.115	0.00322	0.031
27R-3, 75	494.45	F	338	0.951	0.00322	0.034
27R-4, 75	495.95	F	339	1.112	0.00259	0.025
30R-2, 65	521.65	F	332	1.027	0.00315	0.012
30R-3, 65	523.15	F	338	1.174	0.00313	0.012
30R-4, 65	524.65	F	339	0.980	0.00433	-0.014
30R-5, 65	526.15	F	350	1.253	0.00152	0.042
31R-1, 75	529.95	F	332	1.108	0.00269	0.033
31R-2, 75	531.45	F	338	1.169	0.00357	0.013
32R-2, 25	540.55	F	332	1.129	0.00231	0.015
32R-3, 75	542.58	F	338	1.147	0.00301	-0.034
32R-4, 75	544.14	F	339	1.135	0.00459	0.030
32R-5, 60	545.54	F	350	1.208	0.00318	-0.005
33R-2, 50	550.40	F	332	1.189	0.00285	0.024
33R-3, 30	551.70	F	338	1.148	0.00487	0.012
33R-5, 80	555.25	F	350	0.825	0.00163	0.015
33R-5, 80	555.25	F	350	0.825	0.00163	0.015
34R-2, 75	560.40	F	332	1.197	0.00342	0.028
34R-4, 75	563.49	F	339	1.298	0.00403	0.037
35R-2, 75	569.96	F	332	1.110	0.00197	0.028
35R-4, 75	572.99	F	339	1.135	0.00260	-0.005
35R-5, 75	574.49	F	350	1.392	0.00238	0.030
36R-1, 75	578.15	F	332	0.936	0.00301	0.032
36R-3, 75	581.14	F	339	0.895	0.00380	0.022
36R-4, 75	582.66	F	350	0.783	0.00385	-0.000
37R-2, 75	589.29	F	332	1.111	0.00304	0.004
37R-4, 75	592.29	F	339	1.414	0.00278	0.033
37R-5, 75	593.80	F	350	1.248	0.00147	0.024
38R-2, 75	598.01	F	332	1.054	0.00284	0.037
38R-3, 75	599.51	F	338	1.107	0.00314	0.010
38R-4, 75	601.01	F	339	0.952	0.01028	-0.006
39R-2, 75	608.65	F	332	1.093	0.00277	0.009
40R-2, 75	618.25	F	332	1.116	0.00291	0.028
40R-4, 75	621.26	F	339	1.029	0.00403	0.040
41R-2, 75	627.12	F	332	1.110	0.00346	0.025
41R-3, 75	628.57	F	338	1.210	0.00277	0.005
41R-4, 75	630.02	F	339	1.256	0.00405	0.036
43R-2, 75	647.11	F	332	1.126	0.00265	0.038
43R-3, 75	648.61	F	338	1.107	0.00285	0.010
43R-4, 75	650.11	F	339	1.149	0.00228	0.018
44R-2, 75	656.76	F	332	0.988	0.00370	0.005
44R-2, 75	656.76	F	332	0.977	0.00366	0.001

Table 8 (continued).

Core, section, interval top (cm)	Depth (mbsf)	M	P #	TC <sub>corr</sub> (W/m-K)	Std dev (W/m-K)	Drift (°C/min)
44R-3, 75	658.26	F	338	1.479	0.00391	0.025
44R-3, 75	658.26	F	338	1.373	0.00312	0.012
44R-4, 75	659.76	F	339	1.464	0.00467	0.014
44R-4, 75	659.76	F	339	1.520	0.00437	0.022
44R-5, 75	661.26	F	350	1.840	0.01078	0.024
44R-5, 75	661.26	F	350	1.484	0.00884	-0.027
47R-1, 75	684.45	F	332	1.789	0.00229	0.022
47R-2, 75	685.95	F	338	1.361	0.00686	0.024
47R-3, 75	687.45	F	339	1.218	0.00267	0.018
48R-1, 30	693.30	F	332	1.373	0.00271	0.038
48R-2, 30	694.27	F	338	1.100	0.00580	-0.013
48R-2, 100	694.97	F	339	1.131	0.00173	0.028
49R-2, 75	704.95	F	332	1.464	0.00323	0.035
49R-3, 75	706.42	F	338	1.282	0.00329	0.035
49R-4, 45	707.58	F	339	1.395	0.00257	0.010
49R-4, 105	708.18	F	349	2.315	0.00203	0.010
50R-2, 30	713.67	F	332	1.449	0.00198	0.013
50R-2, 100	714.37	F	338	1.253	0.00199	-0.020

Notes: M = method used, either F = full-space or H = half-space; P # = probe number used for test; TC<sub>corr</sub> = thermal conductivity corrected for drift; Std dev = standard deviation of the measurement.

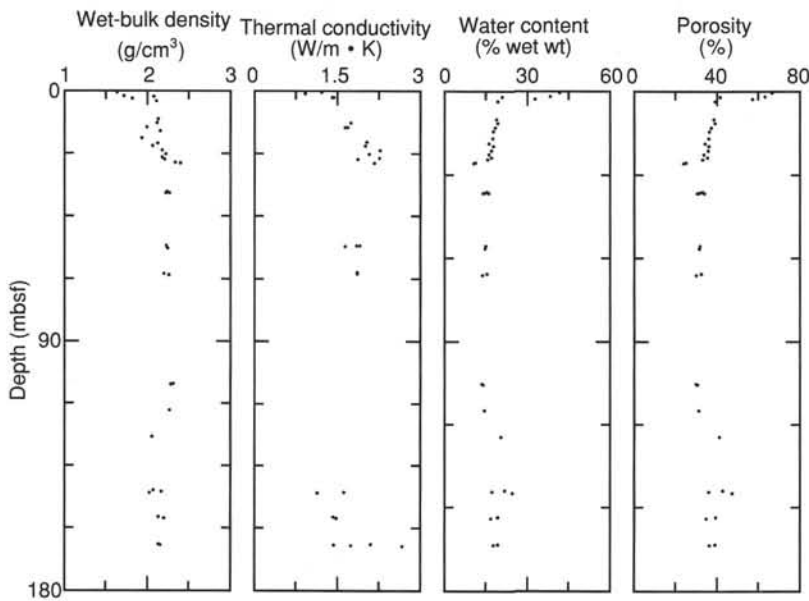


Figure 24. Wet-bulk density (Method B), thermal conductivity, wet water content, and porosity from Holes 913A and 913B (shallow depths).

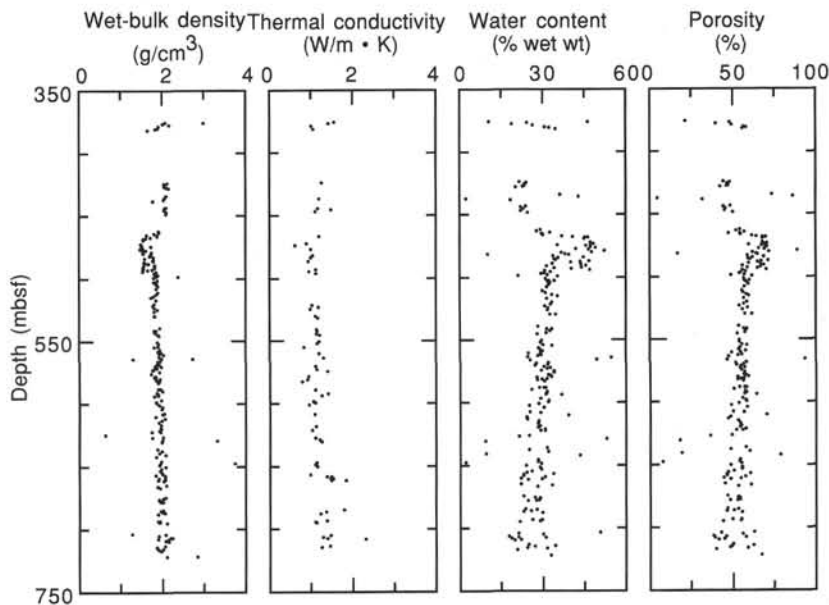


Figure 25. Wet-bulk density (Method B), thermal conductivity, wet water content, and porosity from Hole 913B.

Table 9. Compressional-wave velocity measurements from Hole 913A and 913B.

Core, section, interval (cm)	Depth (mbsf)	Tool	Velocity (m/s)		Core, section, interval (cm)	Depth (mbsf)	Tool	Velocity (m/s)	
			Perp	Par				Perp	Par
151-913A-					27R-2, 137-139	493.57	ham		1686
1H-1, 48-55	0.48	dsv	1536		27R-3, 28-30	493.98	ham	1631	
1H-2, 119-126	2.69	dsv	1640		27R-3, 28-30	493.98	ham		1625
2X-CC, 2-9	4.38	dsv	1606		28R-2, 108-110	502.88	ham	2217	
3H-1, 75-82	10.05	dsv	1604		28R-2, 108-110	502.88	ham	1712	
3H-3, 18-25	12.48	dsv	1655		28R-3, 20-22	503.50	ham	1659	
4H-2, 50-57	19.60	dsv	1492		29R-4, 62-64	515.02	ham	1671	
151-913B-					29R-4, 62-64	515.02	ham		1745
3R-1, 22-24	105.42	ham	1824		29R-5, 26-28	516.16	ham	1629	
5R-CC, 6-8	124.56	ham	1721		30R-1, 133-135	520.83	ham	1633	
7R-1, 20-22	144.00	ham	1754		30R-2, 114-116	522.14	ham	1664	
7R-1, 113-115	144.93	ham	1596		30R-5, 42-44	525.92	ham	1766	
9R-1, 20-22	163.30	ham	1662		31R-1, 40-42	529.60	ham	1635	
9R-1, 57-59	163.67	ham	1722		31R-1, 105-107	530.25	ham	1663	
13W-1, 90-92	240.90	ham	1772		31R-2, 28-30	530.98	ham	2425	
19W-1, 20-22	375.40	ham	1695		32R-1, 145-147	540.25	ham	1647	
19W-1, 120-122	376.40	ham	1640		32R-2, 102-104	541.32	ham	1623	
19W-2, 54-56	377.24	ham	1713		32R-2, 102-104	541.32	ham		1711
19W-3, 66-68	378.86	ham	1594		32R-3, 45-47	542.28	ham	1601	
19W-4, 66-68	380.36	ham	1640		33R-2, 104-106	550.94	ham	1632	
20R-1, 12-14	423.62	ham	1614		33R-2, 121-123	551.11	ham		1585
20R-3, 77-79	427.27	ham	1613		33R-2, 121-123	551.11	ham	1623	
21R-1, 99-101	434.09	ham	1667		33R-4, 125-127	554.15	ham	1590	
21R-4, 88-90	438.48	ham	1644		34R-4, 85-87	563.59	ham	1638	
22R-1, 32-34	443.12	ham	1713		34R-4, 90-92	563.64	ham	1613	
22R-1, 145-147	444.25	ham	1688		34R-6, 53-55	566.35	ham	1591	
22R-2, 133-135	445.63	ham	1651		34R-6, 53-55	566.35	ham		1617
22R-4, 5-7	447.35	ham	1726		35R-1, 86-88	568.56	ham	1581	
23R-1, 95-97	453.35	ham	1671		35R-1, 86-88	568.56	ham		1648
24R-2, 44-46	463.94	ham		2006	35R-6, 31-33	575.55	ham		1650
24R-4, 144-146	467.94	ham	1531		35R-6, 31-33	575.55	ham	1624	
24R-5, 101-103	469.01	ham	1722		35R-7, 15-17	576.89	ham	1677	
24R-5, 101-103	469.01	ham		1580	35R-7, 15-17	576.89	ham		1688
25R-1, 47-49	472.07	ham	1585		36R-1, 9-11	577.49	ham	1676	
25R-1, 47-49	472.07	ham		1756	36R-1, 9-11	577.49	ham		1710
25R-3, 98-100	475.58	ham	1572		36R-1, 79-81	578.19	ham	1557	
25R-3, 98-100	475.58	ham		1757	36R-3, 58-60	580.97	ham		1697
25R-6, 57-59	479.67	ham	1591		36R-3, 58-60	580.97	ham	1587	
25R-6, 57-59	479.67	ham		1713	37R-1, 63-65	587.73	ham	1647	
26R-2, 136-138	483.96	ham	1556		37R-2, 103-105	589.57	ham	1634	
26R-2, 136-138	483.96	ham		1752	38R-4, 94-96	601.20	ham	1773	
26R-4, 89-91	486.49	ham		1716	38R-4, 94-96	601.20	ham		1847
26R-4, 89-91	486.49	ham	1588		39R-2, 20-22	608.10	ham	1482	
26R-6, 103-105	489.63	ham		1781	39R-3, 42-44	609.84	ham	1601	
26R-6, 103-105	489.63	ham	1625		39R-3, 103-105	610.45	ham	2491	
26R-6, 125-127	489.85	ham		1752	39R-5, 132-134	613.74	ham	1687	
26R-6, 125-127	489.85	ham	1606		40R-2, 45-47	617.95	ham	1707	
27R-1, 138-140	492.08	ham	1600		40R-6, 99-101	624.53	ham	1724	
27R-1, 138-140	492.08	ham		1723	41R-2, 123-125	627.60	ham	1746	
27R-1, 141-143	492.11	ham		1703	41R-2, 145-147	627.82	ham	3286	
27R-1, 141-143	492.11	ham	1618		41R-4, 26-28	629.53	ham	1673	
27R-2, 137-139	493.57	ham	1591		42R-1, 62-64	636.02	ham	1651	
					42R-5, 133-135	642.33	ham	1640	

Table 9 (continued).

Core, section, interval (cm)	Depth (mbsf)	Tool	Velocity (m/s)	
			Perp	Par
43R-1, 34-36	645.44	ham	1743	
43R-2, 142-144	647.78	ham	3239	
44R-1, 91-93	655.61	ham	1630	
44R-3, 114-116	658.65	ham	1637	
44R-5, 36-38	660.87	ham	1491	
45R-2, 103-105	666.35	ham	1696	
46R-2, 90-92	676.50	ham	1671	
46R-2, 104-106	676.64	ham	1557	
47R-2, 41-43	685.61	ham	1543	
47R-2, 96-98	686.16	ham	1578	
47R-3, 23-25	686.93	ham	1543	
48R-1, 17-19	693.17	ham	1610	
48R-2, 21-23	694.18	ham	1500	
49R-1, 61-63	703.31	ham	1640	
49R-1, 61-63	703.31	ham		1605
49R-2, 130-132	705.50	ham	1650	
50R-1, 54-56	712.84	ham	1539	
50R-3, 91-93	715.67	ham	1585	
50R-4, 59-61	716.74	ham	1660	
51R-1, 10-12	722.00	ham		4008

Notes: Tool = device used for measurement, either dsv = digital sound velocimeter or ham = Hamilton Frame. Perp = perpendicular, Par = parallel. — = no data.

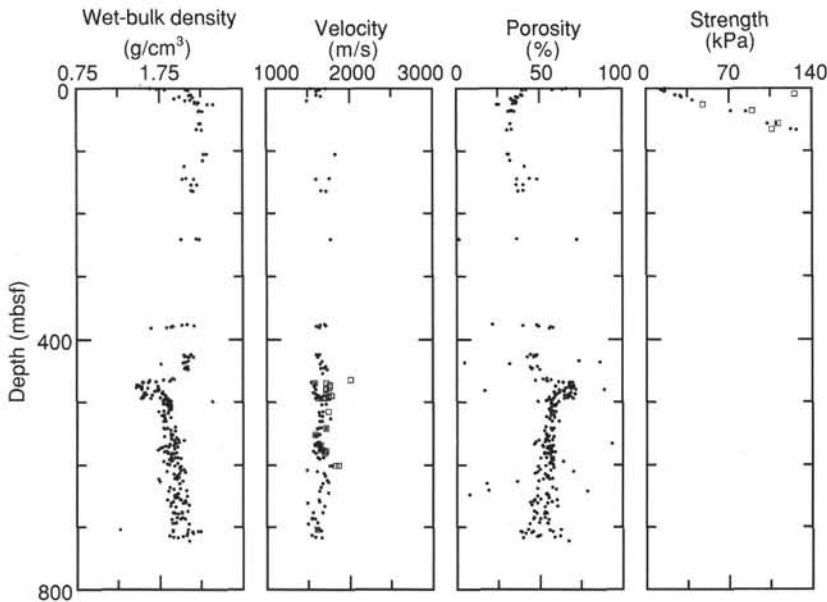


Figure 26. Wet-bulk density (Method B), velocity (closed circles = perpendicular to the bedding plane; open squares = parallel to the bedding plane), porosity (Method C), and vane shear strength ( $y = 9.137 + 1.7544x$ ;  $R = 0.99605$ ) from Holes 913A and 913B.

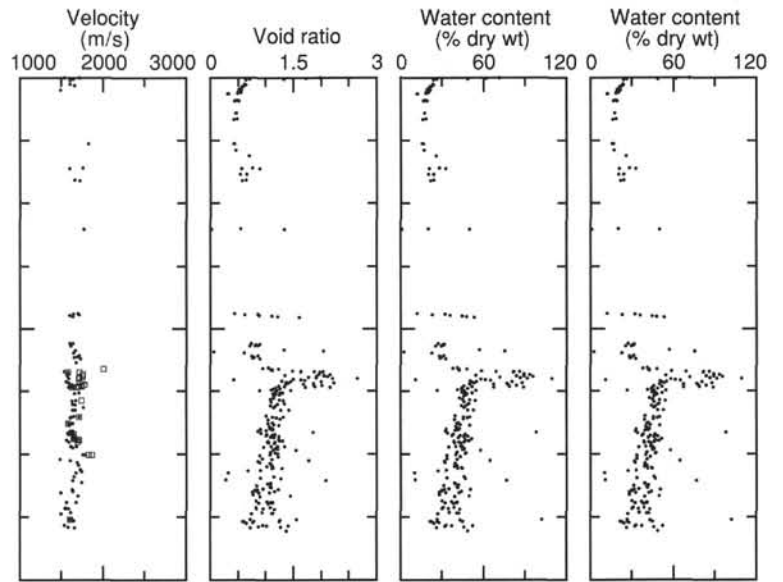


Figure 27. Dry-bulk density (Method C), velocity (symbols as in Fig. 26), void ratio (Method C), and dry water content from Holes 913A and 913B.

Table 10. Shear strength measurements, Site 913.

Core, section, interval (cm)	Depth (mbsf)	SN	Vane (kPa)	Res (kPa)	Pen (kPa)
151-913A-					
1H-1, 87-88	0.87	3	16	8	
1H-1, 99-100	0.99	3	12	10	
1H-2, 119-120	2.69	3	13		
2X-0, 10-11	4.50	3	15		
2X-0, 5-6	4.45	3	16		
3H-1, 112-113	10.42	3	25		
3H-2, 66-67	11.46	3	29	12	
3H-3, 74-75	13.04	3	30	10	
4H-1, 132-133	18.92	3	39	13	
7X-1, 37-38	36.47	3	72		90
9X-1, 63-64	56.13	3			112
9X-1, 121-122	56.71	3	103	32	
10X-1, 49-50	65.59	3	122		
10X-1, 55-56	65.64				106
151-913B-					
3R-1, 12-13	105.32				126
5R-CC, 7-8	124.57				98
7R-1, 109-110	144.89	3	84	27	
9R-1, 62-63	163.72	3	110	46	
10W-CC, 1-2	173.81	3	127		

Notes: SN = numbered spring used to make the measurement. Vane = undrained shear strength; Res = residual shear strength; Pen = unconfined shear strength as measured by the penetrometer.

Table II. Index properties of samples from Holes 913A and 913B.

Core, section, interval (cm)	Depth (mbsf)	WC-d (%)	WC-w (%)	WBD <sup>a</sup> (g/cm <sup>3</sup> )	WBD <sup>b</sup> (g/cm <sup>3</sup> )	GD <sup>a</sup> (g/cm <sup>3</sup> )	GD <sup>b</sup> (g/cm <sup>3</sup> )	DBD <sup>a</sup> (g/cm <sup>3</sup> )	DBD <sup>b</sup> (g/cm <sup>3</sup> )	Por <sup>a</sup> (%)	Por <sup>b</sup> (%)	VR <sup>a</sup>	VR <sup>b</sup>
151-913A-													
1H-1, 66-68	0.66	71.70	41.76	1.64	1.63	2.86	2.84	0.95	0.95	66.66	66.55	2.00	1.99
1H-2, 29-31	1.79	61.79	38.19	1.72	1.70	2.96	2.87	1.06	1.05	64.06	63.37	1.78	1.73
1H-2, 73-75	2.23	26.28	20.81	2.08	2.05	2.84	2.77	1.64	1.62	42.15	41.55	0.73	0.71
1H-2, 129-131	2.79	48.75	32.77	1.82	1.79	2.93	2.80	1.22	1.20	58.22	57.08	1.39	1.33
1H-3, 66-68	3.66	23.90	19.29	2.11	2.07	2.81	2.74	1.70	1.67	39.63	39.01	0.66	0.64
3H-1, 74-76	10.04	23.13	18.79	2.14	2.10	2.85	2.76	1.73	1.70	39.15	38.41	0.64	0.62
3H-2, 75-77	11.55	23.85	19.25	2.11	2.08	2.83	2.76	1.71	1.68	39.67	39.11	0.66	0.64
3H-3, 75-77	13.05	22.66	18.47	2.00	2.08	2.54	2.71	1.63	1.69	35.95	37.44	0.56	0.60
3H-4, 75-77	14.55	21.32	17.57	2.16	2.11	2.82	2.73	1.78	1.74	36.99	36.25	0.59	0.57
3H-6, 25-27	17.05	21.00	17.36	1.93	2.13	2.37	2.75	1.60	1.76	32.72	36.07	0.49	0.56
4H-1, 127-129	18.87	19.28	16.16	2.12	2.17	2.68	2.77	1.78	1.82	33.48	34.28	0.50	0.52
4H-2, 74-76	19.84	21.49	17.69	2.06	2.09	2.63	2.69	1.70	1.72	35.58	36.10	0.55	0.57
4H-3, 74-76	21.34	20.58	17.07	2.18	2.14	2.84	2.76	1.81	1.78	36.31	35.70	0.57	0.56
4H-4, 73-75	22.83	19.04	15.99	2.22	2.15	2.86	2.72	1.87	1.81	34.68	33.53	0.53	0.50
5H-1, 15-17	23.75	20.33	16.89	2.18	2.14	2.82	2.75	1.81	1.78	35.87	35.32	0.56	0.55
5H-1, 100-102	24.60	18.63	15.70	2.21	2.17	2.82	2.73	1.86	1.83	33.85	33.19	0.51	0.50
5H-2, 50-52	25.60	12.59	11.18	2.33	2.30	2.78	2.73	2.07	2.04	25.47	25.11	0.34	0.34
5H-3, 12-14	25.81	11.71	10.48	2.40	2.34	2.84	2.76	2.15	2.10	24.52	23.96	0.32	0.32
7X-1, 14-16	36.24	18.29	15.46	2.23	2.18	2.85	2.75	1.89	1.85	33.70	32.96	0.51	0.49
7X-1, 38-40	36.48	17.57	14.94	2.23	2.18	2.82	2.72	1.90	1.86	32.57	31.82	0.48	0.47
7X-1, 51-53	36.61	16.47	14.14	2.27	2.21	2.82	2.72	1.95	1.89	31.29	30.43	0.46	0.44
7X-0, 13-15	36.78	19.08	16.02	2.23	2.18	2.87	2.78	1.87	1.83	34.80	34.09	0.53	0.52
9X-1, 25-27	55.75	17.63	14.99	2.23	2.18	2.81	2.72	1.90	1.85	32.62	31.86	0.48	0.47
9X-1, 108-110	56.58	17.33	14.77	2.25	2.19	2.83	2.73	1.91	1.87	32.36	31.55	0.48	0.46
10X-1, 71-73	65.81	18.25	15.43	2.20	2.15	2.78	2.69	1.86	1.82	33.12	32.39	0.50	0.48
10X-0, 5-7	66.24	16.07	13.85	2.26	2.21	2.81	2.72	1.95	1.91	30.57	29.91	0.44	0.43
151-913B-													
3R-1, 11-13	105.31	15.60	13.50	2.32	2.27	2.88	2.80	2.00	1.97	30.51	29.92	0.44	0.43
3R-1, 25-27	105.45	16.45	14.13	2.28	2.21	2.85	2.73	1.96	1.90	31.42	30.43	0.46	0.44
4R-0, 2-4	114.92	17.03	14.55	2.27	2.20	2.86	2.73	1.94	1.88	32.20	31.23	0.47	0.45
5R-0, 7-9	124.57	25.67	20.43	2.05	2.08	2.76	2.82	1.63	1.65	40.86	41.37	0.69	0.71
7R-1, 14-16	143.94	27.81	21.76	2.07	2.02	2.89	2.77	1.62	1.58	43.95	42.94	0.78	0.75
7R-1, 60-62	144.40	20.88	17.27	2.17	2.14	2.82	2.76	1.79	1.77	36.50	35.99	0.57	0.56
7R-1, 108-110	144.88	32.59	24.58	2.02	1.97	2.97	2.82	1.53	1.49	48.56	47.26	0.94	0.90
8R-1, 9-11	153.49	23.99	19.35	2.13	2.09	2.88	2.78	1.72	1.68	40.24	39.41	0.67	0.65
8R-1, 64-66	154.04	20.06	16.71	2.20	2.15	2.86	2.75	1.83	1.79	35.90	34.99	0.56	0.54
9R-1, 23-25	163.33	23.82	19.24	2.13	2.09	2.87	2.78	1.72	1.69	40.02	39.26	0.67	0.65
9R-1, 54-56	163.64	21.46	17.67	2.16	2.11	2.82	2.73	1.77	1.74	37.15	36.40	0.59	0.57
13W-1, 10-12	240.10	20.38	16.93	2.20	2.15	2.86	2.76	1.82	1.78	36.25	35.45	0.57	0.55
13W-1, 86-88	240.86	50.06	33.36	2.23	1.76	5.43	2.74	1.49	1.17	72.62	57.25	2.65	1.34
13W-1, 117-119	241.17	0.80	0.79	2.01	2.68	2.03	2.71	2.00	2.65	1.56	2.07	0.02	0.02
19W-1, 22-24	375.42	11.71	10.48	2.08	2.99	2.36	3.85	1.86	2.67	21.26	30.53	0.27	0.44
19W-1, 140-142	376.60	32.24	24.38	2.02	1.95	2.93	2.76	1.52	1.48	47.96	46.43	0.92	0.87
19W-2, 76-78	377.46	23.07	18.75	2.17	2.09	2.92	2.74	1.76	1.70	39.62	38.17	0.66	0.62
19W-3, 63-65	378.83	35.85	26.39	1.91	1.82	2.78	2.51	1.41	1.34	49.25	46.74	0.97	0.88
19W-4, 24-26	379.94	44.28	30.69	1.89	1.76	3.03	2.57	1.31	1.22	56.66	52.58	1.31	1.11
19W-4, 73-75	380.43	47.86	32.37	1.84	1.74	2.96	2.61	1.24	1.18	58.02	54.92	1.38	1.22
19W-5, 28-30	381.48	53.18	34.72	1.65	1.82	2.43	3.10	1.08	1.19	55.78	61.65	1.26	1.61
20R-1, 28-30	423.78	27.30	21.44	2.13	2.03	3.01	2.78	1.67	1.60	44.47	42.51	0.80	0.74
20R-1, 113-115	424.63	31.80	24.13	2.04	2.01	2.99	2.90	1.55	1.53	48.11	47.34	0.93	0.90
20R-2, 32-34	425.32	30.45	23.34	2.05	1.99	2.94	2.79	1.57	1.53	46.61	45.33	0.87	0.83
20R-2, 124-126	426.24	30.40	23.31	2.05	1.98	2.94	2.76	1.57	1.52	46.61	44.97	0.87	0.82
20R-3, 32-34	426.82	30.67	23.47	2.07	2.02	3.02	2.88	1.59	1.55	47.51	46.28	0.91	0.86
20R-3, 76-78	427.26	29.20	22.60	2.10	2.01	3.03	2.79	1.63	1.56	46.33	44.33	0.86	0.80
20R-3, 128-130	427.78	25.20	20.13	2.16	2.11	2.99	2.88	1.72	1.69	42.37	41.47	0.74	0.71
21R-1, 72-74	433.82	56.77	36.21	2.09	1.62	5.10	2.41	1.33	1.03	73.85	57.16	2.82	1.33
21R-2, 72-74	435.32	75.23	42.93	2.06	1.60	8.67	2.78	1.18	0.91	86.42	67.15	6.36	2.04
21R-3, 72-74	436.82	2.30	2.25	2.04	2.71	2.08	2.81	1.99	2.65	4.46	5.93	0.05	0.06
21R-4, 75-77	438.35	22.69	18.49	1.77	2.09	2.12	2.74	1.44	1.70	31.93	37.73	0.47	0.61
22R-1, 32-34	443.12	31.15	23.75	2.09	2.00	3.08	2.84	1.59	1.52	48.39	46.29	0.94	0.86
22R-1, 75-77	443.55	28.11	21.94	2.06	1.99	2.88	2.71	1.61	1.56	44.15	42.64	0.79	0.74
22R-2, 75-77	445.05	29.60	22.84	2.05	1.98	2.91	2.73	1.58	1.53	45.64	44.09	0.84	0.79
22R-3, 75-77	446.55	28.32	22.07	2.09	2.00	2.97	2.74	1.63	1.56	45.04	43.10	0.82	0.76
22R-4, 74-76	448.04	32.62	24.60	2.09	1.97	3.16	2.81	1.58	1.48	50.15	47.25	1.01	0.90
24R-1, 28-30	462.28	41.17	29.16	1.91	1.80	2.95	2.62	1.35	1.28	54.24	51.27	1.19	1.05
24R-1, 101-103	463.01	38.20	27.64	1.93	1.81	2.90	2.55	1.39	1.31	51.98	48.68	1.08	0.95
24R-2, 65-67	464.15	48.05	32.45	1.80	1.75	2.82	2.64	1.21	1.18	56.94	55.32	1.32	1.24
24R-2, 138-140	464.88	42.69	29.92	1.63	1.81	2.17	2.69	1.14	1.27	47.50	52.87	0.90	1.12
24R-3, 29-31	465.29	42.12	29.64	1.88	1.81	2.89	2.68	1.32	1.28	54.32	52.40	1.19	1.10
24R-3, 120-122	466.20	42.78	29.96	1.87	1.81	2.91	2.69	1.31	1.27	54.81	52.91	1.21	1.12
24R-4, 43-45	466.93	58.53	36.92	1.71	1.66	2.80	2.61	1.08	1.05	61.51	59.81	1.60	1.49
24R-4, 114-116	467.64	69.03	40.84	1.61	1.56	2.66	2.43	0.95	0.92	64.15	62.04	1.79	1.63
24R-4, 148-150	467.98	82.21	45.12	1.55	1.48	2.67	2.34	0.85	0.81	68.13	65.23	2.14	1.88
24R-5, 18-20	468.18	86.03	46.25	1.55	1.49	2.77	2.43	0.83	0.80	69.91	67.08	2.32	2.04
24R-5, 93-95	468.93	81.90	45.02	1.54	1.51	2.64	2.48	0.85	0.83	67.82	66.48	2.11	1.98
25R-1, 43-45	472.03	89.49	47.23	1.48	1.44	2.45	2.26	0.78	0.76	68.18	66.36	2.14	1.97
25R-1, 137-139	472.97	93.45	48.31	1.50	1.45	2.63	2.37	0.77	0.75	70.53	68.41	2.39	2.17
25R-2, 52-54	473.62	89.29	47.17	1.51	1.46	2.60	2.36	0.80	0.77	69.37	67.25	2.26	2.05
25R-2, 121-123	474.31	54.54	35.29	1.73	1.67	2.77	2.54	1.12	1.08	59.59	57.52	1.47	1.35
25R-3, 13-15	474.73	84.04	45.67	1.52	1.48	2.54	2.34	0.82	0.80	67.57	65.74	2.08	1.92
25R-3, 98-100	475.58	89.50	47.23	1.53	1.46	2.77	2.36	0.81	0.77	70.72	67.32	2.42	2.06
25R-4, 2-4	476.12	95.82	48.93	1.47	1.42	2.50	2.27	0.75	0.73	70.06	67.97	2.34	2.12
25R-4, 91-93	477.01	72.14	41.91	1.60	1.56	2.71	2.52	0.93	0.91	65.61	63.93	1.91	1.77
25R-5, 18-20	477.78	86.73	46.45	1.53	1.45	2.67	2.27	0.82	0				

Table 11 (continued).

Core, section, interval (cm)	Depth (mbsf)	WC-d (%)	WC-w (%)	WBD <sup>a</sup> (g/cm <sup>3</sup> )	WBD <sup>b</sup> (g/cm <sup>3</sup> )	GD <sup>a</sup> (g/cm <sup>3</sup> )	GD <sup>b</sup> (g/cm <sup>3</sup> )	DBD <sup>a</sup> (g/cm <sup>3</sup> )	DBD <sup>b</sup> (g/cm <sup>3</sup> )	Por <sup>a</sup> (%)	Por <sup>b</sup> (%)	VR <sup>a</sup>	VR <sup>b</sup>
25R-7, 67-69	481.27	61.41	38.05	1.73	1.67	3.01	2.74	1.07	1.04	64.36	62.11	1.81	1.64
26R-1, 9-11	481.19	11.23	10.10	1.71	3.05	1.85	3.91	1.54	2.74	16.84	30.02	0.20	0.43
26R-1, 76-78	481.86	65.11	39.44	1.69	1.64	2.94	2.69	1.03	0.99	65.13	63.12	1.87	1.71
26R-2, 34-36	482.94	50.70	33.64	1.79	1.72	2.89	2.62	1.19	1.14	58.84	56.45	1.43	1.30
26R-2, 127-129	483.87	80.44	44.58	1.58	1.53	2.79	2.55	0.87	0.85	68.66	66.67	2.19	2.00
26R-3, 30-32	484.40	55.08	35.52	1.79	1.71	3.03	2.71	1.15	1.10	61.92	59.25	1.63	1.45
26R-3, 145-147	485.55	51.73	34.09	1.78	1.74	2.88	2.72	1.17	1.15	59.27	57.88	1.46	1.37
26R-4, 37-39	485.97	53.10	34.68	1.79	1.73	2.96	2.72	1.17	1.13	60.53	58.51	1.53	1.41
26R-4, 117-119	486.77	88.14	46.85	1.56	1.51	2.89	2.59	0.83	0.80	71.33	69.03	2.49	2.23
26R-5, 15-17	487.25	76.90	43.47	1.59	1.54	2.76	2.50	0.90	0.87	67.45	65.18	2.07	1.87
26R-5, 95-97	488.05	67.22	40.20	1.66	1.60	2.85	2.57	0.99	0.96	65.14	62.80	1.87	1.69
26R-6, 3-5	488.63	50.20	33.42	1.82	1.77	2.99	2.79	1.21	1.18	59.43	57.75	1.46	1.37
26R-6, 64-66	489.24	77.97	43.81	1.57	1.52	2.66	2.45	0.88	0.86	66.90	65.09	2.02	1.86
26R-7, 34-36	490.44	83.94	45.64	1.54	1.50	2.69	2.46	0.84	0.82	68.77	66.84	2.20	2.02
27R-1, 39-41	491.09	45.79	31.41	1.83	1.80	2.84	2.76	1.25	1.24	55.95	55.25	1.27	1.23
27R-1, 139-141	492.09	78.88	44.10	1.55	1.52	2.60	2.45	0.87	0.85	66.67	65.36	2.00	1.89
27R-2, 35-37	492.55	51.93	34.18	1.76	1.72	2.81	2.64	1.16	1.13	58.74	57.21	1.42	1.34
27R-2, 97-99	493.17	67.52	40.31	1.65	1.61	2.79	2.61	0.98	0.96	64.76	63.22	1.84	1.72
27R-3, 28-30	493.98	88.84	47.04	1.53	1.49	2.73	2.49	0.81	0.79	70.29	68.36	2.37	2.16
27R-3, 96-98	494.66	44.47	30.78	1.86	1.80	2.90	2.72	1.28	1.25	55.71	54.14	1.26	1.18
27R-4, 9-11	495.29	48.71	32.76	1.81	1.75	2.88	2.66	1.22	1.18	57.79	55.88	1.37	1.27
27R-4, 131-133	496.51	43.95	30.53	1.84	1.78	2.82	2.64	1.28	1.24	54.74	53.09	1.21	1.13
27R-5, 56-58	497.26	41.47	29.31	1.89	1.83	2.90	2.71	1.34	1.29	54.02	52.30	1.17	1.10
27R-5, 139-141	498.09	46.02	31.51	1.85	1.77	2.94	2.67	1.27	1.22	56.94	54.55	1.32	1.20
27R-6, 32-34	498.58	26.66	21.05	2.39	2.31	3.70	3.46	1.88	1.82	49.01	47.35	0.96	0.90
27R-6, 86-88	499.12	54.33	35.20	1.79	1.73	3.02	2.76	1.16	1.12	61.53	59.39	1.60	1.46
28R-1, 84-86	501.14	44.62	30.85	1.88	1.80	2.99	2.72	1.30	1.24	56.57	54.17	1.30	1.18
28R-2, 85-87	502.65	47.15	32.04	1.82	1.78	2.86	2.74	1.24	1.21	56.82	55.78	1.32	1.26
28R-2, 99-101	502.79	52.10	34.25	1.79	1.69	2.94	2.56	1.18	1.11	59.90	56.59	1.49	1.30
28R-2, 131-133	503.11	46.49	31.74	1.85	1.72	2.96	2.51	1.26	1.17	57.30	53.26	1.34	1.14
28R-3, 82-84	504.12	48.30	32.57	1.84	1.71	3.00	2.51	1.24	1.15	58.56	54.18	1.41	1.18
28R-4, 68-70	505.48	47.25	32.09	1.89	1.78	3.15	2.72	1.28	1.21	59.22	55.60	1.45	1.25
28R-6, 6-8	507.86	45.91	31.46	1.86	1.74	2.95	2.55	1.27	1.19	56.96	53.27	1.32	1.14
29R-1, 65-67	510.55	42.71	29.93	1.89	1.83	2.96	2.77	1.33	1.29	55.24	53.55	1.23	1.15
29R-2, 102-104	512.42	45.01	31.04	1.86	1.72	2.93	2.49	1.28	1.19	56.30	52.19	1.29	1.09
29R-3, 97-99	513.87	49.82	33.25	1.80	1.71	2.87	2.56	1.20	1.14	58.26	55.46	1.40	1.25
29R-4, 65-67	515.05	54.27	35.18	1.73	1.66	2.77	2.48	1.12	1.07	59.48	56.80	1.47	1.31
29R-5, 84-86	516.74	45.89	31.46	1.85	1.71	2.93	2.46	1.27	1.17	56.73	52.45	1.31	1.10
30R-1, 30-32	519.80	49.69	33.19	1.81	1.77	2.90	2.76	1.21	1.18	58.47	57.22	1.41	1.34
30R-2, 45-47	521.45	48.61	32.71	1.77	1.72	2.75	2.57	1.19	1.16	56.59	54.92	1.30	1.22
30R-3, 44-46	522.94	44.16	30.63	1.80	1.74	2.71	2.53	1.25	1.21	53.91	52.12	1.17	1.09
30R-4, 46-48	524.46	46.91	31.93	1.88	1.73	3.10	2.54	1.28	1.18	58.63	53.79	1.42	1.16
30R-5, 46-48	525.96	46.03	31.52	1.81	1.74	2.79	2.56	1.24	1.19	55.64	53.52	1.25	1.15
31R-1, 30-32	529.50	48.47	32.65	1.80	1.76	2.83	2.69	1.21	1.18	57.27	55.95	1.34	1.27
31R-1, 54-56	529.74	52.79	34.55	1.82	1.74	3.10	2.75	1.19	1.14	61.48	58.63	1.60	1.42
32R-1, 74-76	539.54	39.29	28.21	1.94	1.83	2.98	2.64	1.39	1.31	53.32	50.30	1.14	1.01
32R-2, 86-88	541.16	45.58	31.31	1.85	1.73	2.91	2.53	1.27	1.19	56.39	52.93	1.29	1.12
32R-2, 102-104	541.32	50.00	33.33	1.80	1.75	2.88	2.71	1.20	1.17	58.45	56.93	1.41	1.32
32R-3, 85-87	542.68	48.23	32.54	1.81	1.71	2.89	2.53	1.22	1.15	57.59	54.33	1.36	1.19
32R-4, 85-87	544.24	45.38	31.22	1.88	1.83	3.04	2.86	1.30	1.26	57.40	55.84	1.35	1.26
32R-5, 41-43	545.35	39.00	28.06	1.93	1.87	2.95	2.75	1.39	1.34	52.88	51.09	1.12	1.04
33R-2, 29-31	550.19	41.82	29.49	1.88	1.84	2.88	2.75	1.32	1.29	54.04	52.83	1.18	1.12
33R-3, 35-37	551.75	40.88	29.02	1.91	1.80	2.94	2.61	1.35	1.28	53.99	51.00	1.17	1.04
33R-4, 96-98	553.86	43.08	30.11	1.89	1.81	2.97	2.71	1.32	1.27	55.54	53.29	1.25	1.14
33R-5, 25-27	554.70	49.92	33.30	1.80	1.70	2.89	2.54	1.20	1.14	58.47	55.33	1.41	1.24
33R-6, 57-59	556.52	39.84	28.49	1.95	1.86	3.04	2.74	1.39	1.33	54.15	51.58	1.18	1.07
34R-1, 20-22	558.30	40.95	29.05	1.89	1.84	2.89	2.74	1.34	1.31	53.59	52.28	1.15	1.10
34R-1, 121-123	559.31	42.63	29.89	1.97	1.78	3.26	2.59	1.38	1.25	57.53	51.82	1.35	1.08
34R-2, 61-63	560.26	41.10	29.13	1.93	1.87	3.03	2.82	1.37	1.32	54.82	53.04	1.21	1.13
34R-2, 122-124	560.87	33.00	24.81	2.04	1.96	3.03	2.80	1.53	1.47	49.36	47.42	0.97	0.90
34R-3, 75-77	561.96	41.65	29.40	1.93	1.84	3.05	2.76	1.36	1.30	55.34	52.87	1.24	1.12
34R-3, 141-143	562.62	39.31	28.22	1.93	1.83	2.95	2.63	1.38	1.31	53.07	50.24	1.13	1.01
34R-4, 92-94	563.66	32.55	24.56	1.98	1.94	2.85	2.73	1.50	1.46	47.50	46.43	0.90	0.87
34R-5, 142-144	565.70	97.90	49.47	1.94	1.35	15.54	1.94	0.98	0.68	93.69	64.93	14.84	1.85
34R-6, 47-49	566.29	34.12	25.44	1.87	1.93	2.61	2.77	1.40	1.44	46.51	47.94	0.87	0.92
35R-1, 43-45	568.13	46.69	31.83	1.87	1.74	3.04	2.57	1.27	1.18	58.06	53.90	1.38	1.17
35R-1, 79-81	568.49	37.93	27.50	1.92	1.88	2.88	2.75	1.39	1.36	51.57	50.41	1.06	1.02
35R-2, 34-36	569.55	46.33	31.66	1.82	1.71	2.83	2.48	1.24	1.17	56.09	52.89	1.28	1.12
35R-2, 109-111	570.30	37.13	27.08	1.97	1.90	2.99	2.79	1.44	1.39	52.03	50.27	1.08	1.01
35R-3, 31-33	571.03	43.29	30.21	1.86	1.81	2.88	2.70	1.30	1.26	54.85	53.30	1.22	1.14
35R-3, 140-142	572.12	48.47	32.65	1.78	1.73	2.78	2.61	1.20	1.17	56.84	55.26	1.32	1.24
35R-4, 83-85	573.07	45.96	31.49	1.76	1.70	2.63	2.43	1.21	1.16	54.15	52.14	1.18	1.09
35R-5, 35-37	574.09	41.51	29.33	1.93	1.87	3.04	2.83	1.36	1.32	55.16	53.43	1.23	1.15
35R-6, 90-92	576.14	51.28	33.90	1.73	1.67	2.67	2.47	1.14	1.10	57.14	55.27	1.33	1.24
36R-1, 31-33	577.71	46.59	31.78	1.83	1.78	2.88	2.71	1.25	1.21	56.73	55.19	1.31	1.23
36R-1, 115-117	578.55	49.06	32.91	1.80	1.73	2.87	2.60	1.21	1.16	57.88	55.46	1.37	1.25
36R-2, 38-40	579.26	49.40	33.07	1.84	1.76	3.03	2.71	1.23	1.18	59.32	56.64	1.46	1.31
36R-2, 118-120	580.06	38.46	27.78	1.95	1.88	2.97	2.77	1.40	1.36	52.72	51.00	1.11	1.04
36R-3, 48-50	580.87	45.83	31.43	1.85	1.76	2.93	2.61	1.27	1.20	56.72	53.83	1.31	1.17
36R-3, 101-103	581.40	42.07	29.61	1.90	1.75	2.96	2.50	1.34	1.23	54.81	50.68	1.21	1.03
36R-4, 16-18	582.07	39.00	28.06	1.92	1.88	2.91	2.77	1.38	1.35	52.55	51.35	1.11	1.06
36R-4, 98-100	582.89	43.80	30.46	1.89	1.81	3.01	2.72	1.32	1.26	56.23	53.72	1.28	1.16
37R-1, 82-84	587.92	43.60	30.36	1.96	1.93	3.26</							

Table 11 (continued).

Core, section, interval (cm)	Depth (mbsf)	WC-d (%)	WC-w (%)	WBD <sup>a</sup> (g/cm <sup>3</sup> )	WBD <sup>b</sup> (g/cm <sup>3</sup> )	GD <sup>a</sup> (g/cm <sup>3</sup> )	GD <sup>b</sup> (g/cm <sup>3</sup> )	DBD <sup>a</sup> (g/cm <sup>3</sup> )	DBD <sup>b</sup> (g/cm <sup>3</sup> )	Por <sup>a</sup> (%)	Por <sup>b</sup> (%)	VR <sup>a</sup>	VR <sup>b</sup>
38R-2, 71-73	597.97	47.13	32.03	1.85	1.73	2.97	2.54	1.26	1.17	57.73	53.92	1.37	1.17
38R-3, 71-73	599.47	46.88	31.92	1.86	1.76	3.02	2.66	1.27	1.20	58.01	54.85	1.38	1.21
38R-4, 70-72	600.96	39.80	28.47	1.93	1.86	2.97	2.76	1.38	1.33	53.59	51.76	1.15	1.07
38R-5, 70-72	602.46	33.49	25.09	2.00	1.93	2.95	2.75	1.50	1.45	49.04	47.35	0.96	0.90
38R-6, 71-73	603.97	43.18	30.16	1.99	1.87	3.36	2.90	1.39	1.31	58.60	55.02	1.42	1.22
39R-1, 102-104	607.42	33.62	25.16	2.04	1.98	3.07	2.87	1.53	1.48	50.18	48.51	1.01	0.94
39R-2, 9-11	607.99	40.86	29.01	2.00	1.86	3.28	2.78	1.42	1.32	56.65	52.55	1.31	1.11
39R-3, 55-57	609.97	64.72	39.29	1.83	1.67	3.74	2.82	1.11	1.01	70.22	64.00	2.36	1.78
39R-4, 75-77	611.67	31.66	24.05	2.06	1.97	3.03	2.78	1.56	1.50	48.34	46.23	0.94	0.86
39R-5, 48-50	612.90	31.96	24.22	1.98	1.99	2.83	2.86	1.50	1.51	46.87	47.12	0.88	0.89
39R-6, 70-72	614.62	39.70	28.42	1.92	1.88	2.93	2.80	1.37	1.34	53.19	52.01	1.14	1.08
40R-1, 55-57	616.55	39.34	28.23	1.96	1.90	3.07	2.86	1.41	1.36	54.11	52.33	1.18	1.10
40R-2, 95-97	618.45	40.75	28.95	1.95	1.86	3.09	2.80	1.39	1.32	55.16	52.64	1.23	1.11
40R-3, 69-71	619.69	39.13	28.12	1.98	1.85	3.12	2.69	1.42	1.33	54.33	50.66	1.19	1.03
40R-4, 70-72	621.21	44.17	30.64	1.93	1.77	3.15	2.62	1.34	1.23	57.56	53.05	1.36	1.13
40R-5, 21-23	622.22	41.25	29.20	1.96	1.85	3.13	2.78	1.38	1.31	55.71	52.79	1.26	1.12
40R-5, 33-35	622.34	44.37	30.74	1.74	1.89	2.51	3.00	1.20	1.31	52.12	56.54	1.09	1.30
41R-1, 39-41	626.09	33.20	24.93	2.03	1.95	3.00	2.79	1.52	1.47	49.25	47.47	0.97	0.90
41R-2, 37-39	626.74	27.13	21.34	1.75	1.93	2.17	2.55	1.38	1.52	36.49	40.26	0.57	0.67
41R-4, 67-69	630.04	10.12	9.19	1.99	2.72	2.20	3.27	1.81	2.47	17.85	24.41	0.22	0.32
42R-1, 31-33	635.71	45.82	31.42	1.88	1.75	3.03	2.58	1.29	1.20	57.54	53.54	1.35	1.15
42R-2, 74-76	637.64	33.37	25.02	1.99	1.94	2.91	2.77	1.49	1.46	48.64	47.45	0.95	0.90
42R-3, 30-32	638.70	46.90	31.93	1.92	1.80	3.25	2.79	1.31	1.23	59.77	56.09	1.49	1.28
42R-4, 76-78	640.66	10.43	9.45	2.08	2.34	2.32	2.69	1.88	2.11	19.13	21.52	0.24	0.27
42R-5, 76-78	642.16	76.48	43.34	1.86	1.60	4.91	2.80	1.05	0.91	78.56	67.63	3.66	2.09
43R-1, 73-75	645.83	39.11	28.12	1.97	1.90	3.09	2.86	1.42	1.37	54.14	52.15	1.18	1.09
43R-2, 70-72	647.06	39.23	28.18	1.96	1.85	3.05	2.70	1.41	1.33	53.87	50.86	1.17	1.03
43R-2, 144-146	647.80	2.18	2.13	3.74	3.53	3.97	3.73	3.66	3.46	7.77	7.34	0.08	0.08
43R-3, 70-72	648.56	41.58	29.37	1.92	1.82	3.03	2.68	1.36	1.28	55.12	52.12	1.23	1.09
43R-4, 69-71	650.05	31.31	23.84	2.08	1.96	3.07	2.75	1.58	1.50	48.37	45.69	0.94	0.84
43R-5, 86-88	651.72	40.65	28.90	1.97	1.84	3.14	2.73	1.40	1.31	55.45	51.98	1.24	1.08
43R-6, 71-73	653.07	41.45	29.30	1.93	1.83	3.05	2.71	1.37	1.29	55.25	52.28	1.23	1.10
44R-1, 21-23	654.91	35.00	25.92	1.99	1.92	2.98	2.78	1.48	1.43	50.44	48.66	1.02	0.95
44R-1, 96-98	655.66	31.69	24.07	2.00	1.96	2.86	2.75	1.52	1.49	46.96	45.93	0.89	0.85
44R-2, 64-66	656.65	50.73	33.66	1.84	1.68	3.09	2.47	1.22	1.11	60.44	55.05	1.53	1.22
44R-2, 136-138	657.37	29.87	23.00	2.06	1.99	2.95	2.77	1.58	1.53	46.19	44.65	0.86	0.81
44R-3, 71-73	658.22	29.94	23.04	2.06	2.00	2.94	2.79	1.58	1.54	46.23	44.91	0.86	0.82
44R-4, 16-18	659.17	44.21	30.66	1.91	1.80	3.10	2.69	1.33	1.25	57.22	53.71	1.34	1.16
44R-4, 128-130	660.29	28.07	21.92	2.06	2.02	2.88	2.77	1.61	1.57	44.12	43.13	0.79	0.76
44R-5, 30-32	660.81	42.08	29.62	1.89	1.78	2.92	2.59	1.33	1.26	54.55	51.57	1.20	1.06
44R-5, 98-100	661.49	32.49	24.53	2.03	1.95	2.99	2.77	1.53	1.47	48.62	46.74	0.95	0.88
45R-1, 27-29	664.67	28.08	21.92	2.10	2.02	2.98	2.78	1.64	1.58	44.91	43.27	0.82	0.76
45R-2, 66-68	665.98	49.64	33.17	1.88	1.82	3.22	2.97	1.26	1.22	60.96	59.02	1.56	1.44
45R-2, 137-139	666.69	38.82	27.96	1.94	1.74	2.98	2.37	1.40	1.25	52.98	47.35	1.13	0.90
46R-1, 53-55	674.63	29.82	22.97	2.08	2.02	3.01	2.84	1.61	1.56	46.70	45.27	0.88	0.83
46R-1, 132-134	675.42	36.99	27.00	2.02	1.92	3.14	2.84	1.47	1.40	53.12	50.60	1.13	1.02
46R-2, 44-46	676.04	40.69	28.92	1.92	1.87	2.96	2.82	1.36	1.33	54.05	52.81	1.18	1.12
46R-2, 106-108	676.66	40.17	28.66	1.93	1.87	2.99	2.78	1.38	1.33	53.94	52.16	1.17	1.09
46R-3, 21-23	677.31	40.31	28.73	1.93	1.87	3.01	2.82	1.38	1.34	54.21	52.55	1.18	1.11
46R-3, 65-67	677.75	32.33	24.43	2.02	1.96	2.95	2.77	1.53	1.48	48.18	46.61	0.93	0.87
46R-3, 84-86	677.94	37.84	27.45	1.97	1.91	3.03	2.83	1.43	1.38	52.80	51.05	1.12	1.04
47R-1, 77-79	684.47	30.86	23.58	2.02	1.97	2.89	2.76	1.55	1.51	46.53	45.41	0.87	0.83
47R-1, 118-120	684.88	38.41	27.75	1.96	1.91	3.01	2.86	1.41	1.38	52.97	51.76	1.13	1.07
47R-2, 93-95	686.13	34.69	25.76	2.00	1.94	2.99	2.82	1.49	1.44	50.27	48.81	1.01	0.95
47R-3, 18-20	686.88	29.85	22.99	2.06	2.01	2.94	2.82	1.59	1.55	46.16	45.12	0.86	0.82
47R-3, 75-77	687.45	42.61	29.88	1.90	1.84	2.98	2.78	1.33	1.29	55.34	53.61	1.24	1.16
48R-1, 19-21	693.19	35.37	26.13	1.95	1.90	2.86	2.72	1.44	1.40	49.70	48.45	0.99	0.94
48R-1, 43-45	693.43	42.10	29.63	1.90	1.84	2.98	2.77	1.34	1.30	55.02	53.21	1.22	1.14
48R-2, 20-22	694.17	40.77	28.96	1.93	1.86	3.02	2.79	1.37	1.32	54.59	52.63	1.20	1.11
48R-2, 86-88	694.83	27.33	21.46	2.11	2.04	2.96	2.81	1.65	1.60	44.08	42.79	0.79	0.75
49R-1, 61-63	703.31	102.42	50.60	1.27	1.23	1.68	1.56	0.63	0.61	62.70	60.92	1.68	1.56
49R-1, 128-130	703.98	26.65	21.04	2.08	2.04	2.88	2.78	1.65	1.61	42.78	41.97	0.75	0.72
49R-2, 60-62	704.80	42.98	30.06	1.91	1.90	3.02	3.01	1.33	1.33	55.88	55.80	1.27	1.26
49R-3, 85-87	706.52	21.47	17.68	2.21	2.15	2.93	2.82	1.82	1.77	38.05	37.10	0.61	0.59
49R-3, 120-122	706.87	26.64	21.03	2.24	2.15	3.28	3.04	1.77	1.70	46.03	44.15	0.85	0.79
49R-4, 24-26	707.37	45.06	31.06	1.90	1.83	3.09	2.84	1.31	1.26	57.63	55.54	1.36	1.25
49R-4, 98-100	708.11	22.88	18.62	2.14	2.10	2.85	2.77	1.74	1.71	38.91	38.21	0.64	0.62
49R-5, 35-37	708.98	28.24	22.02	2.08	2.03	2.93	2.81	1.62	1.58	44.65	43.60	0.81	0.77
49R-5, 106-108	709.69	24.37	19.59	2.15	2.08	2.94	2.77	1.73	1.67	41.11	39.68	0.70	0.66
50R-1, 58-60	712.88	33.05	24.84	2.07	2.01	3.12	2.94	1.56	1.51	50.17	48.63	1.01	0.95
50R-2, 50-52	713.91	52.42	34.39	1.86	1.74	3.25	2.75	1.22	1.14	62.45	58.45	1.66	1.41
50R-2, 97-99	714.38	37.05	27.03	1.87	1.91	2.69	2.81	1.36	1.39	49.31	50.41	0.97	1.02
50R-3, 61-63	715.52	32.14	24.32	2.02	1.97	2.94	2.80	1.53	1.49	48.00	46.73	0.92	0.88
50R-3, 119-121	716.10	45.93	31.47	1.91	1.82	3.17	2.83	1.31	1.25	58.72	55.93	1.42	1.27
50R-4, 92-94	717.29	26.06	20.68	1.97	2.07	2.58	2.83	1.56	1.65	39.65	41.84	0.66	0.72
51R-1, 8-10	721.98	48.77	32.78	2.10	1.81	4.31	2.89	1.41	1.22	67.23	57.88	2.05	1.37

Notes: WC-d = water content (% dry sample weight); WC-w = water content (% wet sample weight); WBD = wet-bulk density; GD = grain density; DBD = dry-bulk density; Por = porosity; VR = void ratio.

<sup>a</sup>Value calculated using Method B.

<sup>b</sup>Value calculated using Method C.

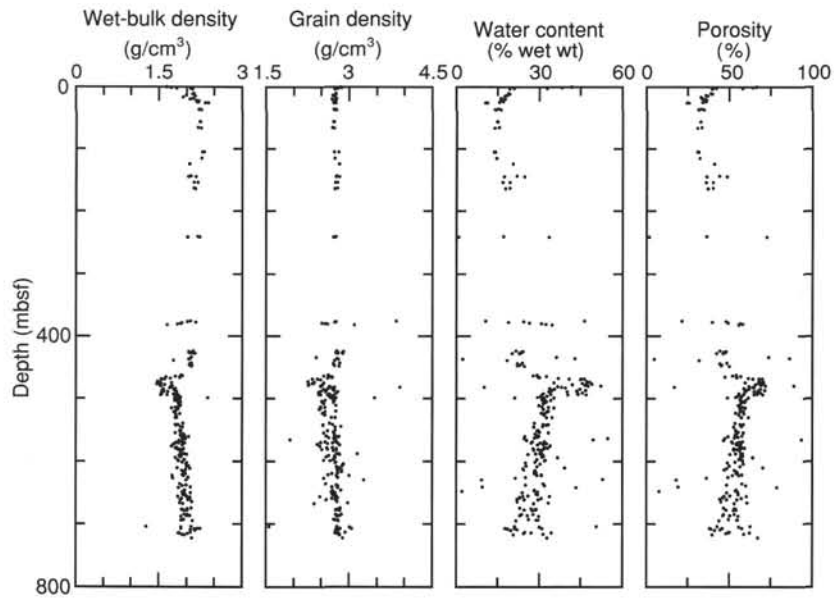


Figure 28. Wet-bulk density (Method B), grain density (Method C), wet water content, and porosity (Method C) from Holes 913A and 913B.